Liver Tissue Mimicking Materials for Image-Guided Needle Interventions

Loes Pluymen

April 2016

TU Delft

LIVER TISSUE MIMICKING MATERIALS FOR IMAGE-GUIDED NEEDLE INTERVENTIONS

By

Loes Pluymen

in partial fulfilment of the requirements for the degree of

Master of Science

in Biomedical Engineering

at the Delft University of Technology,

to be defended publicly on 1st of April 2016

Supervisor:	Dr. J.J. van den Dobbelsteen
Thesis committee:	Prof. dr. J. Dankelman
	Dr. D.J. van Gerwen
	Dr. M.K. Chmarra

PREFACE

During the past year I have been working on my master thesis project on liver mimicking materials for image-guided needle interventions. With this master thesis project I will conclude the master Biomedical Engineering at the TU Delft.

It might not apply to all students working on their graduation project, but I have really enjoyed working on my thesis project up to and including the last phase. The diverse aspects of the subject, ranging from theoretical research, practical work in the lab, Matlab analyses to discussions with clinicians, are some of the reasons why this research topic turned out to be the right choice for me.

However, this project would not have been possible without the help of several people who I would like to thank in this section.

First and foremost, my supervisors John van den Dobbelsteen and Dennis van Gerwen. I really appreciate the way in which you guided me through my graduation project. Most of the time I was given a free rein, but when needed, you pointed me in the right direction. The combination of your different perspectives has been very valuable to me. I also would like to thank the other people from the Misit lab for their enthusiasm and interest in my work. Furthermore, I would like to thank the radiologists from the Jeroen Bosch Hospital for their participation in my research.

Last but not least I would like to thank my friends and family for their support. Tessa, for keeping me company during all those hours spent in the library. Peter, for all our discussions, for being a wonderful lab assistant and, just as importantly, for providing occasional distraction from work.

My parents deserve special thanks for all their support, not only during the graduation process but also during my time as a student in Delft.

SUMMARY

Image-guided needle interventions are needle procedures performed under guidance of ultrasound imaging, CT or MRI. Ultrasound imaging is most frequently applied due to its high safety, portability, expediency and relatively low costs. An opportunity for training these sometimes challenging procedures can be provided by the use of phantoms. Phantoms are artificial organs and are made of tissue mimicking materials. In addition to the purpose of clinical training, phantoms can be used to study needle-tissue interaction or test the performance of surgical tools. Since commercially available phantoms are relatively expensive and often unsuitable for a specific research need, many researchers develop their own phantoms from tissue mimicking materials. A wide variety in materials and production methods exists.

In most studies the phantoms are presented as a tool rather than as subject of study. In studies that do focus on characteristics of phantoms made of tissue mimicking materials, mostly elasticity properties and imaging characteristics of the materials are being investigated. The axial forces in tissue mimicking materials are less often reported upon. The goal of this master thesis project is to provide insight into the extent to which tissue mimicking materials, that are suitable for phantom production, reflect the behaviour of liver tissue during ultrasound-guided needle interventions, with a focus on axial forces. Building on previous research that was conducted at the TU Delft, we will focus on liver tissue.

By reviewing relevant literature, 4 potential tissue mimicking materials are selected based on their mechanical and imaging characteristics that are supposed to determine the behaviour during needle insertions and ultrasound imaging. Materials selected are: gellan gum, polyvinylalcohol (PVA), polyvinylchloride (PVC) and candle gel. Different modalities of the these materials are defined, to be able to study the influence of several variables regarding the composition and manufacturing process of the materials.

In order to define what kind of behaviour should be mimicked, (axial) forces in liver tissue are studied. The data on liver tissue used in the current study were gathered in a preliminary study conducted by T. de Jong. By analysis of the axial forces in liver tissue, criteria for the tissue mimicking materials (TMMs) are defined. These criteria are based on the friction slope during retraction of the needle, and the number and height of the peak forces during insertion (caused by encounters with structures within the liver). Subsequently an experiment is conducted in which axial forces are measured during needle interventions in TMMs. The axial forces in TMMs are compared to the axial forces that are observed in liver tissue with the use of the defined criteria.

In addition to mechanical evaluation of the TMMs, their imaging characteristics are also assessed. Ultrasound images are obtained and compared to those of liver tissue.

A phantom should not only realistically mimic the mechanical and imaging behaviour of the liver, but should also be practical in use. Practical aspects of the materials are therefore evaluated, based on how they were experienced in the current study. Practical aspects include durability, stability over time and costs that are involved.

Combining the results of the three criteria (mechanical, imaging and practical aspects), we came to the following conclusions: Gellan gum does not cause enough friction to meet the retraction slope criterion. Also imaging of gellan gum phantoms is a problem as the material cannot hold shape without its beaker. Furthermore gellan gum is highly susceptible to fungal growth. PVA meets the mechanical criteria and has a liver like appearance under ultrasound. PVC and candle cause more friction than liver tissue and cannot be visualized by ultrasound imaging.

We conclude that PVA has the potential to be a suitable liver TMM according to the criteria that are used in the current study. Therefore PVA is presented to clinicians for practical evaluation. Their opinion about the material is that some samples mimic liver tissue realistically, but other samples are too elastic or too stiff to be comparable to liver tissue.

In addition to insight into the suitability of TMMs to mimic liver tissue in image-guided needle interventions, this thesis presents the influence of specific variables concerning the production or composition of TMMs on both the axial forces measured during needle interventions and imaging characteristics.

TABLE OF CONTENTS

LIST OF FIGURES

LIST OF TABLES

PAPER

Liver mimicking materials for image-guided needle interventions: The suitability of polyvinyl alcohol

L.H. Pluymen
Delft University of Technology

Abstract

Introduction: Phantoms, made of tissue mimicking materials (TMMs), are of great importance to study needle-tissue interaction. This study focuses on the suitability of polyvinyl alcohol (PVA) as liver tissue mimicking material for ultrasound-guided needle interventions. ***Methods:*** Two production variables (concentration of PVA and the number of freeze-thaw cycles) were varied so that 6 different samples were obtained. The samples were subjected to needle insertions (by the inner part of an 18 gauge trocar needle) at 5 mm/s while axial forces were recorded. To evaluate the suitability of PVA as liver TMM, axial forces in PVA samples were compared to axial forces measured in liver tissue, with a focus on friction during retraction and peak forces during insertion. In addition, ultrasound images were obtained and analysed on homogeneity and echogenicity. ***Results:*** PVA shows mechanical and imaging behaviour that is comparable to liver tissue. Both concentration of PVA and number of freeze-thaw (FT) cycles influence the material properties. The most suitable sample with 4% concentration of PVA and subjected to 2 FT cycles has a median friction slope of -0.011 N/mm which lies within the interquartile range (IQR) of friction slopes of liver tissue (-0.006 to -0.013 N/mm). Visualized by ultrasound, this sample shows an appearance similar to human tissue. ***Conclusion:*** By varying the two selected variables a wide range of liver tissue characteristics can be mimicked, including healthy liver tissue. In addition to insight into the suitability of PVA to mimic liver tissue in image-guided needle interventions, the influence of concentration of PVA and number of FT cycles on both the axial forces measured during needle interventions and imaging characteristics has been investigated.

Keywords: Phantom, Needle, Ultrasound, Polyvinylalcohol, Liver

Introduction

Due to the increasing prevalence of obesity and type 2 diabetes, the occurrence of liver disease has also considerably increased [1]. In the last decade, important improvements have been realised in methods to treat liver disease, especially in the field of image-guided minimally invasive procedures [2].

With minimally invasive procedures in the liver (e.g. ablation of liver tumours), positive results have been achieved compared to the regular procedure laparotomy (open surgery) [3]. To provide the clinician with visual feedback during execution of a procedure, minimally invasive procedures are often guided by imaging techniques. Ultrasound imaging is in many cases the preferred modality due to its advantages regarding safety, portability, expediency and low costs [4].

With the rapidly developing field of minimally invasive procedures, needle-tissue interaction has become a widely studied topic in research [5]. A common way to study needle-tissue interaction is by the use of phantoms (representations of organs or tissues made of tissue mimicking materials). Phantoms are, among others, used to validate new equipment, to develop biomechanical models or to test new treatment methods. Furthermore, in a clinical setting, they offer the opportunity for clinical training.

In this paper, we present the results of our search for a durable tissue mimicking material that is representative for liver tissue during ultrasound-guided needle interventions. Both mechanical and imaging properties are studied. With respect to mechanical properties we will focus on axial forces since these are considered to be the most important force component in needle insertions [6].

I.A Related work

Some of the studies in which phantoms are used, focus on developing a model to describe needle-tissue. For example DiMaio et al. [7] used a PVC phantom to study needle forces and soft tissue deformation. In other studies, a specific tissue mimicking material is preselected and compared to soft tissues with respect to its mechanical and/or imaging aspects [8] [9]. Ceh et al. compared several phantom materials, but focused mainly on the imaging characteristics of phantom materials, ignoring mechanical aspects [10]. Also Culjat et al. investigated the imaging performance of tissue mimicking materials by assessing characteristics important for ultrasound visualization [11]. Wedick and Okamura focused on the mechanical aspects of needle-tissue interaction and compared several artificial tissues to ex vivo tissues during needle insertions [12]. However, in studies that focus on both mechanical and imaging characteristics of TMMs, most often elasticity properties are studied to define the mechanical behavior. The axial forces in tissue mimicking materials are less often reported upon. Furthermore, due to a wide variety of materials and methods applied, results are difficult to compare between studies. Therefore, in this work tissue mimicking materials (TMMS) are compared to liver tissue based on both their axial forces and imaging performance. In the first phase of this study, several materials were evaluated regarding their mechanical and imaging characteristics. One material showed best results on both aspects and was therefore selected to be studied further.

I.B. Phantom materials

Materials with elasticity, speed of sound, attenuation coefficient en density properties (based on literature) comparable to liver tissue were evaluated. Materials that are often applied for phantom production and that had suitable characteristics in terms of the above-mentioned aspects were: gellan gum, polyvinyl alcohol (PVA), polyvinylchloride (PVC) and candle gel. We subjected these materials to needle insertions and ultrasound imaging. In addition to the mechanical and imaging properties of the materials, we also assessed some more basic properties such as durability. After conducting

these experiments, we could draw the following conclusions: gellan gum did not cause enough forces during needle interventions and was highly susceptible to fungal growth. To PVC, a considerable amount of plasticizer had to be added with potentially harmful effects. Furthermore, PVC was anechoic to ultrasound. Also candle gel was fully anechoic to ultrasound and the forces during needle insertions were too high compared to those observed in liver tissue. In addition, the material deteriorated rapidly by repeated insertions. However, PVA showed liver like behaviour with respect to both its mechanical and imaging behaviour. As PVA was also able to withstand repeated needle insertions and carried the promise to mimic a wide range of tissues, the material was selected to be studied further.

I.C. Polyvinylalcohol (PVA)

PVA is a synthetic polymer that can be crosslinked both chemically and physically. The latter method is often applied in biomedical applications since no addition of chemical agents is required. PVA is solvable in water and can be physically crosslinked by subjecting the solution to cycles of freezing and thawing. Upon freezing the polymer chains agglomerate causing hydrogen bond formation which ultimately leads to crystalline zones (referred to as junction zones). These crystalline zones act as physical crosslinks and remain present after thawing. The properties of PVA are influenced by a number of variables, among others the concentration of PVA, the degree of polymerization, the amount of hydrolysis (related to the number of acetate groups removed from the polymer chains during the production process of PVA), the thawing rate and the number of freeze-thaw cycles (FT cycles) [13].

II. Materials and methods

II.A. Manufacturing PVA samples

In this study, PVA samples were obtained by physical crosslinking by subjecting the samples to FT cycles, Figure 1. For optimal crosslinking by FT cycles, PVA with a high degree of hydrolysis is favoured over PVA with a low degree of hydrolysis. Furthermore a PVA type with an average degree of polymerization preferable [14]. In this study super hydrolysed PVA (Selvol PVOH 165, Sekisui Chemical Group, NJ, USA) was used. PVA samples were prepared using a hotplate magnetic stirrer (IKA RET Control-Visc S1 Digital Hot Plate Magnetic Stirrer, IKA labor technik, Germany). PVA particles were added to cold water that was stirred intensely. After all PVA particles were submerged, the solution was heated to 93 degrees Celsius. This temperature was maintained for half an hour, after which the solution was poured into a polypropylene beaker and allowed to cool down to room temperature. A cycle consisted of 16 hours of freezing at -19 degrees Celsius, followed by 8 hours thawing at room temperature.

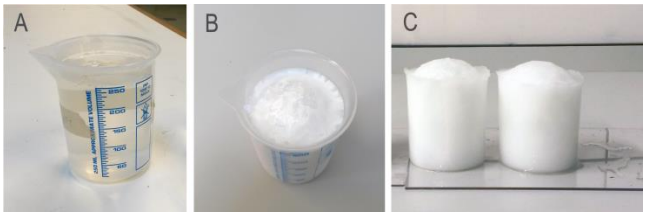

Figure 1 Manufacturing PVA A: PVA in solution, B: After freezing, C: PVA after 3 FT cycles

II.B. Liver data

To be able to characterize liver tissue during needle interventions, a raw data set was used consisting of axial forces during needle interventions in the liver. This data was gathered in a study conducted by T. de Jong [15]. In her study 6 livers (4 animal and 2 human, embedded in gelatin) were each subjected to 20 needle insertions and subsequent retraction. Data of 2 insertions (in animal liver 2 and human liver 2) were not included in our analysis since forces had not been recorded well during these insertions. In total, we thus used data on 118 insertions in liver tissue.

For proper comparison between data obtained by de Jong and the data gathered in the current study, raw data collection methods for this study were identical to those used by de Jong.

The ultrasound images of the liver that were used to characterize the livers appearance under ultrasound were collected from literature.

II.C. Mechanical Characterization

Experimental Setup

The experimental setup that was used to evaluate the forces during needle interventions in the PVA samples consisted of a linear stage and a force sensor to which a needle was connected.

The needle was connected to the force sensor with the help of a connecting element, produced by additive manufacturing. To measure the axial forces during needle interventions, an Aerotech PRO115-400 linear motion stage (Aerotech Inco, PA, USA) was used in combination with Futek LSB force sensor with a capacity of 200 lb (Futek, CA, USA) and parallel conductor with a stiffness of $1.45*10^4$ N/m. The conductor was preloaded to conduct forces in the range of -4 to 4 V.

The needle that was used was a Disposable Two-Part Trocar Needle (Cook Medical, IN, USA). This needle exists of a solid inner needle and a hollow outer needle (cannula). In our experiments, only the inner needle was used, in accordance with the experimental setup of de Jong [15].

Experimental Design

Two production variables that influence the properties of the samples were studied: concentration of PVA (in water) and the number of FT cycles. 6 PVA samples were produced: 4% 1FT, 4% 2FT, 4% 3FT, 7% 1FT, 7% 2FT, 7% 3FT. Every sample was subjected to 13 interventions consisting of 45 seconds insertion, 5 seconds waiting time, followed by 45 seconds retraction. The needle speed was 5mm/s.

All experiments were conducted with the same needle. To exclude the effects of blunting of the needle tip and diminishing of needle coating, the samples were subjected to needle insertions in random order. The puncture locations were predefined to avoid repeated insertion at the same location. Time duration, the position of the needle and the axial forces were recorded during the experiment.

II.C. Data analysis of Liver tissue and PVA

Data was analysed using Matlab 2012b (The MathWorks, Inc., Natick, MA, USA). A moving average filter (filter window 40) was applied to the data to eliminate noise.

The measured axial forces were plotted against their corresponding position to analyse the force patterns during needle insertion and retraction.

Retraction slopes

According to Okamura [16], the forces in the direction of the needle, or axial direction, consist of three components: the stiffness force, friction and cutting forces. The sum of these forces is the total axial force, as is described in the following formula:

$$f_{needle}(x) = f_{stiffness}(x) + f_{friction}(x) + f_{cutting}(x)$$

The stiffness force is needed to deform the tissue up to the moment of puncture. Friction is exerted on the needle shaft during insertion as well as during retraction. Cutting forces are exerted at the needle tip and are caused by both cutting the tissue and deforming the tissue. Both friction and cutting forces are functions of the internal stiffness of the tissue [16].

Since friction is a major force component during the insertion phase (especially for high needle velocities [6]) and even the only force component during the retraction phase, it is important the TMM should cause a similar amount of friction during needle interventions. Therefore a minimal, must-have, mechanical requirement for the TMM is to cause friction comparable to the liver. Several methods to determine friction are applied in literature. One method is to measure axial forces when the needle tip is outside the tissue and all forces are caused by friction along the needle shaft [5] [16]. Another method is to measure forces during retraction and assuming that friction during retraction will be identical to friction during insertion [17]. In our study the latter method was applied. During retraction, the friction is expected to decrease almost linearly due to decreasing surface contact between needle and tissue [6].

For all retractions in both liver tissue and PVA samples, a linear least squared approximation was defined. Subsequently, the slope of this approximation was determined, see Figure 2. A steeper retraction slope results in a more negative retraction slope value.

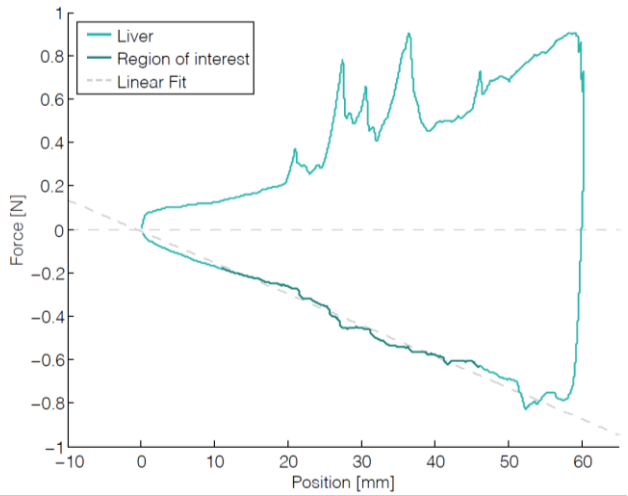

Figure 2 Linear least squares approximation of the retraction in liver tissue

Retraction slope requirement

The requirement for a suitable TMM that was defined was a median retraction slope that lies within the interquartile range (IQR) of retraction slopes observed in liver tissue.

Peak forces

The forces measured during needle insertion in the liver do not increase linearly. Due to encounters with inner structures such as arteries and veins, many force peaks are visible during the insertion phase. Assuming that friction during retraction is comparable to friction during insertion, one can subtract the approximated linear friction during retraction from the forces during insertion to obtain the approximate cutting forces. The method of approximating cutting forces by subtracting friction forces is applied in several studies [16] [18]. The contribution of constant cutting forces to the total insertion forces is very low compared to the contribution of friction. In other words, except from the peaks due to the presence of inner structures, the force that is exerted on the needle tip is low compared to the force that is caused by friction. The peaks, however, are an important phenomenon to investigate since they provide information about the inhomogeneity of the liver. Therefore in this study, in addition to the friction slope during retraction, the peak forces during insertion are examined. The method of analysis is based on previous work by D. van Gerwen [19].

The peak forces are analysed in terms of two measures: peak height and quantity. Peak height is expressed in Newtons, and peak quantity in the number of peaks per decimetre. To identify peak height and quantity, several steps were taken.

Firstly, the part of the curve that accounts for the liver was simplified using a loop version of the Douglas-Peucker Algorithm (DPA). This algorithm uses a convergence criterion that defines the maximum normal distance between the original and the simplified signal, as can be seen in Figure 3. This algorithm was applied to remove small peaks to compare liver tissue and PVA samples with respect to peaks with significant height. A convergence criterion of 0.05 N was applied for this analysis.

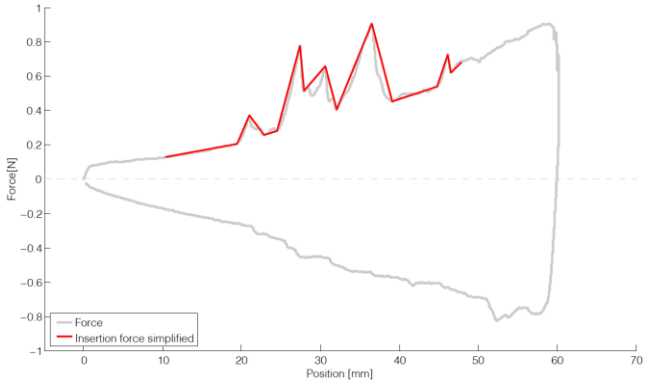

Figure 3 Insertion force simplification with DPA

Peak height was defined as the vertical distance between a peak and its preceding trough, depicted in Figure 4. Since the use of this definition will lead to peak height overestimation of peaks on steeper curves with respect to peaks present on more planar curves, the peaks were defined for the insertion forces while they were projected horizontally. These horizontally oriented insertion forces were obtained by computing the

linear slope of the insertion phase by using a linear least-squares fit. Subsequently, the computed insertion slope was subtracted from the actual insertion forces. During the last step, peak heights of the horizontally displayed signal were computed. This peak data analysis provides information about the force that is measured during encounters with inner structures. However, it does not give insight into the number of inhomogeneities that the needle comes up against. Therefore, the number of peaks was determined as well. Since the number of peaks is dependent on the length of the penetration trajectory, we computed the number of peak forces per distance. The results were visualized in boxplots.

Since in the PVA samples the first peak was due to deformation of the sample before the surface was breached, this peak was excluded from analysis. Also the last peak was excluded from analysis since this peak often just represented the end of the insertion phase, see Figure 4.

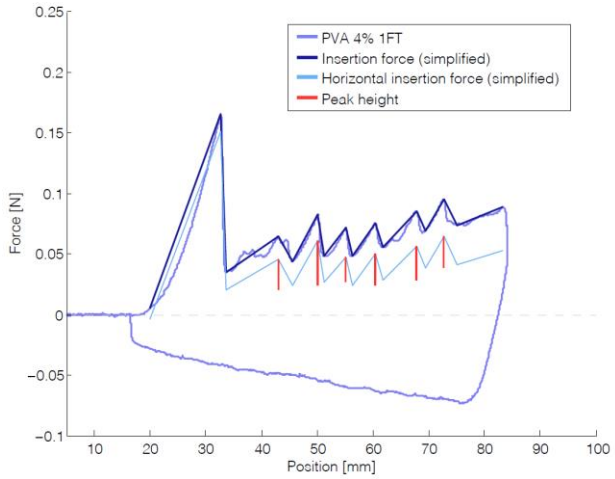

Figure 4 Peaks in PVA

Peak forces requirement

The requirement for a suitable TMM that was defined was a median peak height and a median number of peaks per decimetre (dm) that lie within the interquartile range (IQR) of liver tissue.

II.D. Ultrasound characterization

In order to obtain images without artefacts, the materials were removed from the beakers. Ultrasound images were obtained at different depths, ranging from 2 to 6 cm. 2 PVA samples (4%2FT and 7%3FT) were imaged with a Philips HD7 XE ultrasound system (Philips Medical Systems, The Netherlands). A Philips 15-6L high-resolution linear ultrasound transducer was used (Philips Medical Systems, The Netherlands). Since the PVA samples had a wet surface, no ultrasound gel needed to be used. These specific samples were selected based on their liver mimicking properties, see below.

The ultrasound images of the two PVA samples were compared to ultrasound images of the liver found in literature. Two aspects were evaluated: homogeneity and echogenicity.

III. Results

III.A. Axial force in liver tissue

The axial forces in liver tissue were studied to characterize liver tissue during needle interventions. In this section, the results of the retraction slope analysis and peak forces analysis are presented.

Retraction slopes liver tissue

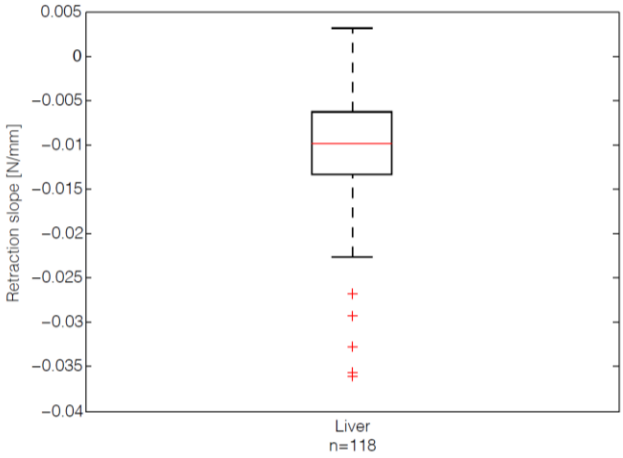

Figure 5 Retraction slopes in liver specimens

The median retraction slope in liver tissue is -0.010 N/mm within an interquartile range of -0.006 and -0.013 N/mm. The results are visualized in the boxplot in Figure 5.

Peak forces liver tissue

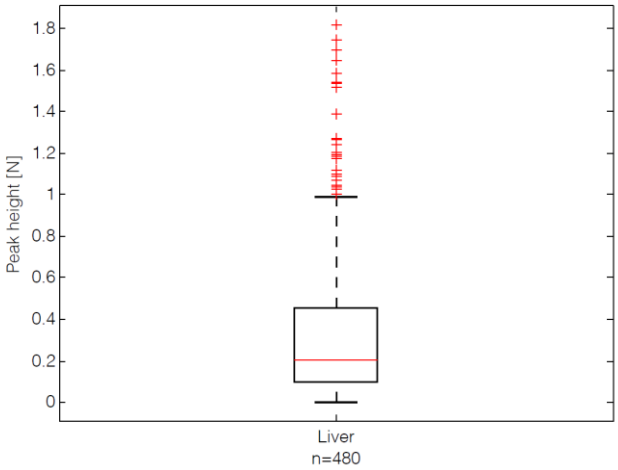

Figure 6 Peak height [N] in liver tissue

The median peak height computed from the horizontally oriented insertion forces is 0.20 N within an IQR of 0.10 N to 0.46 N (Figure 6).

To exclude the influence of specimen thickness and number of insertions, the number of peaks is computed per distance (in decimetres), visualized in Figure 7.

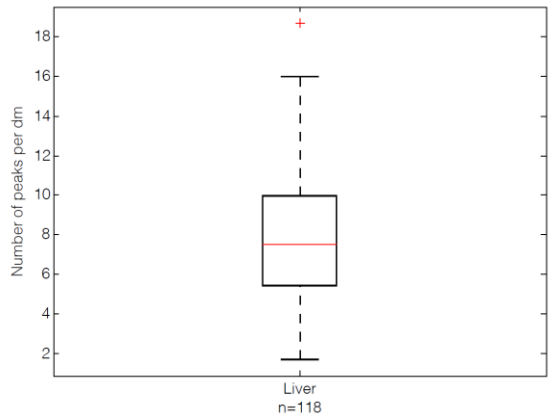

Figure 7 Number of peaks per decimetre in liver tissue

The median number of peaks per dm of all livers combined is 7.5 peaks per dm. 50% from the peaks lie within an IQR of 5.5 peaks per dm to 10.0 peaks per dm.

III.B. Axial force in PVA

The results of the force analysis of PVA are presented in this section. Firstly the retraction slopes are showed, followed by the results of the peak force analysis.

In Figure 8 and Figure 9, typical PVA force position curves can be seen for 4% PVA and 7% PVA respectively.

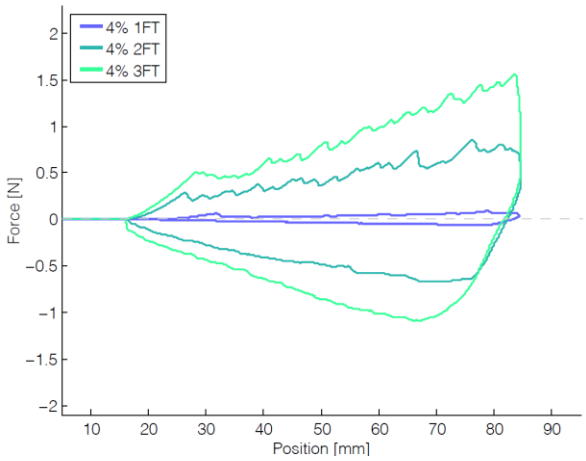

Figure 8 Force-position curves in PVA 4%

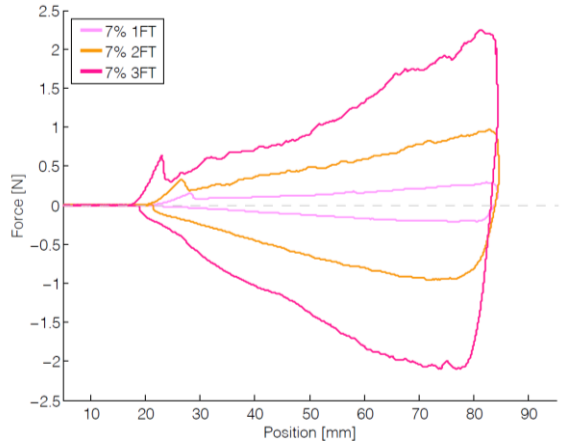

Figure 9 Force-position curves in PVA 7%

Retraction slopes PVA

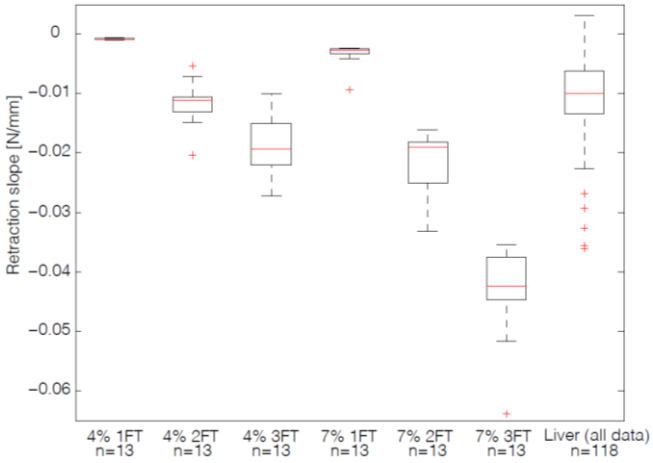

Figure 10 PVA Retraction slopes [N/mm] compared to liver tissue

In Figure 10 the retraction slopes of PVA are visualized in boxplots together with retraction slopes observed in liver tissue.

The median retraction slopes of PVA are presented in Table 1.

Median retraction slope PVA						
Sample	4% 1FT	4% 2FT	4% 3FT	7% 1FT	7% 2FT	7% 3FT
Median retraction slope [N/mm]	-0.001	-0.011	-0.019	-0.003	-0.019	-0.043

Table 1 Median retraction slopes PVA

Both the concentration of PVA and the number of FT cycles influence the retraction slope. Samples with 7% concentration have steeper retraction slopes than samples with 4% concentration PVA. The number of FT cycles has an influence on the measured friction as well. The more cycles the material is subjected to, the more negative the retraction slopes are. The median of 4% PVA subjected to 2 FT cycles lies within the IQR of liver tissue.

Peak forces PVA

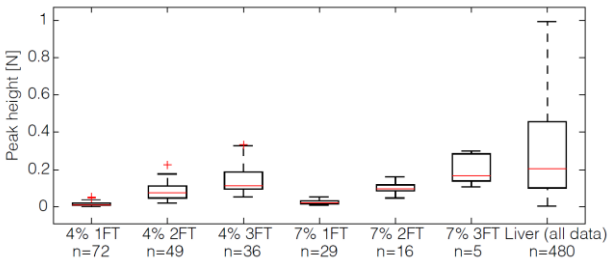

Figure 11 Peak height [N] (outliers liver excluded)

In Figure 11 the peak forces in PVA are presented, together with the peak forces observed in liver tissue. The median peak height can be found in Table 2. The median peak height in both samples with 3FT lie within the IQR of liver tissue.

In Figure 12 the number of peaks per dm are visualized. The number of peaks (per sample) and the number of peaks per dm are presented in Table 2. Regarding the number of peaks per dm, the medians of samples with 4% 1FT and 4% 2FT lie within the IQR of liver tissue.

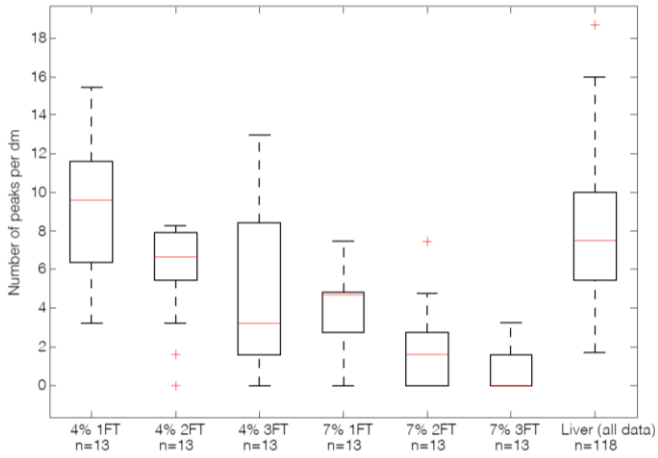

Figure 12 Number of peaks per dm in PVA and liver tissue

Peak forces PVA						
Sample	4% 1FT	4% 2FT	4% 3FT	7% 1FT	7% 2FT	7% 3FT
Median peak height [N]	0.01	0.07	0.11	0.02	0.10	0.16
Number of peaks (per sample)	72	49	36	29	16	5
Number of peaks per dm	9.6	6.6	3.2	4.7	1.6	0

Table 2 Peak forces PVA

III.C. Ultrasound Imaging

In this section ultrasound images (obtained with 2 cm penetration depth) of PVA samples 4% 2FT and 7% 3FT are presented.

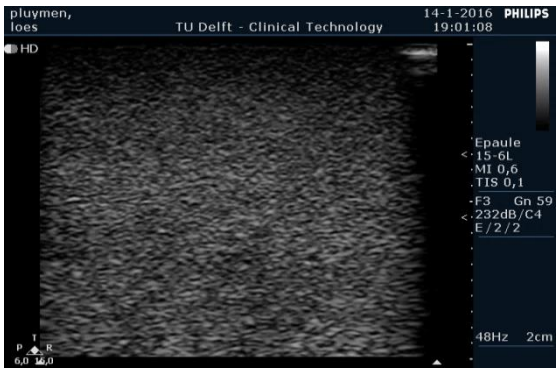

Figure 13 PVA 4% 2FT, 2 cm penetration depth

PVA 4% 2FT has an echogenicity that is comparable to liver tissue, Figure 13. The material is mostly homogenous.

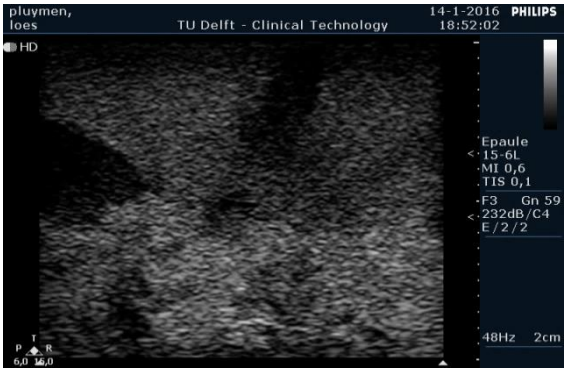

Figure 14 PVA 7% 3FT, 2 cm penetration depth

In PVA 7% 3FT (Figure 14), regions with different echogenicity can be distinguished, and therefore the material is not homogenous.

IV. Discussion

Mechanical requirement 1: Retraction slope PVA

The first mechanical requirement to mimic liver tissue was defined as: The TMM should have a median friction slope within the IQR of friction slopes in liver tissue.

The PVA samples that were tested for mechanical evaluation showed a wide range of friction slopes. Some samples showed less friction than observed in liver tissue, while others showed more friction than liver tissue. Two trends were observed:

- An increase in friction with an increase of number of FT cycles
- An increase in friction with an increase of mass fraction PVA

Although the influence on the mechanical properties of PVA of the number of FT cycles and concentration are described in literature [20] [21], they have not yet been reported with respect to needle-tissue interaction.

From the two trends observed can be concluded that several combinations of a number of FT cycles and a concentration of PVA in water can lead to phantoms with suitable friction characteristics. From the samples that we tested, PVA 4% 2FT had a friction slope within the IQR of liver tissue. However, the spread of the retraction slopes in this sample are smaller than the spread observed in liver tissue. One should keep in mind that the dataset representing liver tissue comprises 6 different specimens, whereas the data representing PVA 4% 2FT just include insertions in 1 sample.

Mechanical requirement 2: Peak forces PVA

The second mechanical requirement to mimic liver tissue was defined as: The TMM should have a median peak height within the IQR of peak height observed in liver tissue, and a median number of peaks within the IQR of the number of peaks present in liver tissue.

An algorithm was applied to exclude small peaks to allow for better comparison between liver tissue and PVA. The insertion forces were simplified to compare significant peak forces only. The influence of the simplifying factor was investigated and a compromise between too much simplification (leading to less informative data) and an insufficient amount of simplification (comparison focusses mainly on small peaks and therefore almost all PVA samples fulfil the criteria) was reached.

When analysing results of the two variables studied here, three conclusions can be drawn:

- Both an increase in FT cycles and an increase in PVA mass fraction leads to an increase in peak height
- Peak height is mostly influenced by the number of FT cycles
- Both an increase in FT cycles and an increase in PVA mass fraction leads to a decrease in number of peaks

During our experiments, we observed an increase in stiffness with an increase in PVA concentration or increasing number of

FT cycles. This is in line with results presented by Jiang [20]. Samples with a higher concentration of PVA or subjected to more FT cycles were stiffer than the other samples and showed less deformation before puncture. Due to the lack of deformation, inner structures are supposed to be cut through more easily. Occasional peaks are probably the result of cutting actions of substantial PVA accumulation.

One should keep in mind, that the properties of PVA are dependent on the freezing and thawing process. As the samples cannot be fully uniformly frozen en thawed, the material properties vary for different positions within the sample. In the current study, the influence of insertion location was not taken into account.

From the samples that we analysed, the medians of samples with 4% 1FT and 4% 2FT lie within the IQR of liver tissue regarding the number of peaks during insertion. The medians of samples with 3FT have sufficient peak height according to the defined criterion. We can conclude that none of our samples meets both criteria that were defined for the peak forces during insertion, however, we are of the opinion that it must be possible to obtain a PVA sample with suitable characteristics on all aspects.

Ultrasound imaging

The PVA samples showed a liver like speckled pattern, probably due to the crystalline regions in the material that diffusively reflected sound waves. An obvious difference could be observed between the PVA 4% 2FT and PVA 7% 3FT samples. The latter showed a more inhomogeneous structure with presence of whimsical structures with higher echogenicity. Concluding from a small additional study in which a PVA 3% 5FT sample was visualized by ultrasound, this inhomogeneity was mostly due to the increase in concentration of PVA (In the additionally made sample PVA 3% 5FT almost no inhomogeneous structures were present).

Limitations

It should be noted that the properties of PVA cryogels are influenced by many more variables than those that were studied in the current work. Among these variables are the amount of hydrolysis, the degree of polymerization, the amount of ions present in the solvent, the type of solvent, the freezing rate and the duration and the thawing rate [22].

A limitation of this work is that the raw data on livers and TMMs were not obtained in the same experiment. Although the same data collection setup was used, the effects of needle blunting and diminishing of needle coating may have influenced the results. Furthermore, the experiments were not conducted by the same person, thereby possibly causing inter-operator differences.

Another aspect to be kept in mind is that the TMM are compared to liver data that did not solely include human livers. Also 4 animal livers have been used as reference, comprising different animals. Furthermore, the data was collected ex vivo. For ethical reasons this is fully understandable, but differences due to among others, lack of perfusion, preservation period and storage conditions cannot be ruled out.

V. Conclusion

The aim of this study was to find a liver TMM suitable for image-guided needle interventions. Regarding the defined criteria on friction slope, peak forces during insertion and ultrasound visualization, we can conclude that PVA is a suitable material to mimic liver tissue during image-guided needle interventions.

The properties of PVA are tuneable to mimic a wide range of tissues. From the PVA modalities investigated in this study, the PVA 4% 2 FT sample proved to provide the best match with liver tissue. This sample had a similar friction slope as liver tissue, showed a comparable number of peaks during insertion and showed human tissue-like characteristics when visualized by ultrasound imaging.

References

1. Welsh, J.A., S. Karpen, and M.B. Vos, *Increasing prevalence of nonalcoholic fatty liver disease among United States adolescents, 1988-1994 to 2007-2010.* The Journal of pediatrics, 2013. **162**(3): p. 496-500. e1.
2. Najmaei, N., et al., *Image-guided techniques in renal and hepatic interventions.* The International Journal of Medical Robotics and Computer Assisted Surgery, 2013. **9**(4): p. 379-395.
3. Buell, J.F., et al., *Experience with more than 500 minimally invasive hepatic procedures.* Annals of surgery, 2008. **248**(3): p. 475-486.
4. Velasco, J.M. and K. Hood, *Percutaneous Ultrasound Guidance Techniques and Procedures*, in *Abdominal Ultrasound for Surgeons*. 2014, Springer. p. 89-107.
5. Abolhassani, N., R. Patel, and M. Moallem. *Experimental study of robotic needle insertion in soft tissue*. in *International Congress Series*. 2004. Elsevier.
6. van Gerwen, D.J., J. Dankelman, and J.J. van den Dobbelsteen, *Needle-tissue interaction forces--a survey of experimental data.* Med Eng Phys, 2012. **34**(6): p. 665-80.
7. DiMaio, S.P. and S.E. Salcudean, *Needle insertion modeling and simulation.* Robotics and Automation, IEEE Transactions on, 2003. **19**(5): p. 864-875.
8. Opik, R., et al. *Development of high fidelity liver and kidney phantom organs for use with robotic surgical systems*. in *Biomedical Robotics and Biomechatronics (BioRob), 2012 4th IEEE RAS & EMBS International Conference on*. 2012. IEEE.
9. Hungr, N., et al., *A realistic deformable prostate phantom for multimodal imaging and needle-insertion procedures.* Medical Physics, 2012. **39**(4): p. 2031-2041.
10. Ceh, D., T.M. Peters, and E.C. Chen. *Acoustic characterization of polyvinyl chloride and self-healing silicone as phantom materials*. in *SPIE Medical Imaging*. 2015. International Society for Optics and Photonics.
11. Culjat, M.O., et al., *A review of tissue substitutes for ultrasound imaging.* Ultrasound in medicine & biology, 2010. **36**(6): p. 861-873.
12. Wedlick, T.R. and A.M. Okamura. *Characterization of robotic needle insertion and rotation in artificial and ex vivo tissues*. in *Biomedical Robotics and Biomechatronics (BioRob), 2012 4th IEEE RAS & EMBS International Conference on*. 2012. IEEE.
13. Surry, K., et al., *Poly (vinyl alcohol) cryogel phantoms for use in ultrasound and MR imaging.* Physics in medicine and biology, 2004. **49**(24): p. 5529.
14. Tao, J., *Effects of Molecular weight and Solution Concentration on Electrospinning of PVA*. 2003, Worcester Polytechnic Institute.
15. de Jong, T., *Needle Deflection in Tissue.* 2015.
16. Okamura, A.M., C. Simone, and M.D. O'Leary, *Force modeling for needle insertion into soft tissue.* Biomedical Engineering, IEEE Transactions on, 2004. **51**(10): p. 1707-1716.
17. Hing, J.T., A.D. Brooks, and J.P. Desai, *A biplanar fluoroscopic approach for the measurement, modeling, and simulation of needle and soft-tissue interaction.* Medical image analysis, 2007. **11**(1): p. 62-78.
18. Hing, J.T., A.D. Brooks, and J.P. Desai. *Reality-based needle insertion simulation for haptic feedback in prostate brachytherapy*. in *Robotics and Automation, 2006. ICRA 2006. Proceedings 2006 IEEE International Conference on*. 2006. IEEE.
19. Van Gerwen, D.J., *Needle-Tissue Interaction by Experiment.* 2013: p. 81-101.
20. Jiang, S., S. Liu, and W. Feng, *PVA hydrogel properties for biomedical application.* Journal of the mechanical behavior of biomedical materials, 2011. **4**(7): p. 1228-1233.
21. Cha, W.I., et al. *Mechanical and wear properties of poly (vinyl alcohol) hydrogels*. in *Macromolecular Symposia*. 1996. Wiley Online Library.
22. Okay, O., *Polymeric Cryogels: Macroporous Gels with Remarkable Properties*. Vol. 263. 2014: Springer.

THESIS

1. INTRODUCTION

1.1 TISSUE MIMICKING MATERIALS

Image-guided needle interventions are needle procedures under guidance of ultrasound imaging, CT or MRI performed percutaneously or during open surgery. These interventions can be challenging due to complex anatomy or visualization limitations. It has been shown that success rates are to a significant extent influenced by the operators experience [1]. However, this experience needs to be obtained. To get acquainted with the feeling of human tissue and its interaction with surgical tools, so called phantoms can be used. Phantoms simulate human tissues or organs and reflect different aspects of reality. In addition to the purpose of clinical training, phantoms can be used to study needle-tissue interaction or test the performance of surgical tools and medical devices.

Commercially available phantoms suitable for interventional radiology are produced by among others CIRS, Blue Phantom and Kyoto Kagaku. Various types of phantoms have been developed, offering different kind of training opportunities. Some phantoms are only suitable for imaging, others for needle interventions, and some can be used for both. However, these phantoms often represent a substantially simplified version of reality and are relatively expensive. Repeated use causes the phantoms to deteriorate rapidly [2]. Furthermore, commercial phantoms rarely simulate pathology [1].

Due to the above mentioned disadvantages of commercial phantoms, alternatives are used both in clinical and in research settings.

There are two alternatives to commercial phantoms. One option is the use of biological tissues. Cadavers, when freshly frozen, retain most of the textural and imaging properties of human tissue [3]. Better available than (human) cadavers, are animal tissues. For the purpose of clinical training for example chicken breast is often being used to simulate soft tissues [4]. However, due to practical and ethical issues, the use of biological tissues is not always a feasible option. Another alternative to commercial phantoms is the use of 'homemade' phantoms, made of tissue mimicking materials. For example gelatin is often applied to mimic soft tissues, due to its low costs and easy manufacturing process [5]. A great advantage of homemade phantoms is that they can be customized to the meet the needs of a specific research activity or training. Furthermore, they can often be produced at low costs.

Although the use of homemade phantoms is often reported upon in literature, not many studies have been performed on the comparison between phantom materials and the degree in which they simulate the original tissue during needle interventions. Often the phantom or material is presented as a tool, rather than as subject of study.

Some of the studies in which phantoms are used, focus on needle-tissue interaction in order to model the interaction between needle and tissue [6] [7]. In other studies, a specific tissue mimicking material is selected and compared to soft tissue with respect to its mechanical and/or imaging aspects [5] [8]. Ceh et al. compared several phantom materials, but focused mainly on the imaging characteristics of phantom materials used for image-guided needle interventions [9]. Also Culjat et el. investigated the imaging performance of tissue mimicking materials by assessing characteristics important for ultrasound visualization [10]. Wedick and Okamura focused on the mechanical aspects of needle-tissue interaction and compared several artificial tissues to ex vivo tissues during needle insertions [11]. However, in studies that focus on both mechanical and imaging characteristics of TMMs, most often elasticity properties are studied to define the mechanical behavior. The axial forces in tissue mimicking materials are less often reported upon. Furthermore, due to a wide variety of materials and methods applied, results are difficult to compare between studies. Therefore, in this work tissue mimicking materials (TMMS) are compared to liver tissue based on both their axial forces and imaging performance.

The motivation for this this master thesis project, was the need for more insight into the properties of ultrasound compatible TMMs, during needle insertions. In line with research performed previously at TU Delft, this work will focus on materials used to mimic liver tissue.

1.2 PROBLEM DEFINITION AND OBJECTIVE

There is no complete insight into the accuracy in which TMMs that are suitable for phantom production reflect the behavior of liver tissue during image-guided needle interventions.

This study aims to provide an overview of potential phantom materials and the way they reflect the behavior of liver tissue in image-guided needle interventions, leading to the most suitable phantom material.

The present work will investigate to what extent TMMs mimic liver tissue in image-guided needle interventions. The materials will be evaluated based on both mechanical performance and imaging characteristics. Furthermore, the practical aspects with respect to phantom production will be reviewed.

The initial objective of this master thesis project is to find a material that mimics liver tissue in its healthy state. However, the material properties of the TMMS should be extendable towards the pathologic spectrum of liver tissue characteristics. This is however outside the scope of this thesis.

1.3 APPROACH

TMMs will be evaluated using three criteria:

- Mechanical properties
- Imaging properties
- Practical aspects

At first, important liver characteristics will be defined and determined by reviewing relevant literature. Subsequently TMMs will be selected based on agreement with the determined liver characteristics.

After this theoretical phase, an experiment will be conducted in which TMMs will be compared to liver tissue. With respect to the data of liver tissue available for this thesis, the comparison will focus on axial forces during needle interventions. The raw dataset representing axial forces in liver tissue that will be used was obtained in a preliminary study performed by T. de Jong [12]. Data representing axial forces in needle insertions in the selected TMM will be collected during this study.

After the TMMs mechanical properties have been assessed, the materials will be compared to liver tissue regarding their imaging properties. Ultrasound images will be obtained and compared to ultrasound images of liver tissue that are found in literature.

In the last phase of this research project, the practical aspects of the TMMs will be evaluated and the TMMs will be presented to clinicians.

The individual steps that will be taken in this project are visualized in Figure 1.

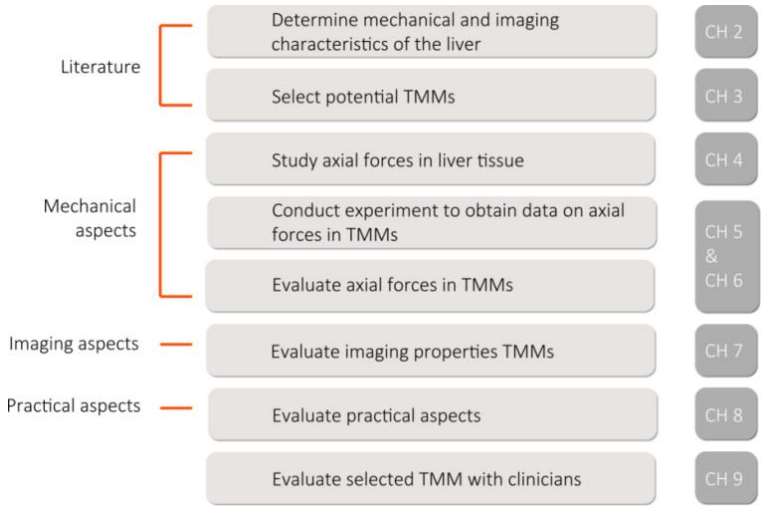

Figure 1 Organization of the thesis

1.4 ORGANIZATION OF THE THESIS

This thesis is organized as follows: Chapter 2 will provide the reader with theoretical background information about the mechanical and imaging characterization of the liver and about needle tissue interaction. In chapter 3, phantom materials reported in literature are discussed. This chapter will conclude with the selection of TMMs that will be further evaluated in this research project. After axial forces in liver tissue have been analysed in chapter 4, the axial forces in TMMs are presented in chapter 5 followed by a further investigation of one TMM presented in chapter 6. In chapter 7 the imaging characteristics of TMMs are studied. In chapter 8 the practical facets of the TMMs will be evaluated, followed by a report of the evaluation with clinicians in chapter 9. Subsequently, the discussion and final conclusions of this research are presented.

2. THEORETICAL BACKGROUND

A literature survey was conducted prior to this master thesis project to be able to select potential liver tissue mimicking materials worthy of further investigation. The results of this literature survey provided interesting background information that is presented in the current chapter.

In the following section 2.1 the features and organization of the liver will be explained, followed by a section on most frequently performed needle interventions in 2.2. In section 2.3 related research on needle-tissue interaction is presented. Mechanical and imaging characteristics of the liver, presented in section 2.4 resp. 2.5., will serve as a guideline to define requirements for the phantom materials.

2.1 LIVER TISSUE AND PATHOLOGY

In this chapter most important liver characteristics will be explained, both on macro and micro level. Subsequently, commonly observed pathologies are described.

2.1.1. MACRO LEVEL

The liver is involved in many vital processes, and liver malfunctioning can have severe consequences. The organ plays a major role in the metabolism of carbohydrates, proteins and fat. In spite of irregular food intake, the liver ensures a constant availability of glucose. Another important function is the detoxification and elimination of foreign substances. Furthermore, the organ serves as storage for vitamins and iron and is involved in the production and secretion of bile. As the liver is an expandable organ, by storage of large quantities of blood in its vessels it can act as a blood reservoir [13].

The liver is the biggest solid organ of the human body, weighing about 1200-1500 grams. The organ is located in the right upper part of the abdomen. Based on the outer appearance, the liver can be subdivided into 4 primary lobes: the right, left, caudate and quadrate lobe. More often the liver is discussed in terms of eight segments based on the internal anatomy, as can be seen in Figure 2. The outer surface of the liver is covered by a capsule, called the Glisson's capsule.

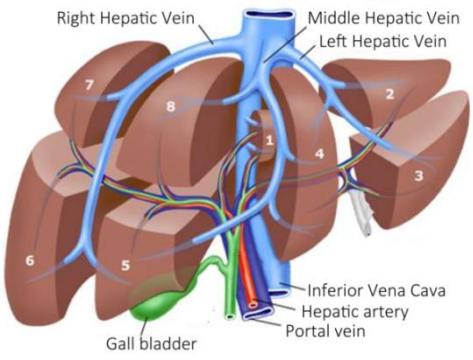

Figure 2 Liver segments, retrieved from [14] (adjusted)

Blood is carried towards the liver via the hepatic artery and the portal vein. The hepatic artery originates from the celiac trunk in the aorta and thus provides oxygen rich blood. It accounts for 25% of the blood flow towards the liver. The portal vein supplies the remainder of its blood flow and provides the liver with nutrient rich blood from the stomach, intestines and spleen. Blood is drained by the hepatic veins, that empty into the inferior vena cava [14].

2.1.2. MICRO LEVEL

The liver consists of 50.000 to 100.000 liver lobules, which are its functional and structural units. These lobules have a hexagonal shape and consist of plates of hepatic cells constructed around a central vein in longitudinal direction, see Figure 3.

Blood flows towards the central vein and from which it continues to the hepatic veins. At each of the six corners a portal triad is located, that contains three basic structures: a branch of the hepatic artery, a branch of the portal vein and a bile duct [14].

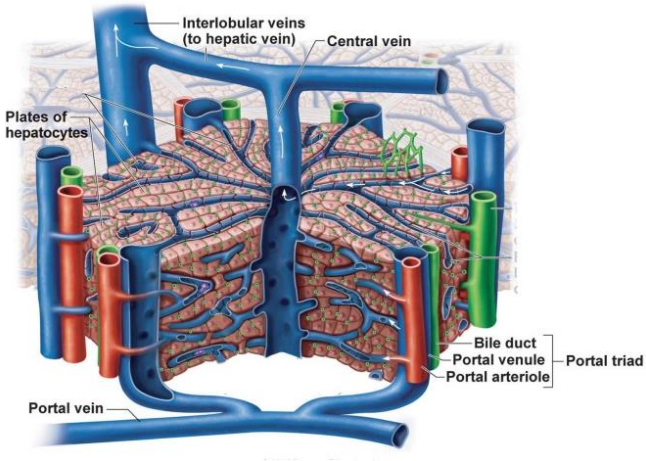

Figure 3 Liver lobule, retrieved from [14]

2.1.3. PATHOLOGY

Related to its many functions, the liver is vulnerable to a wide array of metabolic, toxic, microbial and circulatory disorders. Due to the increasing prevalence of obesity and type 2 diabetes, liver disease is becoming more prevalent. The most common primary liver disorders are hepatitis, alcohol induced liver disease, non-alcoholic fatty liver disease (NAFLD) and hepatocellular carcinoma (HCC). More common than HCC are liver metastases from primary tumours of other bodily organs. They account for 72% of the malignant tumours found in the liver [15].

Fibrosis, or scarring of liver tissue, is often seen in early stage of liver disease. Final stage fibrosis is called cirrhosis and can result in liver failure.

Symptoms of liver damage may take weeks or months or some even years to become apparent. This means that liver diseases are often only detected a significant period after onset. When 80 to 90% of the functional liver capacity is affected, hepatic failure can occur. The prognosis for patients suffering from hepatic failure is severe, with a mortality rate of 80% without liver transplantation [16].

2.2 NEEDLE INTERVENTIONS

Needle interventions are part of many diagnostic and therapeutic procedures. In this section, two commonly performed needle interventions in the liver are discussed: biopsy and ablation.

2.2.1.BIOPSY

Liver biopsies have been used to diagnose liver diseases for more than 100 years. Although today the use of imaging techniques also provides useful diagnostic information, biopsies are still a valuable tool to assess liver disease and functioning. Liver biopsies can be performed percutaneously, transvenously and laparoscopically. Also during abdominal surgery biopsies can be taken. The most commonly used method is percutaneous biopsy, in which a needle is inserted via the skin. Transvenous liver biopsy can both be performed via the femoral or, more common, via the jugular veins. This method was introduced to avoid coagulopathy (clotting disorder) that is induced by the bleeding following from percutaneous biopsy, or in patients with significant ascites (fluid accumulation in the abdominal cavity) or morbid obesity [17]. Laparoscopic liver biopsy is often

performed when a liver lesion is discovered during laparoscopy. It has the advantage of a direct view on the liver. This reduces the risk on sampling errors (causing the wrong diagnosis) and bleeding after the biopsy is taken [18]. Most common complications of biopsies are haemorrhage and biliary leakage [19]. Most biopsies are performed under guidance of imaging [20].

2.2.2.ABLATION

In addition to resection (surgical removal), tumorous tissue can be removed by ablation. Different types of ablation are being used, all of them based on needle interventions. One way of performing ablation is by the instillation of a chemical agent. A commonly used agent is ethanol. Chemical ablation is very suitable for encapsulated tumours like HCC, as the capsule around the tumour prevents the injected agent from spreading to healthy tissue. Ablation can also be achieved by thermal treatment. By exposing the tumorous tissue to extreme temperatures, the targeted cells are destroyed. When using low temperatures, the technique is called cryo-ablation. Ablation therapies using high temperatures are high intensity focused ultrasound (HIFU) ablation, laser ablation, microwave coagulation therapy and radio-frequency ablation (depicted in Figure 4). Ablation is often used often to treat small tumours. For larger tumours, multiple ablations can be needed. Each ablation takes several minutes. The procedure can either be performed surgically, percutaneously or laparoscopically.

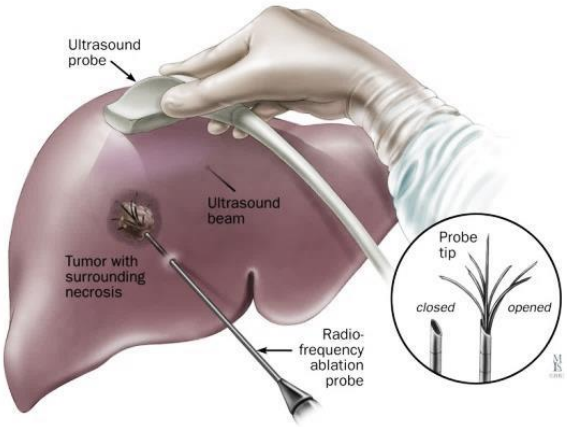

Figure 4 Ultrasound-guided ablation, retrieved from www.hopkinsmedicine.org

2.3 NEEDLE-TISSUE INTERACTION

The response of tissues upon needle insertions has been widely studied. This is, among others, due to its relevance for improvement of minimally invasive procedures [21]. Studies performed to investigate needle-tissue interaction focus, inter alia, on forces generated during needle insertions, tissue deformation and needle deflection. Factors that significantly influence the interaction between needle and tissue are needle design, type and state of punctured tissue, and needle insertion method and velocity.

2.3.1 INTERACTION PARAMETERS

In this section three items that influence the needle tissue interaction will be briefly discussed: needle properties, tissue characteristics and interaction parameters.

NEEDLE PROPERTIES

The shape of the tip and the diameter of the needle have a significant influence on the interaction between needle and tissue. The larger the diameter of the needle, the more tissue is displaced and compressed. Thereby forces normal to the needle shaft increase, resulting in higher friction forces. This was showed by Okamura [22], who found that the slopes of the force-position curves are steeper for thicker needles, indicating a higher amount of friction. Force-position curves will be explained in section 2.4.4. Also needle bending is influenced by

the needles diameter: a thicker needle will have less deflection. Mc. Gill et al. [23] showed that the use of stiffer needles leads to less needle deflection.

Various types of needle tip designs exist. The tips can have a blunt, 3-sided, or beveled shape (Figure 5). Every needle tip has his own interaction with tissue in terms of produced forces and needle deflection. Logically, less force is needed to insert needles with sharper tips. Related to the number of cutting edges at the tip, cone tips require the highest amount of force, followed by beveled tips. For insertion of triangular tips the least amount of force is needed. Needle deflection is influenced by symmetry of the needle tip. Asymmetrical bevel tips cause more deflection than symmetrical triangular tips. However, also in insertions with symmetrical needles deflection is observed. This deflection is due to inconsistencies within the punctured material [22] [24].

Figure 5 Various needle tips: blunt, beveled, conical, sprotte, diamond, Tuohy, retrieved from [25]

Figure 6 Two-part disposable trocar needle, retrieved from www.cookmedical.com

In practice often two-part needles are used. These needles consist of a hollow outer needle, and solid inner needle, see Figure 6. After insertion of both parts, the sharp inner needle that served to cut the tissue, is removed. Subsequently, a device can be inserted through the outer needle. As will described later, these needles will be used in the experiments conducted in this study.

TISSUE PROPERTIES

The majority of studies conducted to asses mechanical properties of liver tissues make use of tissues ex vivo. Since the absence of perfusion is affecting the mechanical behaviour to a significant extent, question is whether these kind of experiments is representative for the in vivo situation [26]. Some researchers try to overcome this issue by simulating perfusion in ex vivo tissues.

Also the preservation period of the liver in ex vivo experiments influences to a great extent the tissue properties, as was demonstrated by Yarpuzlu [27]. On the other hand, results from in vivo experiments are more easily influenced by variable test conditions and can be affected by respiratory movements [28].

In addition to differences between ex vivo and in vivo measurements, the difference between species should be taken into account. Studies are based on, among others, bovine, porcine, canine and human livers. Lastly, the pathological state has a significant influence on the tissue properties. Many researchers studied the effect of fibrosis and liver tumours on tissue stiffness and showed that liver stiffness is significantly increased in case of fibrosis [29]. This is not further explored here since this master thesis project focuses on comparison of TMMs to healthy liver tissue.

INSERTION PARAMETERS

During needle interventions, needles are not inserted at a constant velocity nor with constant force [30]. To allow for comparison and interpretation of forces during needle interventions, in most studies needles are

inserted at constant speed [25]. Forces measured during needle-tissue interaction are shown to increase with needle velocity [6]. Also Webster et al. showed that forces directly depend on needle velocity, and additionally concluded that deflection was not significantly affected by needle velocity [31]. On the contrary, Mc Gill et al. [24] showed a decrease of needle deflection caused by an increase of needle insertion velocity (for insertion velocities higher than possible for manual insertion).

2.3.2 INTERACTION

As described above, the interaction parameters (needle properties, tissue properties and insertion parameters) influence the needle tissue interaction in terms of, among others, measured forces, needle deflection and tissue deformation. This master thesis project will focus on the influence of tissue properties on the measured forces (in particular axial forces during needle insertion and retraction, see Figure 7. The other parameters (needle properties and insertion parameters) are kept constant. In the following section forces in needle tissue interaction are discussed.

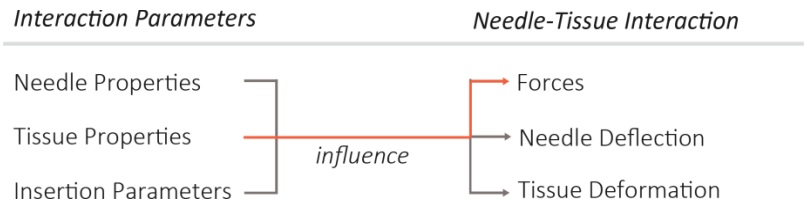

Figure 7 Needle-tissue interaction parameters

AXIAL FORCES DURING NEEDLE INSERTION AND RETRACTION

Several phases of needle insertion can be distinguished. The first phase is known as the deformation phase, in which the needle is pushing the tissue without breaching the surface, Figure 8.A. When the needle tip subsequently enters the tissue, the insertion phase starts. During this phase, forces are exerted both on the needle tip and on the needle shaft, Figure 8.B. By contrast, during the retraction phase, the needle shaft is the only part forces are being exerted on [25].

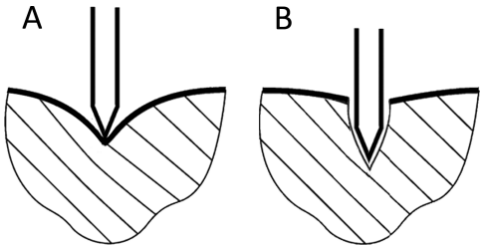

Figure 8 A: Tissue deformation, B: Needle insertion, retrieved from [25] (adjusted)

According to Okamura [22], the forces in the direction of the needle, or axial direction, consist of three components: the stiffness force, friction and cutting forces. The sum of these forces is the total axial force, as is described in Equation 1. The stiffness force is needed to deform the tissue up to moment of puncture. Friction is exerted on the needle shaft during insertion as well as during retraction. Friction can be caused by tissue adhesion and damping. Cutting forces are exerted at the needle tip and are caused by both cutting the tissue and deforming the tissue. Both friction and cutting forces are functions of the internal stiffness of the tissue [22].

$$f_{needle}(x) = f_{stiffness}(x) + f_{friction}(x) + f_{cutting}(x)$$

Equation 1 Axial forces (x = position of the needle tip)

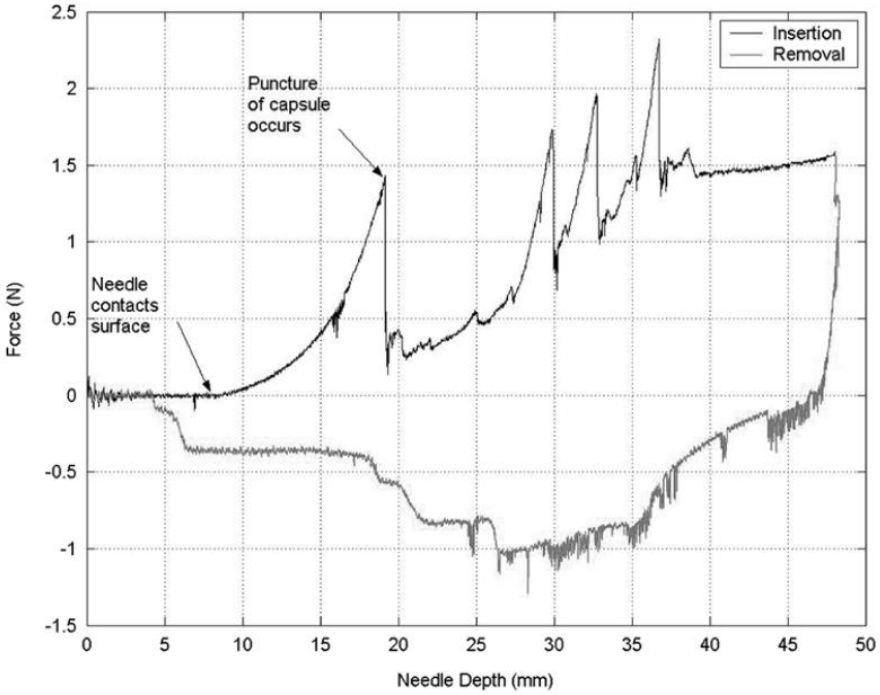

Figure 9 Force position diagram, retrieved from [22]

In Figure 9, a force position diagram can be seen. The three phases of deformation, insertion and retraction can be distinguished. The deformation phase spans the part of the curve from first contact with the needle (left arrow) to puncture of capsule (right arrow). When the capsule is breached (punctured), the force position curve shows a sharp decrease, after which the insertion phase starts. During the insertion phase, the force gradually increases due to increasing contact surface with the needle. Three prominent peaks are visible during the insertion phase, indicating the presence of inner structures within the tissue. When the needle has reached it maximal depth, the needle is retracted. During the retraction phase, all forces are due to friction along the needle shaft [22].

2.4 MECHANICAL CHARACTERIZATION LIVER

As described in the previous section, forces reflecting needle-tissue interaction are heavily dependent on the experimental setup. In most studies different test conditions are used, thereby hampering inter-study comparison. Instead of trying to compare forces described in literature, in this study underlying characteristics are defined. One of the most influential properties of the liver is its stiffness. The stiffer the organ, the more it will show resistance to deformation. While stiffness is a property of an organ, elasticity is a property of the tissue itself. Although elasticity measurements do also vary due to different measuring methods, the results are better comparable between studies than friction. Therefore the present study will investigate elasticity characteristics of liver tissue to provide literature based criteria for the selection of TMMs.

2.4.1 ELASTICITY AT SMALL STRAINS

Soft biological tissues exhibit nonlinear elastic behaviour. In other words, in these materials stress does not increase linearly with strain. Most soft tissues show a nonlinear elastic behaviour for strains above 10% [32]. The elastic modulus is often determined from a linear region at lower strains, to still be able to determine a representative value, as can be seen in Figure 10. Although the behaviour of liver tissue is highly nonlinear, the elastic modulus is still a convenient measure for comparison between tissue types or conditions [32].

Techniques to determine elasticity of liver tissue include indentation, aspiration, elastography and compression and tension tests [33]. Indention and aspiration can be performed in vivo, for example during open surgery. These techniques are based on force displacement relationships determined by compression and suction respectively. In vivo characterization of liver tissue can also be done by elastography, visualizing the response of tissue to an applied distortion by medical imaging [34]. Compression and tension tests are performed ex vivo.

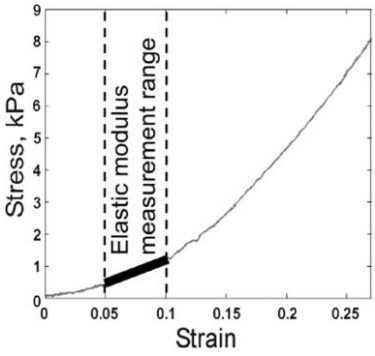

Figure 10 Elastic modulus measurement of a non-linear elastic material, retrieved from [32]

2.4.2. OTHER ASPECTS

As described above, the liver can be described as non-linear elastic. However, soft tissues like the liver exhibit both elastic (time independent) as viscous behaviour (time dependent) and are therefore denoted as viscoelastic. Viscoelastic materials are time and history dependent exhibiting different behaviour under different test conditions. Other features of viscoelastic materials are hysteresis (energy dissipation during loading and unloading), creep (increase in strain during constant stress), stress relaxation (decreasing stress during constant strain) and strain rate dependency (Figure 11) [35] [36].

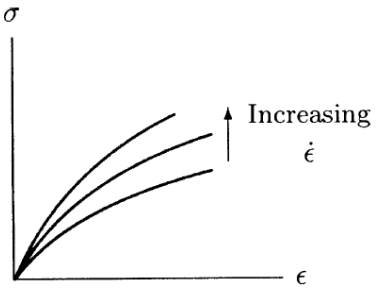

Figure 11 Strain rate dependent viscoelastic behaviour, retrieved from [35]

In addition to the properties described above, the liver is anisotropic (its characteristics depend on the direction in which they are measured) and also non-homogenous (its characteristics depend on the place in which they are measured) [36].

2.4.3 CONCLUSION

In this study, the elastic modulus of liver tissue is determined by comparing Young's moduli of liver tissue documented in literature for low strains. The Young's modulus for liver is tissue is defined as approximately 5 kPa based on comparison of several sources. The articles that have been used as reference, combined with the applied measuring method and reported Young's moduli can be found in Table 13 in appendix A. The influence of viscoelasticity, non-homogeneity, and anisotropy on the reported Young's moduli in literature is not taken into account in this work, to allow for better comparison between studies.

2.5 IMAGING CHARACTERISTICS LIVER

Needle interventions are often guided by ultrasound, MRI or CT imaging. Ultrasound is most commonly used to guide interventions, due to its many advantages. The possibilities for real time monitoring, its high safety, portability, expediency and relatively low costs make ultrasound a very attractive modality [37]. Ultrasound is used for diagnostic purposes as well as interventional procedures, both percutaneous as intra operatively. The latter is referred to as intraoperative ultrasound (IOUS). In IOUS the transducer is placed directly on the organ by which high resolution images can be obtained [38].

In the following section concepts of ultrasound and corresponding characteristics of the liver will be presented.

2.5.1 ULTRASOUND IMAGING

Ultrasound means high frequency sound, above the audible range for humans. With ultrasound imaging an image is created by constructing the reflection of high frequency sound waves.

The reflection of ultrasound waves that is used for image reconstruction is dependent on the acoustic impedance of a material. Acoustic impedance is the resistance of a material to ultrasound waves. At boundaries between adjacent materials, some of the ultrasound waves are reflected and some are transmitted. The difference in acoustic impedance of two adjacent tissues, determines the amount of reflection [39]. In bodily tissues, both air (low acoustic impedance) and bone (high acoustic impedance) produce a strong reflection of ultrasound waves, because their acoustic impedance is considerably different from the tissues that surround them. A high amount of reflection results in brightness on the ultrasound image, or high echogenicity. An-echogenic structures appear black on ultrasound, as none of the ultrasound waves are reflected.

Reflection can either be specular (one-directional), or diffuse. Diffuse reflection is also referred to as scattering and occurs when the waves encounter irregular shaped objects, as can be seen in Figure 12 [39]. In soft tissues the amount of scattering is relatively small compared to specular reflection at organ boundaries, however, both specular reflection and scattering are important for image formation in soft tissues. The grainy appearance of soft tissue is also referred to as speckle [40].

When ultrasound waves travel through tissue, there will be a loss of wave amplitude with increasing depth of penetration. This loss of energy is called attenuation and is, among others, due to absorption, reflection and scattering. In soft tissues, 80% of the attenuation is caused by absorption and results in heat production. The higher the frequencies used, the more the ultrasound waves will be attenuated leading to a loss of penetration depth. To describe the attenuation in a tissue, the attenuation coefficient is used, the relation of attenuation to distance expressed in decibels per unit length at a certain frequency.

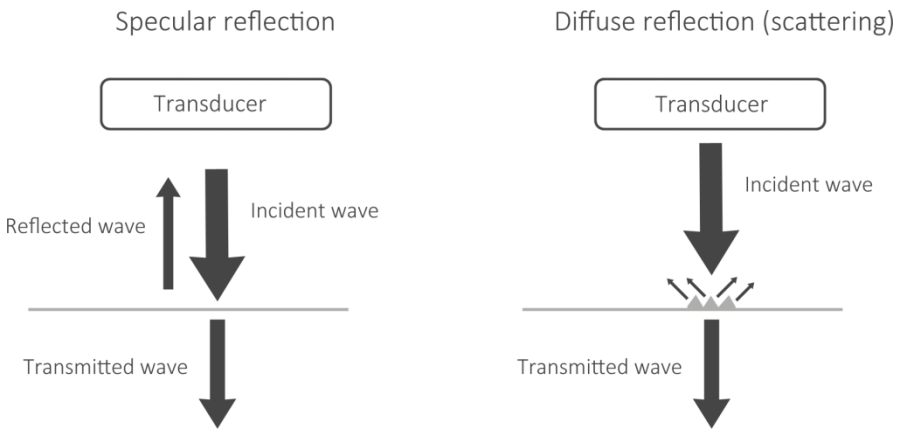

Figure 12 Specular versus diffuse reflection, retrieved from www.vaultrasound.com (adjusted).

In conclusion, important characteristics with respect to ultrasound imaging are acoustic impedance and attenuation coefficient. These aspects are used to select TMM materials that are suitable for ultrasound imaging.

As acoustic impedance is the product of the density of a material and the speed of sound through the material, we will compare liver TMMS with liver tissue based on both characteristics. Speed of sound in liver tissue is reported to be 1540 ms^{-1} and its density 1060 kg m^{-3} [15]. Attenuation in soft tissues increases approximately linear with frequency and is defined (by comparing several sources) to vary between 0.4 and 0.7 dB cm^{-1} MHz^{-1} [41].

2.5.2 LIVER VISUALIZED BY ULTRASOUND

A healthy liver has a homogenous and echogenic texture with a fine mottled pattern. Several anechoic structures are visible that represent vessels, ducts and arteries. Healthy livers have a smooth surface, while cirrhotic livers are identifiable by their nodular surface. Below several images of healthy tissue (Figure 13) and diseased liver tissue (Figure 14 and Figure 15) are shown.

HEALTHY LIVERS

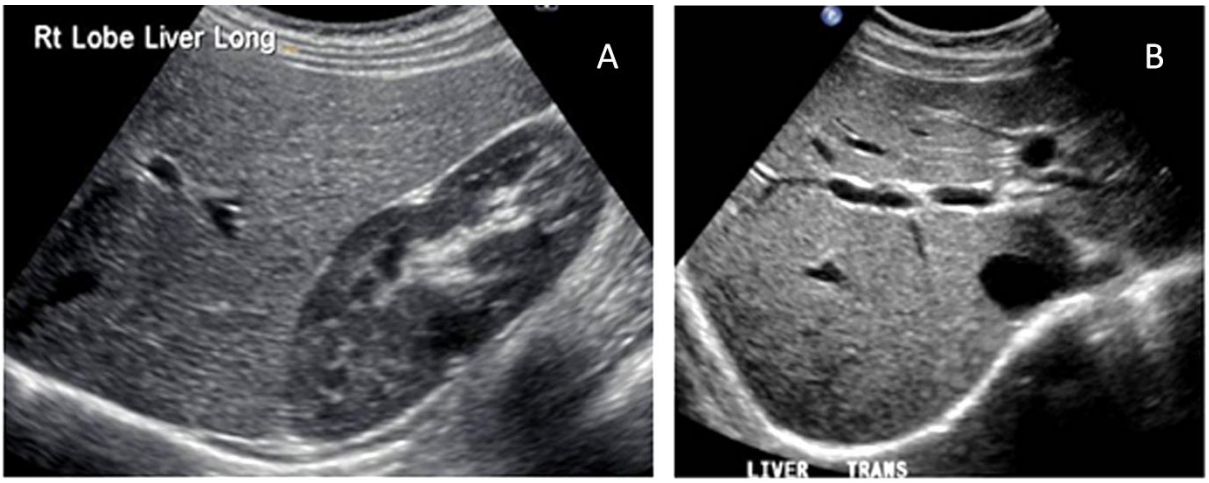

Figure 13 A: Right lobe of healthy liver (and kidney) B: Right lobe of liver (with portal vein), retrieved from www.ultrasoundpaedia.com

The hyperechoic edge (Figure 13 A and B) respresents the posterior border of the liver.

DISEASED LIVERS

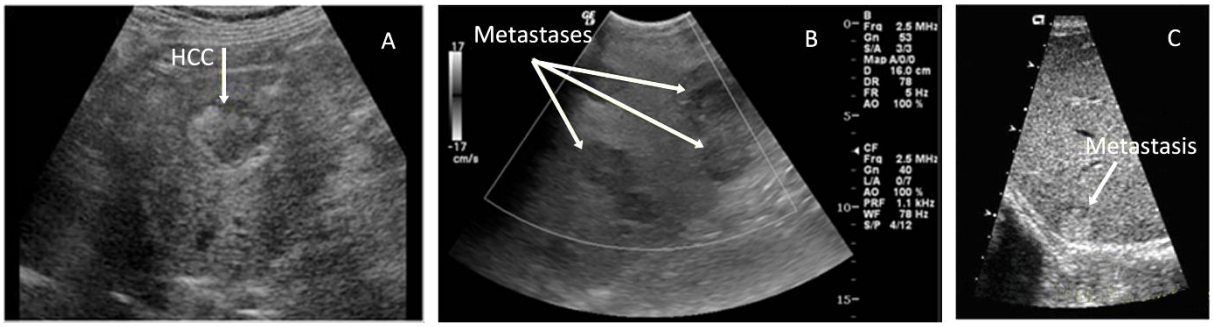

Figure 14 A: Liver with HCC, B: Liver with hypo-echoic metastases, C: Liver with a hyper-echoic metastasis, retrieved from www.ferrantiphoto.com

The appearance of hepatocellular carcinoma (HCC) varies. They can be hypo-echoic (darker) or hyper-echoic (lighter). Also the appearance of liver metastases can vary. They can be hypo-echoic or hyper-echoic but typically show a hypo-echogenic margin as can be seen in Figure 14 B and C.

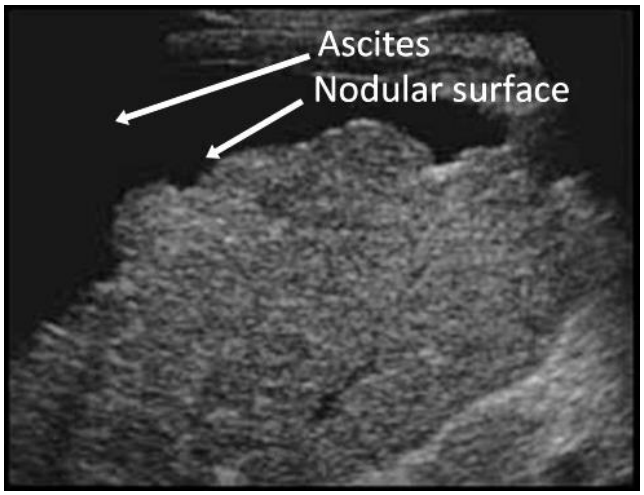

Figure 15 Cirrhotic liver, retrieved from www.ferrantiphoto.com

Cirrhosis is diagnosed by its nodular surface, depicted in Figure 15. In this image also ascites (fluid accumulation in the abdominal cavity) is evident as a fluid is present between the abdominal wall and the liver.

3. LIVER MIMICKING MATERIALS

Most tissue mimicking materials that are described in literature are based on the use of polymers. Polymers are macromolecules consisting of connected monomers. They display a wide range of varieties, properties and applications.

In 3.1 the major aspects of polymers is briefly explained, together with a categorized overview of the reviewed polymers. It will be demonstrated that, considering their mechanical and imaging characteristics, four materials seem promising to be used as liver tissue mimicking material. In section 3.2 to 3.5 an elaboration on the properties of these materials and associated variables can be found.

3.1 OVERVIEW OF PHANTOM MATERIALS

Liver tissue is often mimicked by the use of polymers. Polymers can either be from biological origin, or synthesized from monomers by polymerization reactions. Their structure can be linear, branched or cross-linked [42], see Figure 16.

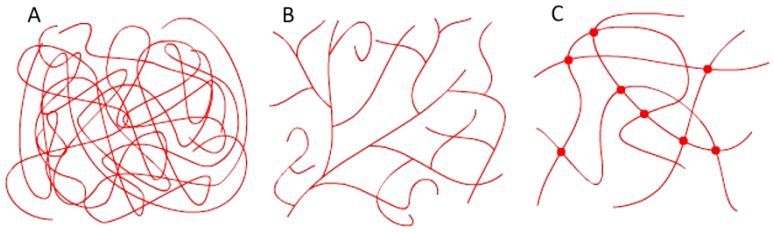

Figure 16 A: Linear polymer, B: Branched polymer, C: Cross-linked polymer, retrieved from www.design-and-technology-education.com

Crosslinking can be achieved chemically (by addition of a crosslinking agent) or by physical interaction between the molecules. The amount of crosslinking has a significant influence on the material properties. The more crosslinking, the lower the elasticity will be [43]. Crosslinked polymers often show increased strength compared to linear polymers. An important concept regarding polymers is the degree of polymerization. The degree of polymerization indicates the number of linked monomers. In general, a higher degree of polymerization will lead to an increase in mechanical strength.

Polymers can be the main component of a tissue mimicking material, or act as mesh-work in which a fluid can be held. When this fluid is water, the material is referred to as a hydrogel. An increase in crosslinking will lead to a decrease in the water holding capacity [44].

A subdivision of polymers used as tissue mimicking material can be seen in Figure 17.

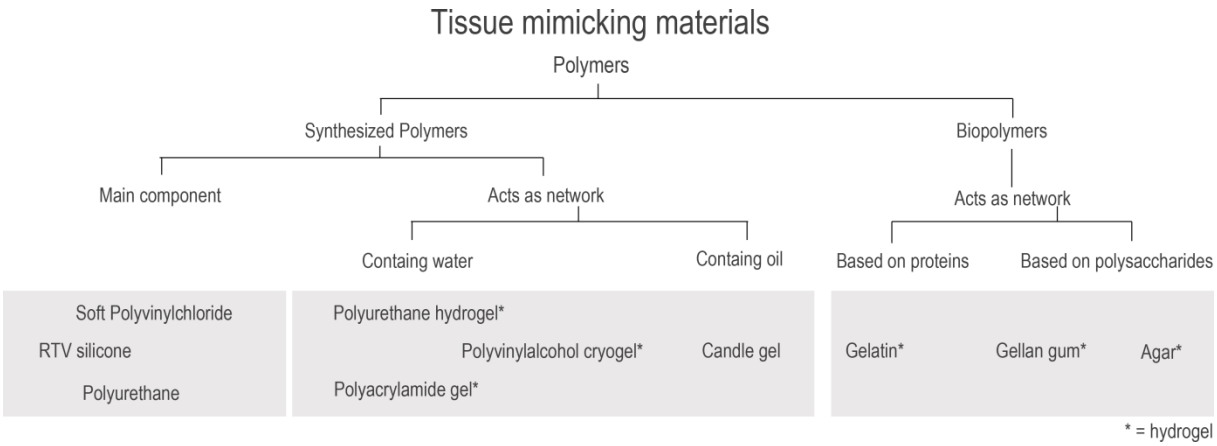

Figure 17 Polymers used as tissue mimicking material

In a previously conducted literature study laying some groundwork for this thesis, all materials in the coloured boxes in Figure 17 have been compared to the characteristics of liver tissue.

Gellan gum, polyvinylalcohol cryo-gel (PVA), soft polyvinylchloride (PVC), and candle gel were described in literature as having promising properties for mimicking liver tissue and were therefore selected for inclusion in this study, see Table 1. Their properties regarding elastic modulus, density, speed of sound, attenuation coefficient and shelf life (by which they were selected for further investigation in the current study) that are reported in literature can be found in Table 14, 15, 16 and 17 in appendix A.

Materials included in the current study
Material
Gellan gum
Polyvinyl alcohol (PVA)
Soft Polyvinyl chloride (PVC)
Candle gel

Table 1 Materials included in the current study

Some of the materials covered did not seem to be suitable as tissue mimicking material for image-guided needle interventions and were therefore not included in the current study. Materials excluded from further investigation, together with the reason for exclusion, are listed in Table 2.

Materials excluded from further investigation		
Source	**Material**	**Reason for exclusion**
Based on literature	RTV silicone	Speed of sound too low
	Polyurethane hydrogel	Production principle not described in literature
	Polyacrylamide gel	Expensive, toxic production process
	Gelatin	Fast degradation
	Agar	Fast degradation
Based on requested samples	Polyurethane	Density too high

Table 2 Materials excluded from further investigation

An elaboration on the selected materials will be provided in the following sections.

3.2 GELLAN GUM

Gellan gum is a hydrogel obtained dissolving gellan (the powder) in water. Gellan is a polysaccharide with a high gelling efficiency (a measure for the degree in which it gels a fluid to which it is added) [45]. The material was discovered in 1978, and is nowadays used as food additive, in pharmaceuticals, for cell culture and tissue engineering [46].

3.2.1. PRODUCTION

Gellan gum is produced by fermentation of carbohydrates by the bacterium Pseudomonas elodea [47]. The repeating unit of the native polymer contains two acyl groups (functional group containing a double bonded oxygen atom), namely an acetyl and glyceryl group. Due to the presence of acyl groups, the native form of the polymer is called high acyl gellan gum. By exposing gellan gum to high temperatures under certain conditions, the acyl groups can be removed, resulting in deacylated or low acyl gellan gum. During this process both acyl groups are hydrolysed (cleaved by addition of water) [48]. The molecular structures of both types of gellan gum can be seen in Figure 18.

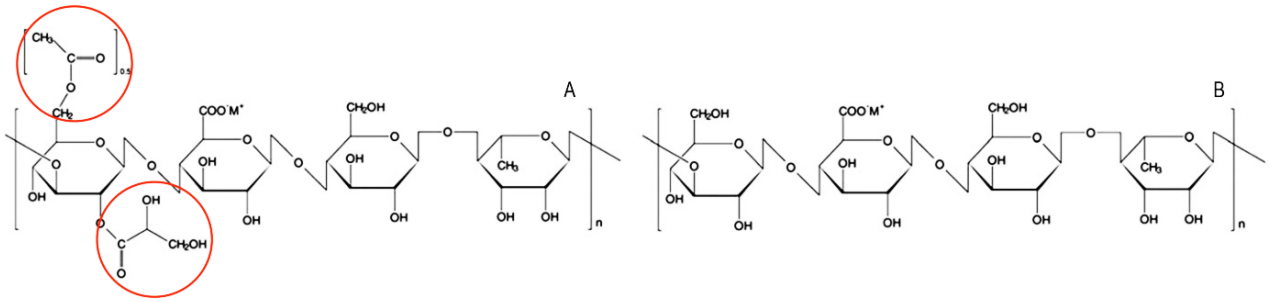

Figure 18 A: High acyl (acyl groups encircled in red) , B: Low acyl, retrieved from [49]

3.2.2. GELATION PRINCIPLE

Figure 19 Gelation principle gellan gum. A: Random coils, B: Double helix formation, C: Junction zone assembly, retrieved from [50]

Like in gelatine, the gelation principle of gellan gum is based on helix formation. In a heated solution, the molecules have a disordered structure consisting of single random coils (Figure 19.A). Upon cooling, these coils form double helices resulting in a certain ordered structure (Figure 19.B). Subsequently, the double helices aggregate into bundles that act as junction zones (Figure 19.C). The junction zones are linked together by untwined polysaccharide chains at the ends of the helices [46]. Cations (positive ions) play an important role in the gelation process of gellan gum. Both monovalent cation (ion with valence of one, that can form one chemical bond) and divalent cations (ion with valence of two, that can form two chemical bonds) promote gel formation in gellan gum. Divalent cations act as direct bridges between the double helices and are most effective in facilitating gel formation. The double helix aggregation principle promoted in absence or presence of cations can be seen in Figure 20. In spite of the presence of acyl groups in high acyl gellan gum, its helical

structure is similar to the helical structure of low acyl gellan gel. However, in low acyl gellan gum the binding sites for cations are more suitable for helix aggregation than the binding sites in high acyl gellan gum [49]. This difference in helix agglomeration could be an explanation for the difference between properties of high versus low acyl gellan gum.

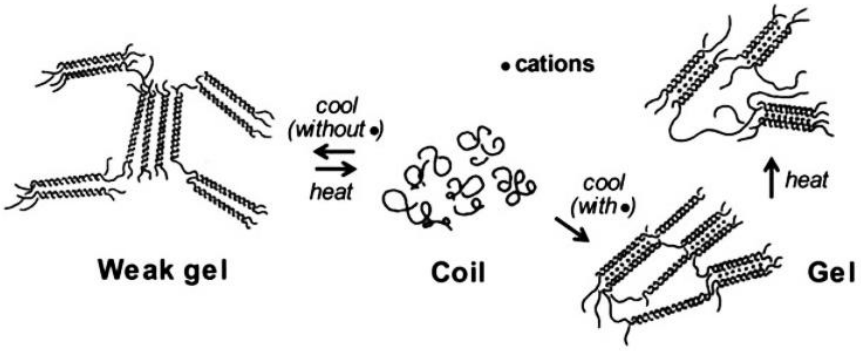

Figure 20 Gelation of gellan gum with and without the presence of cation, retrieved from [49].

With high acyl gellan gum soft and elastic gels can be produced, while the use of low acyl gellan gum results in more firm and brittle gels. By combining both forms, gels with intermediate properties can be obtained [51]. In most studies high acyl gellan gum is used to mimic soft tissues.

3.2.3. PRODUCTION CHOICES GELLAN GUM

In the present study, while the assumption is made that tap water that will be used to produce gellan gels, contains enough cations to promote gelation, the influence of two variables will be investigated:

- The concentration of gellan gum powder in water
- The ratio of high versus low acyl gellan gum

From a pilot study it was concluded that high concentrations of gellan gum were needed to obtain friction forces comparable to friction forces measured in liver tissue. Although the maximum dissolvable concentration described in literature is 5%, it turned out to be hard to dissolve gellan powder in higher concentrations than even 1%. When using a magnetic stirring plate, the upper side of the solution already cooled resulting in gelation. The thickness of the solution did not allow an uniform temperature and therefore no homogenous solution could be obtained. To accomplish an uniformly heated solution, the samples will be prepared by use of a microwave. A more thorough explanation about the method of preparation and material specifications is presented in section 5.1.

3.3 PVA

Polyvinyl alcohol is a synthetic polymer with many applications in the textile and pharmaceutical industry. Since the properties of PVA are controllable over the range of human tissue properties, the material is often used for the production of various phantoms [32]. Furthermore, PVA is biocompatible and can therefore be applied in soft contact lenses and as tissue substituent in cartilage defects [52]. In addition to its attractive mechanical properties, PVA has suitable properties as TMM for ultrasound and magnetic resonance [53].

3.3.1. PRODUCTION

Contrary to what the name suggests, PVA is not produced by polymerization of vinyl alcohol. This is due to the fact that the monomer vinyl alcohol does not exist in a stable form [54]. Hence, polyvinylalcohol is obtained by polymerization of vinyl acetate (PVAc), see Figure 21.A. After polymerization, PVAc is subjected to a hydrolysis

reaction resulting in polyvinylalcohol (PVA), Figure 21.B. PVAc is difficult to fully hydrolyse, and therefore PVAc monomer units remain to some extent present in the polymer, Figure 22.

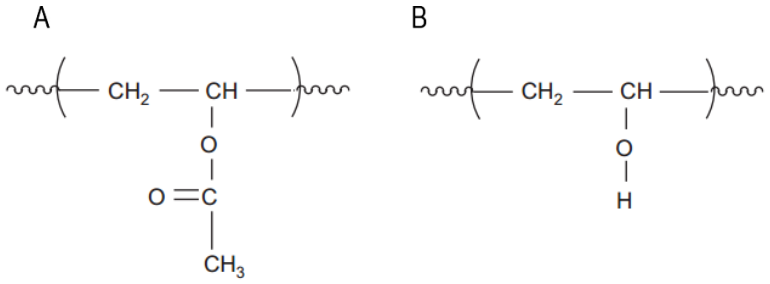

Figure 21 A: Poly(vinyl acetate) (PVAc), B: Poly(vinyl alcohol) (PVA), retrieved from [55]

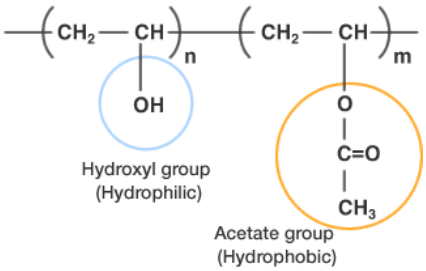

Figure 22 Partially hydrolysed PVA (n = number of hydroxyl groups, m = number of acetate groups)

The degree of polymerization (DP) is the number of linked monomers, including both vinyl acetate and vinyl alcohol monomer units, Equation 2.

$$\text{Degree of Polymerization} = n + m$$

Equation 2 (n = number of hydroxyl groups, m = number of acetate groups)

The amount of hydrolysis is the part of vinyl alcohol monomers to the total number of monomers. Since every monomer has one residual group this can be seen as the number of hydroxyl groups to the total number of residual groups (hydroxyl and acetate groups). With n the number of vinyl alcohol monomers and m the number of vinyl acetate monomers, the degree of hydrolysis can be determined by Equation 3.

$$\text{Degree of Hydrolysis} = \frac{n}{n+m} * 100$$

Equation 3 (n = number of hydroxyl groups, m = number of acetate groups)

The higher the degree of hydrolysis, the more hydroxyl groups are present in the polymer. One would expect that a higher number of these hydrophilic groups would increase the polymers solubility, however, this is not entirely correct. In PVA with high degree of hydrolysis, the absence of bulky acetate groups allows the hydroxyl groups to come close together, resulting in strong hydrogen bonds between the OH groups. Since too many hydrophobic acetate groups will make the polymer too hydrophobic to dissolve in water, there is an optimum of the amount of hydrolysis concerning solubility in water at room temperature [56]. At higher temperatures, all types of PVA can be dissolved in water, as can be seen in Figure 23.

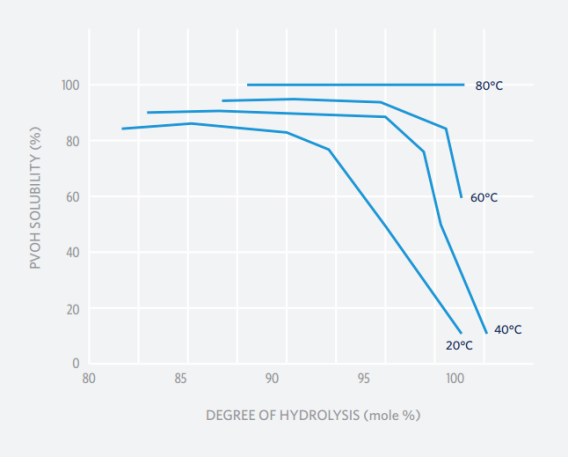

Figure 23 Solubility of PVA in water, retrieved from www.sekisuichemical.com

3.3.2. GELATION PRINCIPLE

PVA can be crosslinked in several ways. The chains can be connected both chemically through addition of crosslinking agents, or physically by physical interactions within the material. While chemical crosslinking results in permanent bonds, physical crosslinking results in thermo-reversible gels. Physical crosslinks can be formed by microcrystalline aggregates, entangled chains, ionic interactions between charged atoms, and hydrogen bonds [57].

Mixing PVA with the commonly used chemical crosslinker sodium tetraborate, or borax, results in a highly viscous gel. PVA crosslinked with borax is referred to as slime, and is sold in many toy stores for children.

One method of physical crosslinking of PVA is by subjecting the material (in solution) to cycles of freezing and thawing. When the solution freezes, the solvent forms poly crystals that compress the PVA chains. As a result, hydrogen bonding occurs between the OH groups of the polymer. By formation of hydrogen bonds, a crystalline structure is obtained [58]. Upon thawing, the crystalline regions stay present and act as physical crosslinks (Figure 24). The number of freeze thaw cycles affects the number of crystalline regions that is formed, therewith influencing the material properties [59]. A higher degree of crosslinking will result in a stiffer material. In addition to the number of FT cycles, the properties of PVA cryo-gel are influenced by many other aspects such as polymer concentration in the solution, thawing rate and, to a lower extent, freezing time [57].

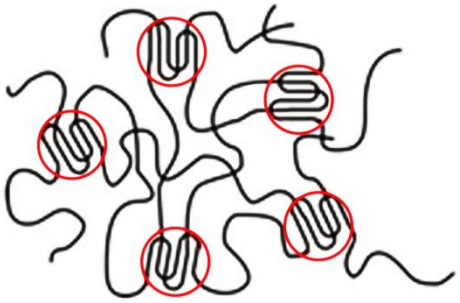

Figure 24 PVA network with crystalline regions acting as physical crosslinks, retrieved from www.tvt.kit.edu

As explained before, PVA with a higher level of hydrolysis contains less acetate groups. Since the pendent acetate groups prevent the chains from folding up closely, high level hydrolysis PVA is used when crystallite formation is desired. Additionally, since shorter chains (lower degree of polymerization) fold up more easily than longer chains, PVA with a low DP is favoured over PVA with high DP when crystallinity is wanted [60]. However, one should keep in mind that a lower degree of polymerization also results in lower (tensile) strength.

By crosslinking PVA, a porous structure is obtained. During every FT cycle larger pores with stronger pore walls are obtained, as can be seen in the images in Figure 25 presented in a study by Zhang [61]. We note that in this study the samples were subjected to directional freezing, by which an organised structure was obtained. Our samples will be frozen in the refrigerator and will therefore have a more random pore orientation.

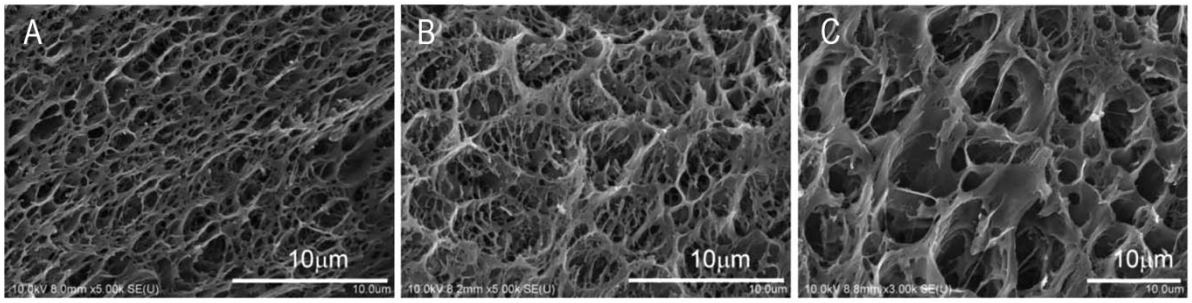

Figure 25 PVA structure (obtained by directional freezing) A: PVA 10% 1FT B: PVA 10% 3FT C: PVA 10% 5FT, retrieved from [61]

3.3.3.PRODUCTION CHOICES PVA

In the experiments described in chapter 5, two properties of PVA are investigated: influence of the number of FT cycles and the influence of concentration. To clearly show the effect of freeze thaw cycles, a type of PVA is selected with a high potential for crystallization. As explained above, bulky acetate side groups hinder crystallization, therefore a high degree hydrolysis PVA (99%+) is used in the experiments. Considering that long chains impede crystallite formation, a type of PVA with average molecular weight has been selected, i.e. average chain length. Based on literature on development of phantoms as well as literature about the selected PVA type, 4% and 7% w/w concentrations are chosen to be investigated. To obtain a first indication of the material properties influenced by these variables, samples with the two concentrations were subjected to 1, 2 and 3 freeze thaw cycles. An extensive description of the production process can be found in section 5.1.

3.4 PVC

One of the most common thermoplastic materials employed today is polyvinylchloride (PVC). PVC has a wide range of applications, ranging from footwear to sewage pipes and kitchen floors.

3.4.1. PRODUCTION

The monomer vinyl chloride is made by a reaction between chlorine and ethylene. Subsequently, PVC can be obtained by polymerization of the monomer vinyl chloride.

PVC is a thermoplastic, so softens when heated and hardens when cooled. This process is reversible and can be repeated many times. PVC has primarily an amorphous structure and therefore the material has no specific melting point. However, around 170-180 °C, PVC undergoes significant changes.

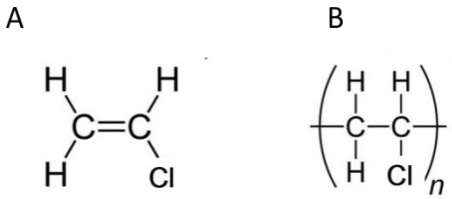

Figure 26 A: monomer vinyl chloride, B: repeating monomer unit of polyvinyl chloride

The structure of PVC can be seen in Figure 26. The properties of the material are influenced by its average molecular weight and molecular weight distribution. These features are determined by the amount of polymerization.

3.4.2. PLASTICIZERS

PVC is originally a rigid and hard material, but can be produced in more soft and flexible forms by the addition of plasticizers. The combination of PVC with a plasticizer is designated as PVC-P (PVC-plastisized). Dry blend compounds without any plasticizer are also called PVC-U (PVC-unplastisized). Plasticizers are often based on organic substances with a high boiling temperature, such as phthalates, adipates and phospates. 95% of the used plasticizers are phthalate esters [62]. Most plasticizers are toxic to some extent.

PVC/plasticizer mixtures are referred to as plastisol, available in several ratios. The higher the amount of plasticizer in a plastisol, the softer gels are obtained. When a PVC/plasticizer mixture is heated, the PVC particles adsorb the plasticizer. This first stage is called gelation. After adsorption (plasticizer molecules solvating the PVC resin surface), absorption occurs with PVC particles swelling. When the mixture is further heated (above 150 °C), the PVC particles and plasticizer melt together resulting in a homogeneous material.

This stage is designated as fusion stage. All steps are visualized in Figure 27. Upon cooling, the polymer chains partially crystallize. The plasticizer molecules and PVC molecules are connected via intermolecular van der Waals forces and hydrogen bonds. Since the plasticizer is not bound chemically (intra molecular) to the PVC molecules, most plasticizers are able to migrate towards the surface. From there they can evaporate into the atmosphere, dependent on the temperature of the environment. Another reason for plasticizer migration is contact with another polymer compatible with the plasticizer. This phenomenon can result in damage to surface coating or materials, and is therefore an important aspect to consider [63].

Different theories are developed about the mechanism in which plasticizers change the properties of PVC. A common belief is that after fusion of plasticizer and PVC, more space is created between the PVC chains, causing them to move more freely. Plasticizers are thought to break the bonds between the PVC molecules and prevent reformation of the chains [63].

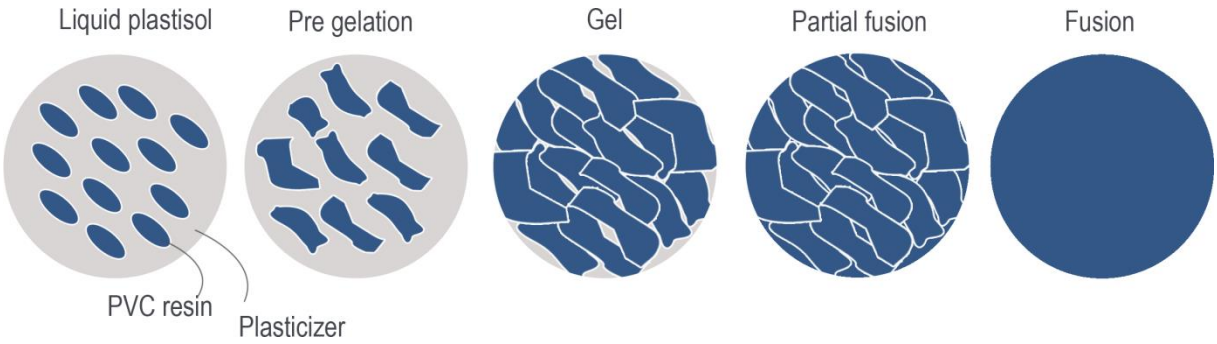

Figure 27 Working principle PVC, retrieved from www.richardgreaves.com (adjusted)

3.4.4. PRODUCTION CHOICES PVC

The current study will investigate the influence of the quantity of plasticizer that is added to the PVC. As was the case for gellan gum, during a pilot study was concluded that homogenous heating is difficult using a hotplate magnetic stirrer. Therefore the samples were prepared with the use of a microwave. A more thorough description of the production process will be provided in section 5.1.

3.5 CANDLE GEL

Candle gel is a transparent gel wax that is used in fancy candles. The material consists of 5% polymer resin and 95% mineral oil [64]. Several types of polymers can be used to manufacture candle gel. Candle gel can be purchased as ready-made material, or produced by mixing mineral oil with a polymer resin. Candle gel is available in different viscosity grades, dependent on the amount of polymer that is added. Oudry et al. [65] used different mixtures of white mineral oil with a copolymer (polymer consisting of blocks of different monomers). The higher the concentration of copolymer, the stiffer the produced phantom. Also the speed of sound and attenuation increase with an increase in copolymer concentration [65].

Candle gel is used to produce phantoms suitable for several imaging modalities such as MRI, CT and ultrasound [66]. Candle gel is a thermo-reversible material and can be reused easily. Upon heating, the material liquefies and can subsequently be reshaped.

3.6 DISCUSSION

In the previous sections the basic material properties and production principles of the 4 selected TMM are described. The variables that are assumed to be most relevant for the selection of an appropriate liver TMM and best controllable within the scope of this study are summarized in Table 3. Choices regarding the production of the samples were made based on literature and a few pilot studies conducted in the current work.

Variables of the selected materials			
Material	**Variables that will be studied**	**Sample design choices**	**Influential variables not taken into account (a.o.)**
PVA	# Freeze thaw cycles	1,2,3 FT cycles	Thawing rate
	Concentration	4%, 7%	Freezing time
			Degree of Polymerization
			Amount of Hydrolysis
			Type of solvent
Gellan gum	Concentration	1%, 2%	Ions in solution
	Ratio HA/LA	100/0, 75/25, 50/50	Degree of Polymerization
PVC	Ratio plastisol/plasticizer	100/0, 80/20, 60/40	Degree of Polymerization
Candle gel	-	100%	Degree of Polymerization
			Concentration of oil

Table 3 Variables of the selected materials

There are a few aspects regarding the selection process of the materials to be included in further experimental research that warrant specific mentioning:

- The materials have been selected based on their resemblance to liver tissue regarding elastic behaviour in the region of small strains (as already alluded to in section 2.4 since in this domain the livers behaviour is linear elastic). However, the behaviour of the selected TMMs could be very different from liver tissue at larger strains domains.
- Materials are selected based on elasticity properties and not on insertion and retraction forces. Although the concepts of forces in needle insertions and retractions and elasticity of tissues are in literature reported to be related, this relationship is not made explicit. A material that is comparable to the liver regarding elasticity properties, does therefore not necessarily cause the same forces in reaction to needle insertions as liver tissue.
- As described in the previous sections, the material properties are influenced by many variables. Some of these variables need to be kept constant although they are not easily controllable. This could influence the results on the material behaviour regarding the studied variables.

The influence of the selected variables on the insertion and retraction forces in the 4 TMMs will be investigated. The performance of these materials regarding both mechanical and imaging characteristics will subsequently be compared with liver tissue. This will be extensively described in chapters 4 to 7.

4. CHARACTERIZATION OF LIVER TISSUE IN NEEDLE INTERVENTIONS

In this chapter the characteristics of the liver in response to needle insertions will be investigated, to be able to define desired phantom material characteristics. This will be done by analysis of force-position diagrams recorded during needle interventions in liver tissue. The data used for analysis of the liver characteristics are not acquired in this study, but taken from a study conducted by T. de Jong [12]. Based on her data, requirements for the TMMs will be defined. For proper comparison between forces in liver tissue and TMMs, it is essential that data about the TMMs will be collected using the same method. Therefore in the next section (4.1), a description of the data acquisition method applied in the study by de Jong is provided, followed by the methods that will be used to analyse the raw data in this work. Two phases of the needle intervention process are distinguished: the insertion phase and the retraction phase. The results regarding the liver behaviour during these phases is presented in section 4.2 and 4.3 respectively. In section 4.4 the discussion and conclusion are presented.

4.1 METHODS

The work presented in this chapter is fully based on raw data collected in a previous study by de Jong. This means that for this study, data collection methods were prescribed since they obviously had to be identical for targeted (liver) and TMM data collection.

The data analysis of data representing the retraction phase was similar to the one used by the Jong. For the insertion phase, methods were developed in this study in order to define more realistic TMM requirements. These methods were based on the work of D. van Gerwen [67].

Since data on human livers was only limited available for this study, it was supplemented with data on animal livers. The livers used in this study were considered healthy tissues, since no evidence for pathologies was found during preparation of the samples according to de Jong [12].

4.1.1 DATA ACQUISITION

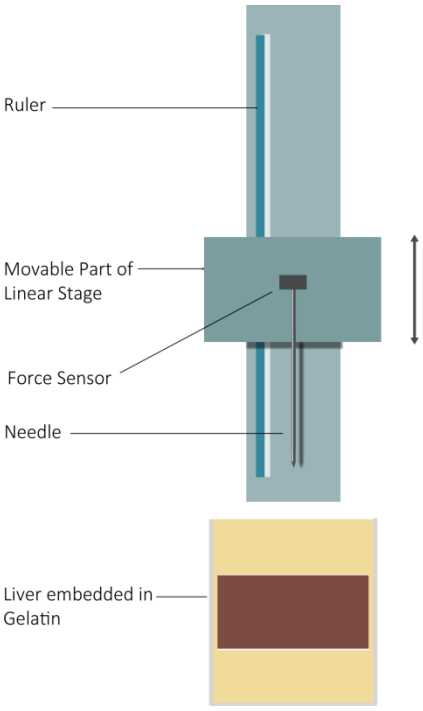

Figure 28 Experimental setup that was used to gather liver data

In the work carried out by the Jong, forces were measured during needle insertion and retraction. An 18 gauge trocar needle was attached to an Aerotech PRO115-400 linear motion stage (Aerotech Inco, Pittsburgh, USA) and inserted in the liver in vertical direction. The needles that were used were Disposable Two-Part Trocar Needles (Cook Medical, Bloomington, USA), of which only the inner component of the needle was inserted. Forces were measured with an ATI nano17 six-axis force/torque sensor (ATI Industrial Automation, Apex, USA). Four animal (1 sheep, 3 bovine) and two human livers were each subjected to 20 interventions. The livers were embedded in gelatine, to mimic the natural environment of the liver. Two needles were used for all liver specimens. Before the record was initiated, the needle was moved inside the upper gelatin layer, with the tip approximately 10 mm above the embedded liver (inside the upper gelatin layer). Subsequently the samples were punctured with a speed of 5 mm/s moving through the liver specimen into the lower gelatine layer. Before retraction was initiated, the needle was maintained in its maximal position for 50 to 60 seconds. During the measurements, data on forces, position and time were recorded.

The experimental setup is depicted in Figure 28. A full description of this experimental setup can be found in the study by de Jong [12].

4.1.2 ANALYSIS OF LIVER DATA

Data was analysed using Matlab 2012b (The MathWorks, Inc., Natick, Massachusetts, United States). A moving average filter (filter window 40) was applied to the data to eliminate noise.

The forces measured were plotted against their corresponding position to analyse the force patterns during needle insertion and retraction, see Figure 29. The forces in gelatin are not of interest in this study, therefore for every specimen the analysis is performed on the part of the trajectory where at least the tip of the needle was inside the liver, visualized by the darker part on the curve in Figure 29 (denoted as regions of interest). The retraction and insertion phase were analysed using different methods, as is described in the following sections.

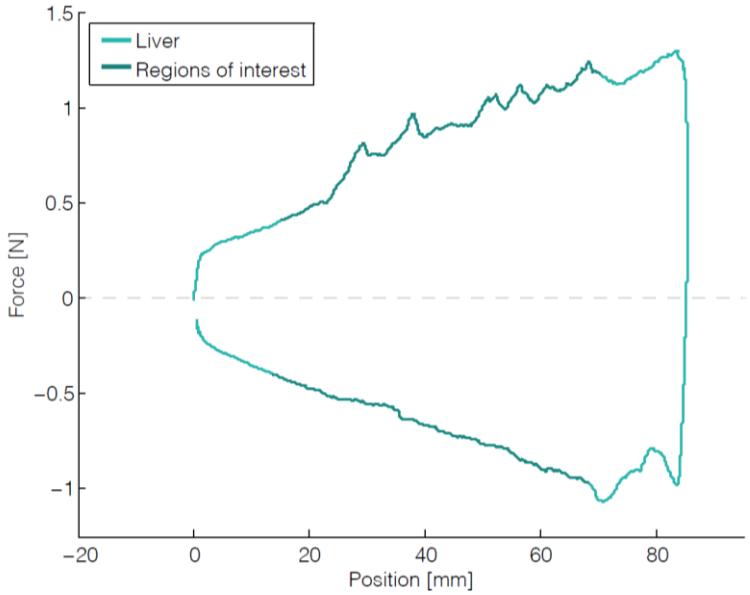

Figure 29 A force-position curve of the liver

Compressive forces acting on the needle are taken as positive, with the part of the curve above the horizontal axis representing the insertion forces. Tensile forces are taken as negative, with the part of the curve below the horizontal axis representing the retraction phase.

4.2 RETRACTION FORCES IN LIVER TISSUE

As described in section 2.3, during retraction all measured forces are due to friction between tissue and needle shaft. Forces are maximal at the beginning of the retraction phase, short after movement has been initiated at the needles maximum position. Forces measured during needle retraction decrease almost linearly, due to decreasing contact with the needle.

4.2.1 METHODS TO ANALYSE RETRACTION FORCES IN LIVER TISSUE

The part of the retraction phase that accounts for the liver is analysed to determine the amount of friction during the retraction phase. This part of the curve is visualized in dark green in Figure 30. For every retraction curve, a linear least squares approximation was determined for the force-position diagram (dashed grey line in Figure 30). The slopes of the linear relation, or friction slopes, were visualized in a boxplot diagram. A more negative retraction slope indicates higher friction during retraction.

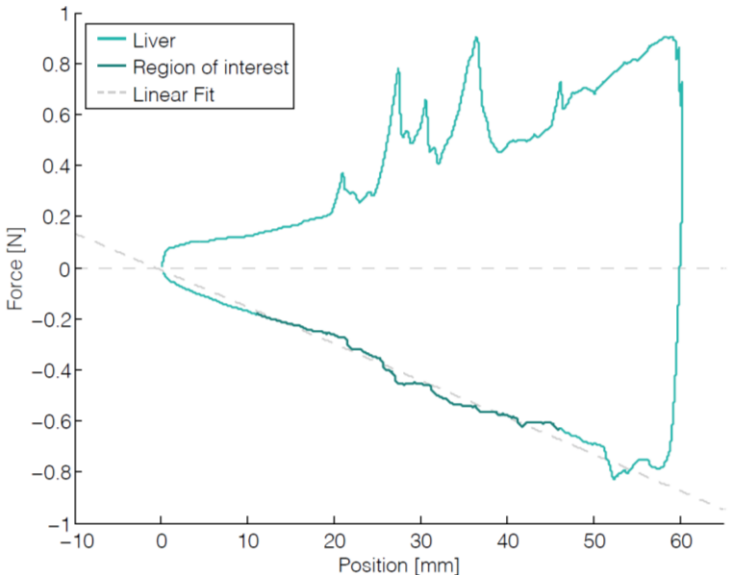

Figure 30 Linear least squares approximation for the friction slope in liver tissue

4.2.2 RESULTS – RETRACTION FORCES IN LIVER TISSUE

The force-position diagrams representing the 6 livers can be found in appendix B.

The retraction slopes of all livers are visualized in Figure 31.

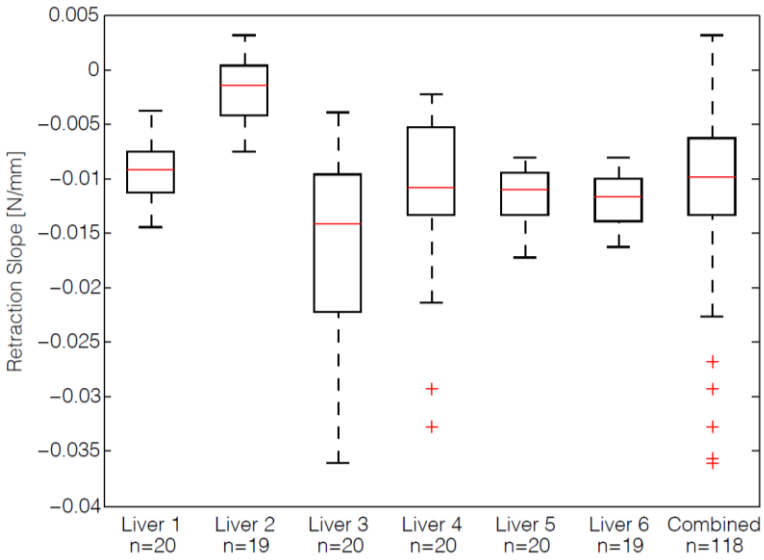

Figure 31 Retraction slopes of the 6 livers, and all data combined

The interquartile range of retraction slopes for all livers is: -0.006 to -0.013 Nmm^{-1}. The median of all retraction slopes is -0.010 Nmm^{-1}. This can be seen in the rightmost boxplot visualizing the retraction slope of all livers combined.

In liver 2 friction during retraction was considerably lower than in other livers (a median of -0.002 Nmm^{-1} compared to the median of all livers combined of -0.010 Nmm^{-1}). The forces in liver 2 almost remained unchanged during retraction and during some retractions forces even increased, as is indicated by the positive slope values. Liver 3 shows more variability between retraction slope values compared to the variability between other livers.

4.2.3 CONCLUSION RETRACTION FORCES IN LIVER TISSUE

From Figure 31 we can conclude that liver 1, 5 and 6 have comparable friction characteristics. The medians (-0.009, -0.011 and -0.012 Nmm^{-1}) as well as the variation of the values of these livers resemble, as can be concluded from the shapes of the boxplots. From the results presented in Figure 31, one could conclude that animal livers (livers 1 to 4) show more inter and intra specimen variation. However, the similarity between the human livers is probably coincidence as human tissues are very unique and known to cover a broad spectrum of characteristics.

Since the median retraction slope is not representative for all livers due to the wide variety of liver tissues, we will use the IQR of all specimens as a guideline for the TMMs. The suitability criterion that will be applied for a TMM (representing healthy liver tissue) is that their median friction slope must lie within the IQR of the retraction slopes of liver tissue, so between -0.006 Nmm^{-1} and -0.013 Nmm^{-1}.

4.3 INSERTION FORCES IN LIVER TISSUE

The forces measured during needle insertion in the liver do not increase linearly. Due to encounters with inner structures such as arteries and veins, many peaks are visible during the insertion phase. In section 2.3 is explained that forces during insertion are caused by friction along the shaft of the needle, and cutting and deformation forces at the tip of the needle. Assuming that friction during retraction is comparable to friction during insertion, one can subtract the approximated linear friction during retraction from the forces during insertion to obtain the approximate cutting forces. The method of approximating cutting forces by subtracting friction forces is applied in several studies [22] [68]. The contribution of constant cutting forces to the total insertion forces is very low compared to the contribution of friction, see Figure 32. In other words, except from the peaks due to presence of inner structures, the force that is exerted at the needle tip is low compared to the force that is caused by friction. The peaks, however, are an important phenomenon to investigate since they provide information about the inhomogeneity of the liver. Therefore in the following section we will examine the peak forces during insertion. As mentioned above, this analysis is based on work by D. van Gerwen [67].

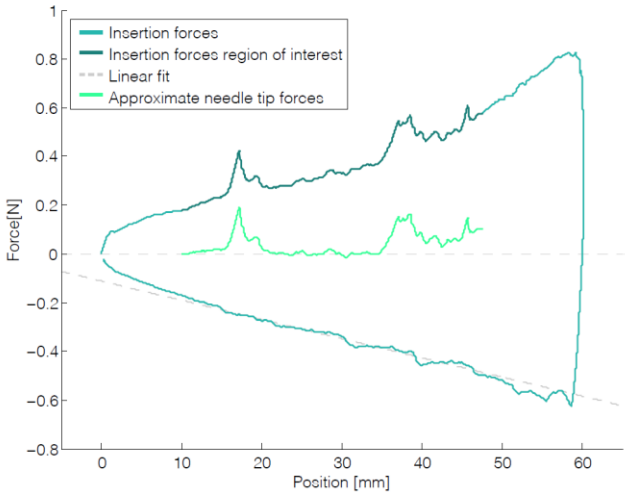

Figure 32: Approximated needle tip forces obtained by subtracting friction (during retraction) from insertion forces.

4.3.1 METHODS TO ANALYSE INSERTION FORCES IN LIVER TISSUE

As explained above, we consider the constant force exerted on the needle tip when cutting the homogenous parts of the liver, negligible. The aspects we are interested in, are the peak forces caused by encounters with inner structures inside the liver. These peak forces were analysed in terms of two measures: peak height and quantity. Peak height is expressed in Newtons, and peak quantity in number of peaks per decimetre (dm). To identify peak height and quantity, several steps were taken.

Firstly, the part of the curve that accounts for the liver was simplified using a loop version of the Douglas-Peucker Algorithm (DPA). This algorithm uses a convergence criterion that defines the maximum normal distance between the original and the simplified signal, as can be seen in Figure 33. This algorithm was applied to remove small peaks. A convergence criterion of 0.05 N was chosen for this analysis.

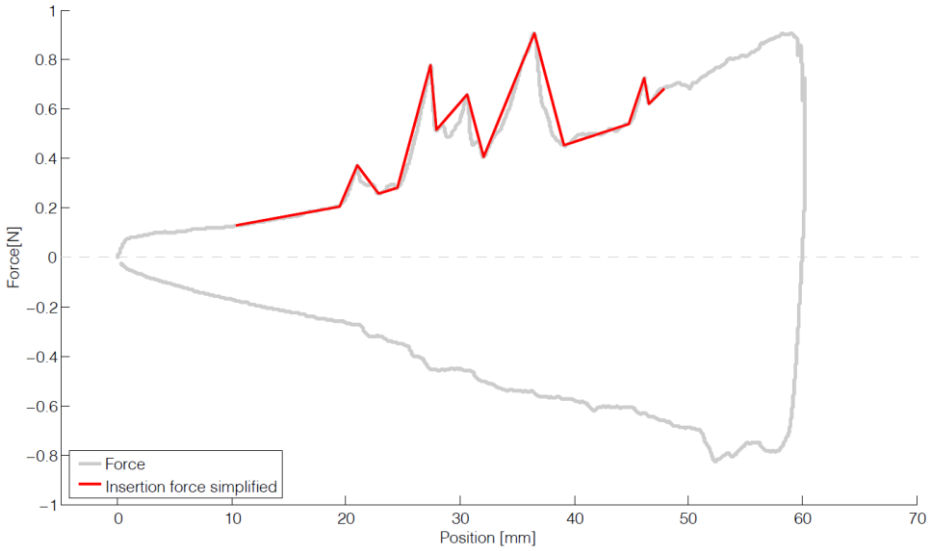

Figure 33 Insertion force simplification with DPA

Peak height was defined as the vertical distance between a peak and its preceding trough, depicted in Figure 34. Since the use of this definition will lead to peak height overestimation of peaks on steeper curves with respect to peaks present on more planar curves, the peaks were defined for the insertion forces while they were projected horizontally. These horizontally oriented insertion forces were obtained by computing the linear slope of the insertion phase by using a linear least-squares fit. Subsequently, the computed insertion slope was subtracted from the actual insertion forces.

Figure 34: Definition of peak height

During the last step, peak heights of the horizontally displayed signal were computed and presented in boxplots. This peak data analysis provides information about the force that is measured during encounters with inner structures. However, it does not give insight into the number of in-homogeneities that the needle comes up against. Therefore the number of peaks was determined as well. Since the number of peaks is dependent on the length of the penetration trajectory, we computed the number of peak forces per distance. The results were visualized in boxplots.

The steps described above are visualized in Figure 35.

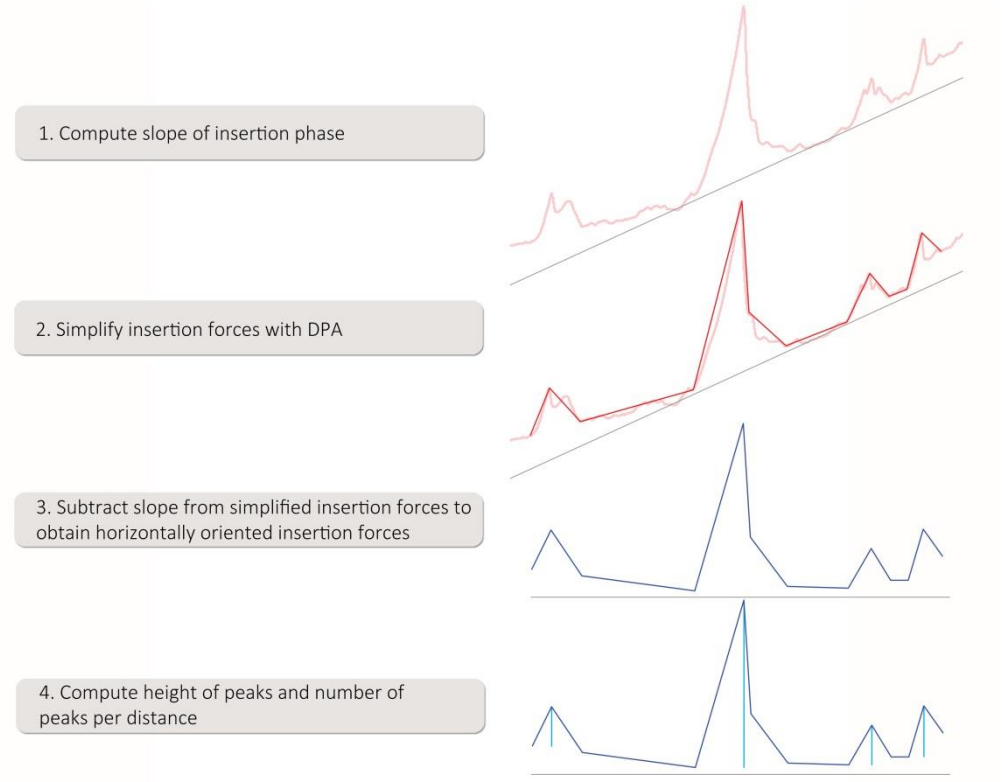

Figure 35 Analysis method of peak forces

4.3.2 RESULTS – INSERTION FORCES IN LIVER TISSUE

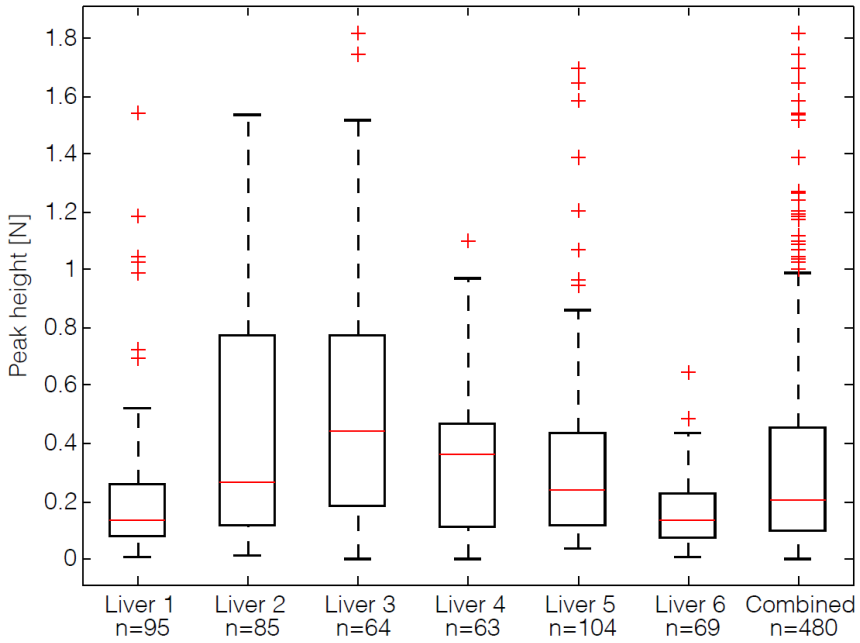

Figure 36 Peak forces in liver specimens

In Figure 36 peak height in liver specimens is presented. The median peak height from horizontally oriented insertion forces is 0.14 N, 0.27 N, 0.45 N, 0.36 N, 0.24 N and 0.14 N for liver 1 to 6 respectively. The peak height of all peaks together lie within an IQR of 0.10 N to 0.46 N with a median of 0.20 N.

The number of peaks per liver are 95, 85, 64, 63, 104, 69 peaks respectively. Note that for liver 2 and 6 only 19 insertions were included in the analysis instead of 20 insertions in other specimens. To exclude the influence of specimen thickness and number of insertions, the number of peaks is computed per distance, visualized in Figure 37.

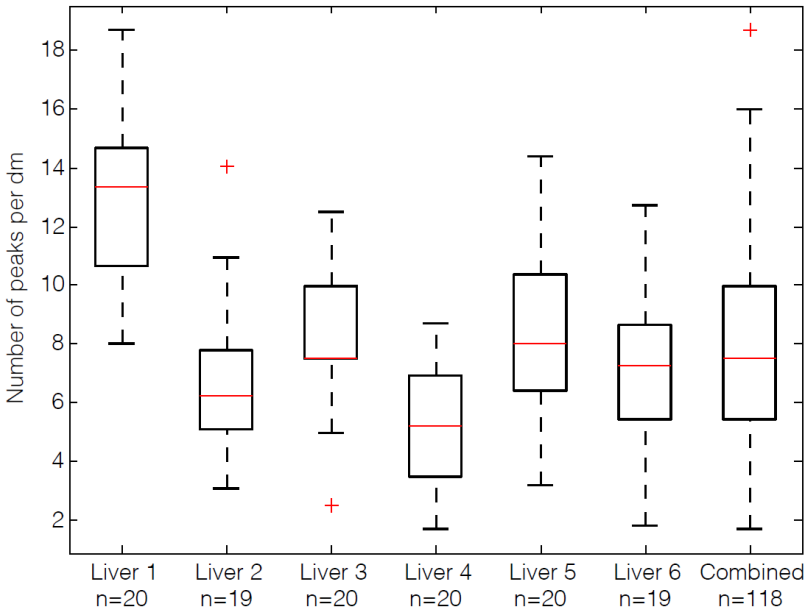

Figure 37 Number of peaks per decimetre in liver specimens

The median number of peaks per dm is 13.3, 6.2, 7.5, 5.2, 8.0 and 7.3 for liver 1 to 6 respectively, visualized in the first 6 boxplots from the left. Liver 1 shows a higher number of peaks per dm (median 13.3) compared to the median of all livers combined (7.5 peaks per dm). 50% from the peaks lie within an IQR of 5.5 peaks per dm to 10.0 peaks per dm, with a median of 7.5 peaks per dm as can be seen in the rightmost boxplot.

4.3.3 CONCLUSION INSERTION FORCES IN LIVER TISSUE

As mentioned before, we assume that friction during insertion is similar to friction during retraction. When we subtract the friction component (based on friction during retraction) from the forces during insertion, the forces exerted at the needle tip remain. Except for the peaks that are visible, we can conclude that these forces are considerably low and can therefore be neglected. The peaks forces however, cover a rather large part of the total force measured during insertion (concluding from the force-position diagrams) and were therefore investigated.

Based on peak height and the amount of peaks visible during needle insertion, we can conclude that the liver is in-homogenous, in accordance with literature. The nature of the encountered in-homogeneities in terms of the forces they exert on the needle, varies over a broad range with extremes up to 1.8 N (measured in liver 3). These are considerable forces, compared to the friction force which approximately reaches 1 N at the moment of maximal contact surface between liver and needle. However, the median peak height is significantly lower than these extreme peaks with a value of 0.20 N. The livers used in this experiment have a high variability, especially regarding the number of peaks. The inter specimen difference could be, amongst others, due to differences between species, individuals, or sample preservation and preparation. Furthermore, an important

factor to consider is the locus of insertion, which significantly influences the results. The dataset available does not take this into account.

The requirement regarding peak forces is that the number of peaks in the force position diagram of the TMM should lie within a range of 5.5 peaks per dm and 10.0 peaks per dm, with peak heights in the range of 0.10 N and 0.46 N. In addition, with exclusion of the peaks, the forces during insertion should be similar to forces during retraction.

4.4 DISCUSSION AND CONCLUSION

In this section the limitations of the above described procedures are described, followed by a conclusion about the TMM requirements.

4.4.1. LIMITATIONS

When drawing conclusion about the results presented in the previous sections, several aspects/limitations need to be considered.

In this study, liver interventions were performed in the liver at equally spaced distances throughout the whole organ. In reality, when performing needle interventions, clinicians will avoid puncturing major structures. Therefore, probably less inner structures will be punctured compared to the number of structures that were encountered in this study. This theory is also presented by Jiang [69], who showed the difference between safe and dangerous insertions in liver tissue.

Furthermore, the requirements for TMMs are based on forces measured during insertion at constant speed. A phantom material that responds in exactly the same way to needle insertions at constant speed does not necessarily provide the right tactile feedback to the clinician. Therefore, in the last phase of this study, evaluation with clinicians will provide insight into the suitability of the selection criteria described in this chapter.

Additionally, when comparing the results presented in this chapter to those that will be obtained by evaluating the forces in TMMs, the wear of the needle coating as well as diminishing of needle sharpness could be confounding. In the current study was concluded that diminishing of needle sharpness or needle coating did not influence the results significantly (discussed in appendix E), however we cannot guarantee that needle conditions in the experiment performed to obtain liver data (carried out by de Jong) were similar to needle conditions in the experiment by which TMM characteristics were defined (presented in the subsequent chapter).

We assume the constant cutting forces to be negligible, and chose to compare TMMs with liver tissue with respect to their retraction slopes, peak height and quantity. However, in a TMM it could be possible that the constant cutting force covers a significant portion of the insertion forces (and/or the friction during insertion is not similar to the friction during retraction). This topic will be revisited in chapter 5.

Lastly, an important issue in this analysis is the limited amount of data. 6 livers were subjected to needle interventions, 4 of which were not human tissues. Considering the large variability between individuals, the livers characteristics are not defined very accurately.

4.4.2. CONCLUSION - DEFINITION OF TMM REQUIREMENTS

Since friction is the major force component during the insertion phase and even the only force component during the retraction phase, it is important the TMM should cause a similar amount of friction during needle interventions. Therefore a minimal, must-have, mechanical requirement for the TMM is to cause friction

comparable to the liver. The amount of friction in TMMs will be measured by analysis of forces during retraction. The results of these measurements will be presented in the following chapter. This will be done by the same method that was applied to analyse the liver.

A subsequent step could be modification of materials with suitable friction characteristics to induce peak forces similar to the liver. This could be accomplished by addition of certain particles. This is however outside the scope of this thesis, since many new variables would be introduced that will probably also influence the amount of friction. However, when peak forces will be caused by a natural property of a TMM, they will be analysed using the methods presented in 4.4.1.

The defined requirements are summarized in Table 4.

Table 4 TMM requirements

Liver property	**TMM requirement**
Friction during retraction [N/mm]	Median retraction slope between -0.006 N/mm and -0.013 N/mm
Peak height [N]	Median peak height between 0.10 N and 0.46 N
Number of peaks/dm	Median number of peaks/dm between 5.5 peaks/dm and 10.0 peaks/dm

Table 4 TMM requirements

5. MECHANICAL CHARACTERIZATION OF TMMS - RETRACTION SLOPES

Phantom materials have been selected and forces in liver tissue are analysed. Based on this analysis, requirements for TMMs are defined. The subsequent step will be to investigate whether forces during needle retractions in TMMs lie within the defined range.

Phantom recipes described in literature, in combination with several for this thesis conducted pilot studies, are used to make several versions of the materials regarding composition and production process that match the properties of liver tissue. The production parameters are summarized in Table 4 in section 3.6. In the current chapter the mechanical characteristics of the tissue mimicking materials in response to needle retractions will be investigated. This chapter is organized as follows: In section 5.1 the materials will be described, together with the experimental setup and methods that will be used to analyse the resulting data. Subsequently, the results are presented in section 5.2. In section 5.3 the discussion and the conclusion about the suitability of the TMMs are presented. This conclusion is drawn from the results in section 5.2, based on the criterion regarding the retraction slope described in section 4.4.

5.1 METHODS

In this section, sample components, requisites and methods for preparation and assessment of the samples, together with the experimental setup will be discussed. Lastly, the method of analysis will be presented.

5.1.1. MATERIALS

6 gellan gum samples, 6 PVA samples, 3 PVC samples and 1 candle gel sample were prepared for evaluation of forces during needle interventions. The number of samples correlated with production variables per material. (for example in gellan gum 2 variables are investigated with each 3 variations = 6 samples). Samples were prepared in 250 ml glass beakers with a diameter of 6 cm. Since the PVA samples had to be subjected to FT cycles, the PVA solutions were poured into plastic beakers able to withstand expansion of their contents. Component specifications and quantities per sample are summarized in Table 5.

Gellan gum samples were prepared by adding the required amounts of high and low acyl gellan gum to the quantity of water specified in Table 5. After mixing thoroughly, the solution was heated in a microwave at 700 watt for 45 seconds. After stirring the solution it was heated for another 45 seconds at 700 Watt. The samples were allowed to cool at room temperature.

PVA samples were prepared using a hotplate magnetic stirrer (IKA RET Control-Visc S1 Digital Hot Plate Magnetic Stirrer, IKA labor technik, Germany). PVA particles were added to cold water that was stirred intensely. After all PVA particles were submerged, the solution was heated to 93 °C. This temperature was maintained for half an hour, after which the solution was poured into a plastic beaker and allowed to cool down to room temperature. During cooling, a skin was developed covering the solution. This skin was removed before the samples were subjected to FT cycles. A cycle consisted of 16 hours of freezing at -19 °C, followed by 8 hours thawing at room temperature.

PVC samples were prepared by the use of a microwave (700 Watt). Both components were mixed and heated for 1 minute. Then the solution was stirred and heated for an additional minute. This process was continued until the initially white solution turned transparent. After the last heating phase, the solution was stirred very gently allowing small air bubbles to rise to the surface. Subsequently, the solutions were allowed to cool down at room temperature.

Candle gel was purchased as ready-made material. The gel was weighed and heated using the hotplate of the magnetic stirrer. After the material was fully melted, it was gently stirred to avoid entrapment of air bubbles. The sample was allowed to cool down at room temperature.

Table 5 Component specifications and quantities per sample

TMM	**Sample components**	**Sample 1**	**Sample 2**	**Sample 3**	**Sample 4**	**Sample 5**	**Sample 6**
Gellan gum	High acyl gellan gum (Kelcogel LT100 - High Acyl Gellan Gum, Modernist Pantry, York, ME, USA)	2,5 g	1,875 g	1,25 g	5 g	3,75 g	2,5 g
	Low acyl gellan gum (Kelcogel F - Low Acyl Gellan Gum Modernist Pantry, York, ME, USA)	0 g	0,625 g	1,25 g	0 g	1,25 g	2,5 g
	Water	247,5 ml	247,5 ml	247,5 ml	245 ml	245 ml	245 ml
PVA	Super hydrolyzed PVA (Selvol PVOH 165, Sekisui Chemical Group, NJ, USA)	10,5 g*	10,5 g*	10,5 g*	18,4 g*	18,4 g*	18,4 g*
	Water	240 ml	240 ml	240 ml	232,5 ml	232,5 ml	232,5 ml
PVC	Plastisol (Plastileurre Soft, Bricoleurre, Mont Saint Aignan, France)	250 g	200 g	150 g	-	-	-
	Plasticizer (Assouplissant, Bricoleurre, Mont Saint Aignan, France)	0 g	50 g	100 g	-	-	-
Candle gel	Candle gel (Crystal kaarsen-gel, Aduis, Nijmegen, The Netherlands)	250 g	-	-	-	-	-

*Table 5 Component specifications and quantities per sample (*corrected for percentage of volatiles, see appendix C).*

5.1.2 EXPERIMENTAL SETUP

The needle was attached to the force sensor with the help of a connecting element. This connecting element, referred to as needle holder, was especially designed for this experiment and produced by additive manufacturing, see Figure 38. To measure the axial forces during needle interventions, an Aerotech PRO115-400 linear motion stage (Aerotech Inco, Pittsburgh, USA) was used in combination with Futek LSB force sensor with capacity of 200 lb (Futek, CA, USA) and parallel conductor with a stiffness of $1.45*10^{4}$ Nm^{-1}. The conductor was preloaded to conduct forces in the range of -4 to 4 V.

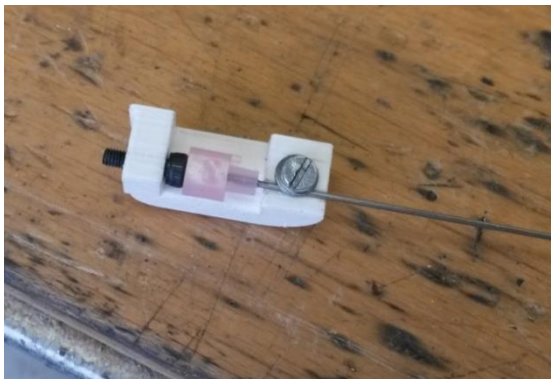

Figure 38 Additive manufactured needle holder

To exclude the effects of blunting of the needle tip and diminishing of needle coating, the samples were in randomized order subjected to needle insertions and subsequent retractions. In addition, the puncture locations were predefined to avoid repeated insertion at the same location. Every sample was subjected to 13 interventions consisting of 45 seconds insertion, 5 seconds waiting time, followed by 45 seconds retraction. Time duration, position of the needle and axial forces were recorded during the experiment. As the same settings needed to be applied as in the study performed by de Jong, needle speed was 5 mm/s and the inner part of a disposable two-part trocar needle was used (Cook Medical, Bloomington, USA). All experiments were conducted with the same needle. The experimental setup is depicted in Figure 39.

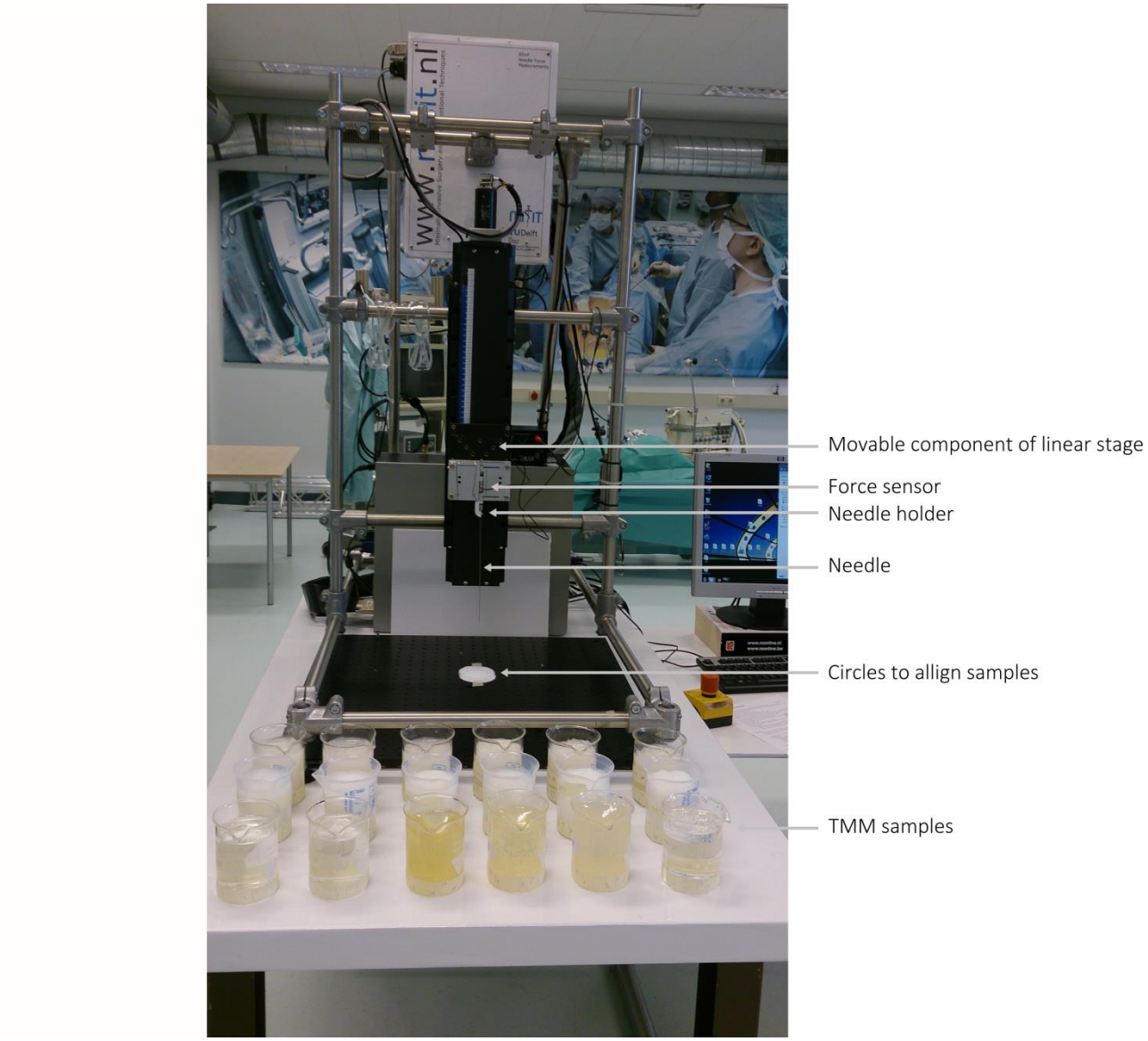

Figure 39 Experimental Setup

5.1.3 ANALYSIS

For all samples the retraction slopes were defined. The data was analysed using the same methods that were applied to analyse the liver described in section 4.3.1. A linear least squares approximation of the forces during retraction of the needle was made to determine the retraction slope in samples. In order to define the retraction slope accurately, the first and last part of the retraction phase were not included in the analysis. The remaining part of the retraction phase, referred to as the region of interest, is defined as 95% to 5% of the maximum retraction force, visualized for candle gel in Figure 40. After this maximum, the force starts to decrease approximately linearly.

The results were visualized in boxplots together with retraction slopes of all livers used in this study. A more negative retraction slope value indicates higher friction along the needle shaft during retraction.

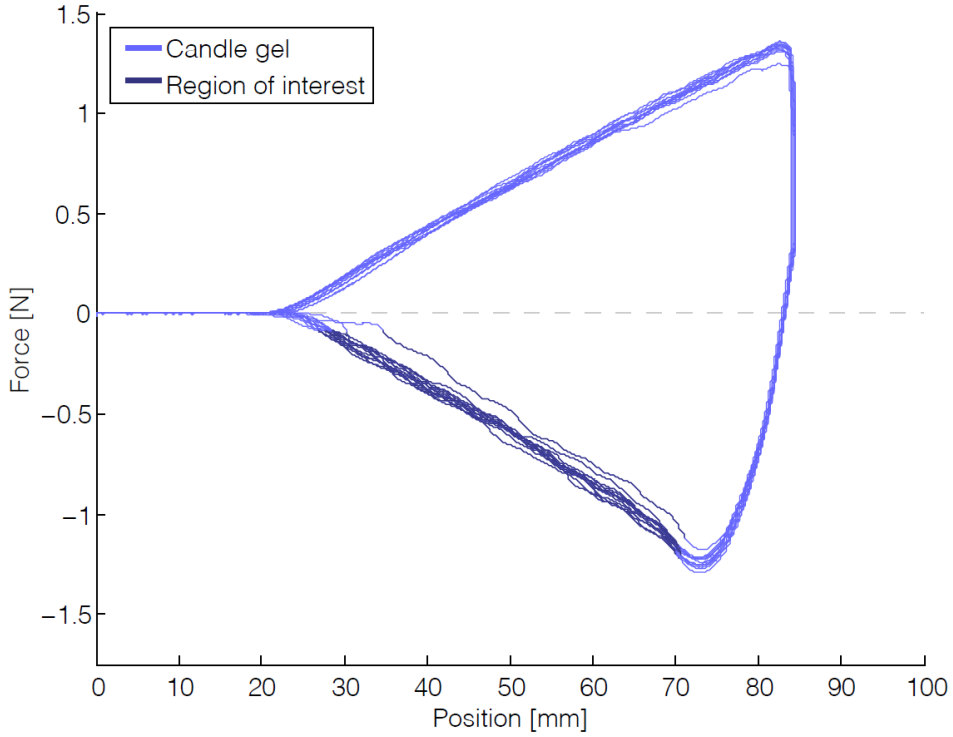

Figure 40 Region of interest visualized for candle gel

5.2 RESULTS – RETRACTION SLOPES IN TMMS

The force position diagrams of all materials, together with the average linear fit of all retractions can be found in appendix D. The slopes of the retraction forces are depicted in Figure 41 to Figure 45 for gellan gum, PVA, PVC and candle gel respectively.

Both insertion as retraction force position curves are of candle gel and PVC are straight. The forces in gellan gum are lower compared to other TMMs. In gellan gum and PVA, peak forces are present during insertion. For all materials the cutting forces (except for the peak forces in PVA) are negligible as forces during insertion are comparable to forces during retraction.

Median retraction slopes gellan gum						
Sample	**1% 100/0**	**1% 75/25**	**1% 50/50**	**2% 100/0**	**2% 75/25**	**2% 50/50**
Median retraction slope [N/mm]	$-1.4*10^{-3}$	$-7.2*10^{-4}$	$-5.5*10^{-4}$	$-3.3*10^{-3}$	$-2.2*10^{-3}$	$-1.4*10^{-3}$

Table 6 Median retraction slopes gellan gum (samples are described by the concentration of gellan gum, followed by the ratio of high acyl versus low acyl gellan gum)

Figure 41 shows the results of the gellan gum samples. The median retraction slopes can be found in Table 6.

Both concentration and ration of HA/LA influence the retraction slope. Retraction slopes are steeper in 2% gellan gum samples than in samples with a concentration of 1% gellan gum. Furthermore, the samples with 2% gellan gum show more variation in friction slope. Samples with high ratio HA/LA have more negative retraction slopes than samples with lower ratios of HA/LA.

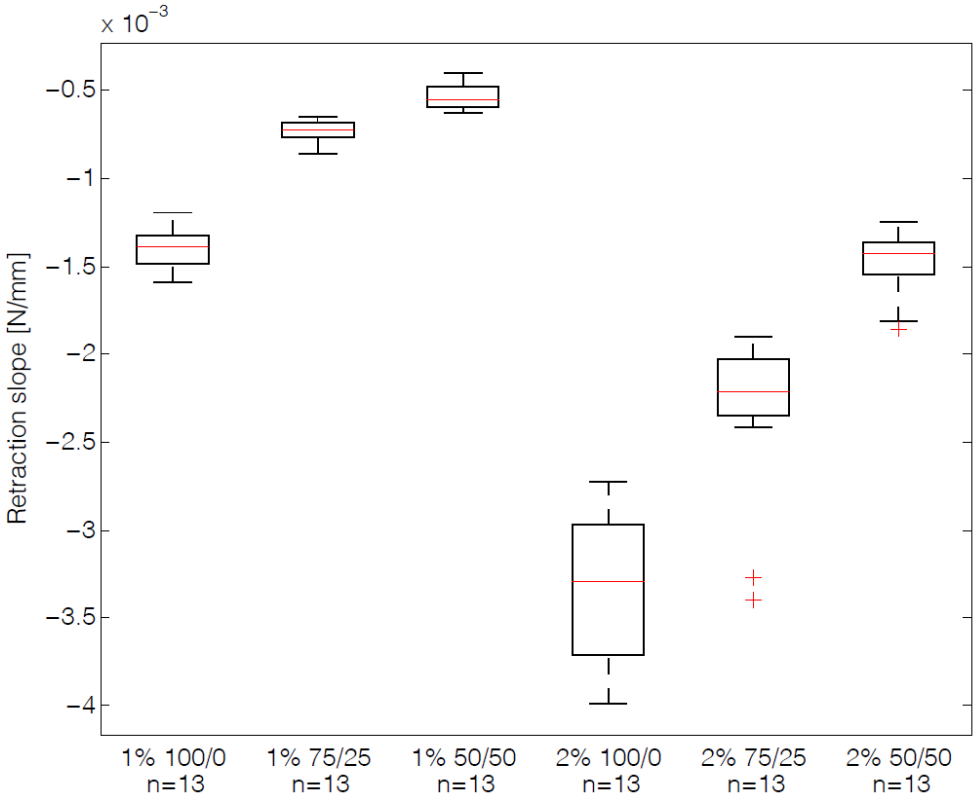

Figure 41 Retraction slopes in gellan gum

Figure 42 shows the same data as Figure 41, with addition of the retraction slopes in liver tissue. None of the retraction slope values of gellan gum lie within the IQR of the livers retraction slopes.

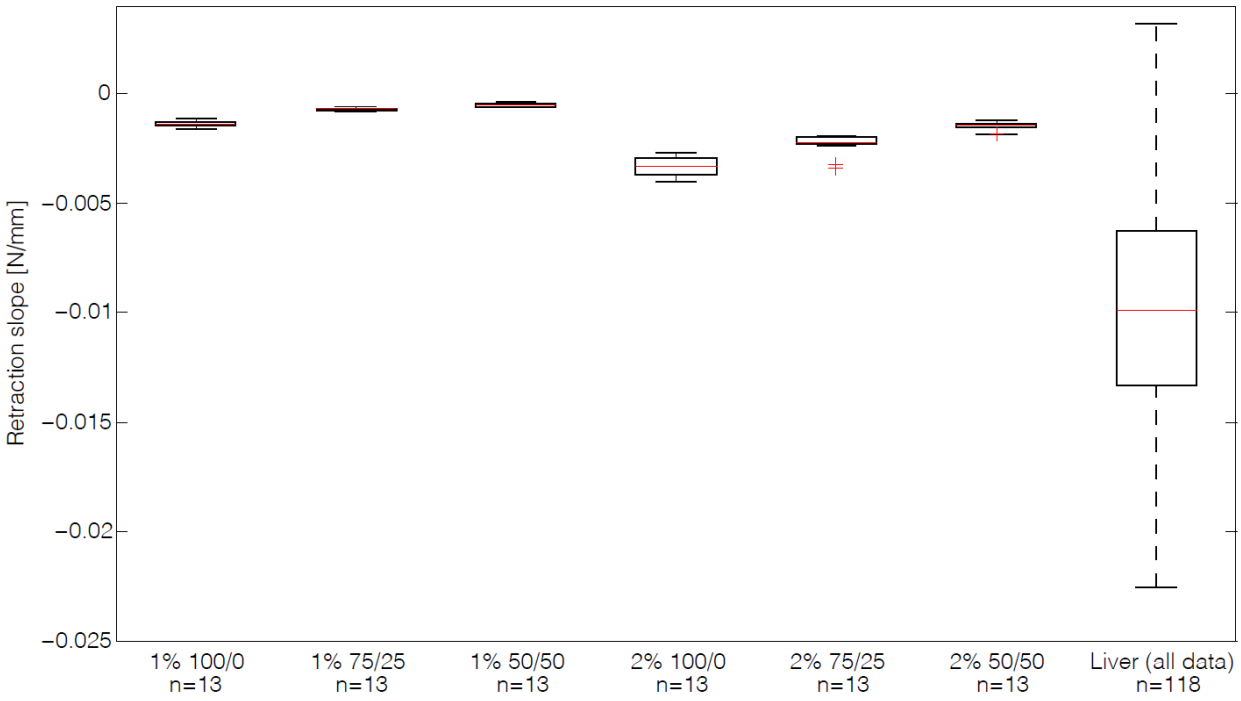

Figure 42 Retraction slopes gellan gum compared to retraction slopes in liver tissue

The retraction slopes of needle interventions in PVA are visualized in Figure 43. The median retraction slopes can be found in Table 7.

Median retraction slopes PVA						
Sample	**4% 1FT**	**4% 2FT**	**4% 3FT**	**7% 1FT**	**7% 2FT**	**7% 3FT**
Median retraction slope [N/mm]	-0.001	-0.011	-0.019	-0.003	-0.019	-0.043

Table 7 Median retraction slopes PVA (samples are described by concentration of PVA, followed by number of FT cycles)

Also in PVA the two examined variables influence the retraction slope. Samples with 7% concentration have steeper retraction slopes than samples with 4% concentration PVA. The number of FT cycles has an influence on the measured friction as well. The more cycles the material is subjected to, the more negative the retraction slopes are. The median of 4% PVA subjected to 2 FT cycles lies within the IQR of liver tissue.

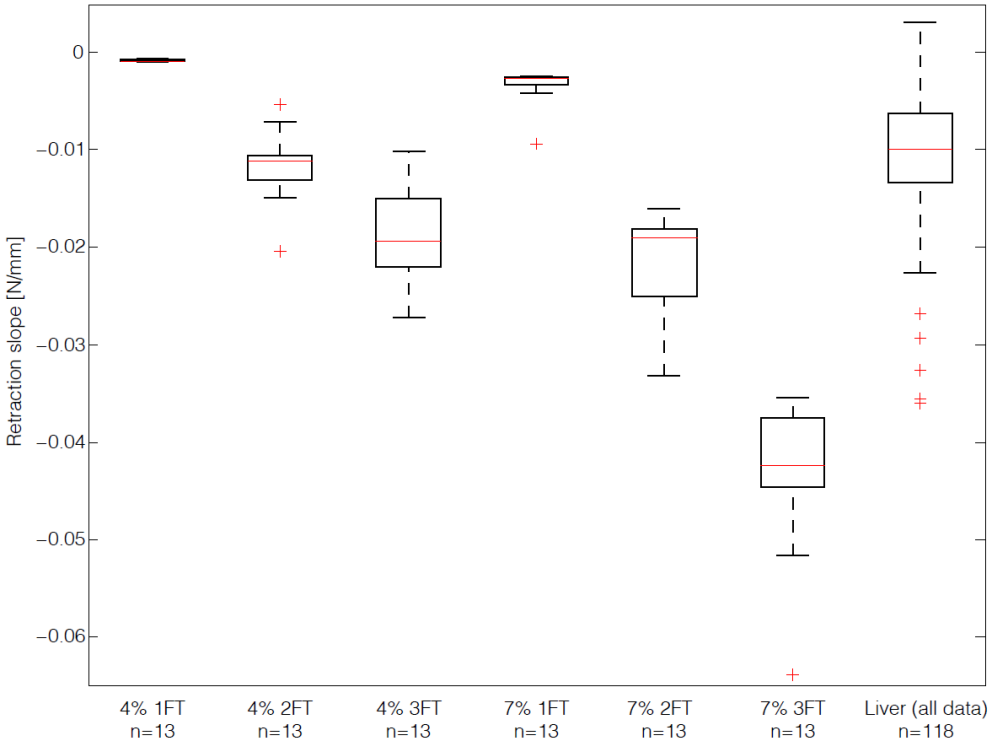

Figure 43 Retraction slopes PVA

Median retraction slopes PVC			
Sample	**100**	**80**	**60**
Median retraction slope [N/mm]	-0.085	-0.054	-0.020

Table 8 Median retraction slopes PVC (samples are described by the percentage of plastisol)

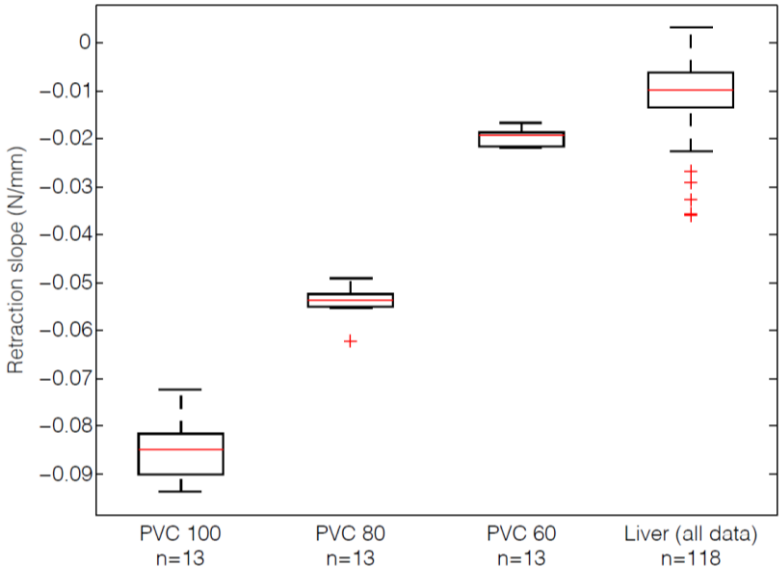

Figure 44 Retraction slopes PVC

The retraction slopes of the three PVC samples together with the retraction slopes of liver tissue are presented in Figure 44. The median retraction slope of the PVC samples can be found in Table 8.The addition of plasticizer results in less friction following a linear trend. None of the retraction slope values of PVC lies within the IQR of liver tissue.

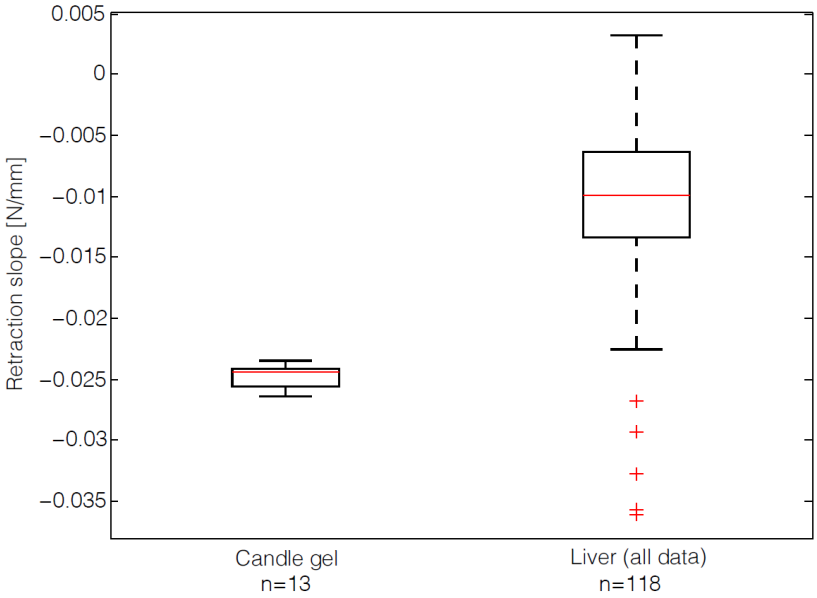

Figure 45 Retraction slopes candle gel

The retraction slopes determined for the forces in candle gel are presented in Figure 45. The median retraction slope of candle gel is -0.024 Nmm^{-1}. As was the case for gellan gum and PVC, none of the retraction slope values are within the IQR of liver tissue.

5.3 DISCUSSION

In this section the results are discussed, followed by a conclusion about what materials are suitable as liver TMM regarding their friction slope during retraction of the needle.

5.3.1 DISCUSSION OF THE RESULTS

The requirement that was defined for the TMM is a median retraction slope within the IQR of retraction slopes of liver tissue. The results presented in the previous section show that only PVA sample 2, with 4% PVA concentration, subjected to 2 FT cycles meets this requirement. However, in gellan gum and PVC, trends are observed that could lead to samples with suitable properties. In this section an interpretation of the results is provided.

GELLAN GUM

As can be seen in Figure 41, friction increases with increasing amount of gellan gum. In addition, the use of high acyl (HA) gellan gum causes more friction than low acyl (LA) gellan gum. This could be due to the fact that HA gellan gum is more elastic and more clingy than LA gellan gum, by which tissue adhesion is increased. As explained in 2.3, friction is, among others, influenced by tissue adhesion [22]. Tissue adhesion to the needle (visualized in Figure 46) will impede insertion, and cause more friction (during retraction the direction of deformation will be opposite but with the same effect).

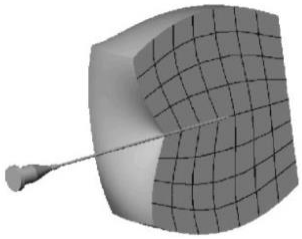

Figure 46 Tissue adhesion, retrieved from [6]

Theoretically, friction in gellan gum samples could be increased by increasing the concentration of gellan gum powder in samples consisting of 100% HA gellan gum. However in reality, a higher percentage gellan gum powder than 2% turned out to be difficult to dissolve. No homogeneous solution could be obtained for concentrations higher than 2%. Also the 2% gellan gum samples were not completely homogenous as can be concluded from the force peaks during the insertion phase induced by un-dissolved gellan gum powder (as can be seen in the force-position diagrams of gellan gum in appendix D).

Although gellan gum is often used to mimic soft tissues, not much has been reported about the suitability of gellan gum to mimic soft tissue regarding its friction properties during needle interventions. One study that focussed on modelling friction forces in soft tissues, gellan gum was found to be a suitable TMM. However, in this study a concentration of 6% gellan gum was used (HA/LA specifications were not reported) [70].

PVA

The amount of friction increases with increasing amount of FT cycles. The effect is more prominent for the samples with a concentration of 7% than for the samples with a concentration of 4%. Also concentration influences the amount of friction that is measured. When samples are subjected to a similar number of freeze thaw cycles, a higher concentration of PVA leads to more friction. Furthermore, PVA shows more intra sample variation than the other TMMs, especially in the samples that were subjected to 3 FT cycles. It seems that variation increases with the number of FT cycles. This could be due to the non-homogeneous nature of the material. As explained in section 3.3, the material properties are dependent on thawing rate. Since thawing rate will not be uniform throughout the sample, the material properties will not be consistent for all insertion locations. As can be seen in the force position diagrams of PVA in appendix D, a significant number of peaks is present during the insertion phase. Peak forces in PVA will be further discussed in chapter 6. For now the

conclusion on PVA is that the properties of PVA are adjustable within a broad range, both to mimic tissues that cause low friction and to mimic tissues that cause a higher amount of friction. Of the samples that were tested in this study, sample 2 (4% 2FT) meets the defined criterion. Probably other combinations between concentration and number of FT cycles will lead to samples that meet the requirement as well. This will not be further investigated in the current study.

The suitability of PVA to mimic soft tissues in needle interventions is often reported, but not with respect to its friction characteristics in needle interventions. Jiang et al [69] concluded that PVA phantoms showed resembling forces during needle interventions as those observed in porcine tissue. In their experiment 3% PVA was used, however, due to a very different setup than the one we applied (the main solvent that was used was not water, the number of FT cycles was not mentioned and needle speed was 1 mm/s) we cannot compare the results.

PVC

As described in the previous section, none of the PVC samples lie within the IQR of liver tissue. However, the linear trend observed in the PVC samples indicates that with an increased amount of plasticizer, a sample could be obtained with retraction slopes within the livers IQR. In a separate experiment, that was not included in initial setup of this study, it was demonstrated that by adding more plasticizer PVC can meet the retraction slope criterion. See appendix E.

According to Hungr [8], PVC does not feel biologically realistic due to the lack of lubricating fluid inside. In Hungrs study a prostate phantom is fabricated from PVC with different amounts of softeners bought from the same supplier as we did. The softest version that was used in Hungrs study was the 100% plastisol sample in our study (with the highest amount of friction of all PVC samples that we evaluated). Assuming that prostate tissue causes the a comparable amount of friction as liver tissue, this could be a reason for the unrealistic friction properties of described phantom.

CANDLE GEL

The friction in candle gel is too high compared to liver tissue. The properties of candle gel cannot be adjusted since there are no variables that can be varied (in the current study). Therefore candle gel is not suitable as liver TMM, with respect to our requirement.

5.3.2 LIMITATIONS

Specific variables of the TMM have been selected that were assumed to be most impactful and best controllable within this study. Based on these variables, conclusions were drawn regarding the suitability of the materials. However, when other variables would have been chosen, the results and conclusions could have been different.

Since gellan gum is widely used as phantom material in literature, it is surprising that in this study, even after extensive experimenting (among others by adding several amounts of potassium and sodium ions), suitable samples could not be obtained. The high acyl gellan gum samples remained very flabby and low acyl samples became friable with high mass fraction of gellan gum powder. It can only be speculated that our failure to replicate results as reported in literature is due to the production methods used in our lab. In most studies in which gellan gum phantoms are used, preservatives are added to preclude rapid deterioration, and these additives might lead to improved mechanical performance. This could be a subject for further investigation.

In the previous section was concluded that PVC could possibly be a suitable TMM when more plasticizer would be added to the plastisol. However, caution should be taken as some plasticizers are very toxic. Hungr et al. [8]

developed a prostate phantom made of PVC with plasticizer, both purchased from the same supplier as was done in this study. They stated that the used softener was diethyl hexyl adipate. Diethyl hexyl adipate is not found to be carcinogen in humans and is widely used as phthalate substitute as a plasticizer in PVC films employed as food wrapping material [71]. Although our supplier did inform us that his plasticizer is based on adipates, he did not want disclose information about the specific type of plasticizer and therefore the use of diethyl hexyl adipate cannot be confirmed with absolute certainty, and toxicity cannot be ruled out.

The properties of candle gel could not be varied as it was purchased as ready-made material. Since the available sample did not meet the specified criterion, candle gel is in this experiment discarded as suitable TMM.

5.3.3. CONCLUSION – MECHANICAL CHARACTERIZATION OF TMMS

We can conclude that PVA (4% 2FT) is a suitable phantom material with respect to the retraction slope requirement, while PVC can be adjusted to meet the requirement (concluded from the additional experiment presented in appendix E). Gellan gum and candle gel, as fabricated in the current study, are not suitable based on their mechanical properties.

As was mentioned above, in PVA peak forces are observed. Since PVA meets the retraction slope criterion, these peak forces are worthy of further investigation. In the subsequent chapter will be investigated whether the observed peaks are similar to those observed in liver tissue in terms of peak height and number of peaks.

6. PEAK FORCES IN PVA

In chapter 5 was concluded that PVA 4% 2FT met the mechanical friction requirements. Also another interesting aspect was observed, namely the presence of peak forces during the insertion phase. In this chapter the properties of PVA, regarding the height and number of peak forces, will be further analysed. To be able to determine the influence of concentration and freeze thaw cycles, all PVA samples will be studied. In section 6.1 the methods of analysis are described, followed by the results presented in section 6.2.

6.1 METHODS

For the investigation of peak forces in PVA, the data obtained in the experiment described in 5.2 will be analysed further. The analysis methods were comparable to those applied to analyse the liver (described in 4.2) but not completely identical. Since the PVA samples were, unlike the liver, not embedded in gelatin, the material was significantly deformed by the needle before the needle breached the surface of the samples. The resulting peak that is visible in the force-position diagram is not caused by in-homogeneities within the material, but by its elasticity. Therefore the first peak was not included in the peak analysis. Also the last peak was excluded from analysis, since this 'peak' often just represented the end of the insertion phase, as was the case for the liver, see Figure 47. Peak height was defined as the vertical distance between a peak and its preceding trough. The same convergence criterion (0.05N) was used as that was applied to analyse the liver. Peak heights and number of peaks per decimetre were visualized in boxplots and a representative force-position diagram for every sample is presented in 6.2.

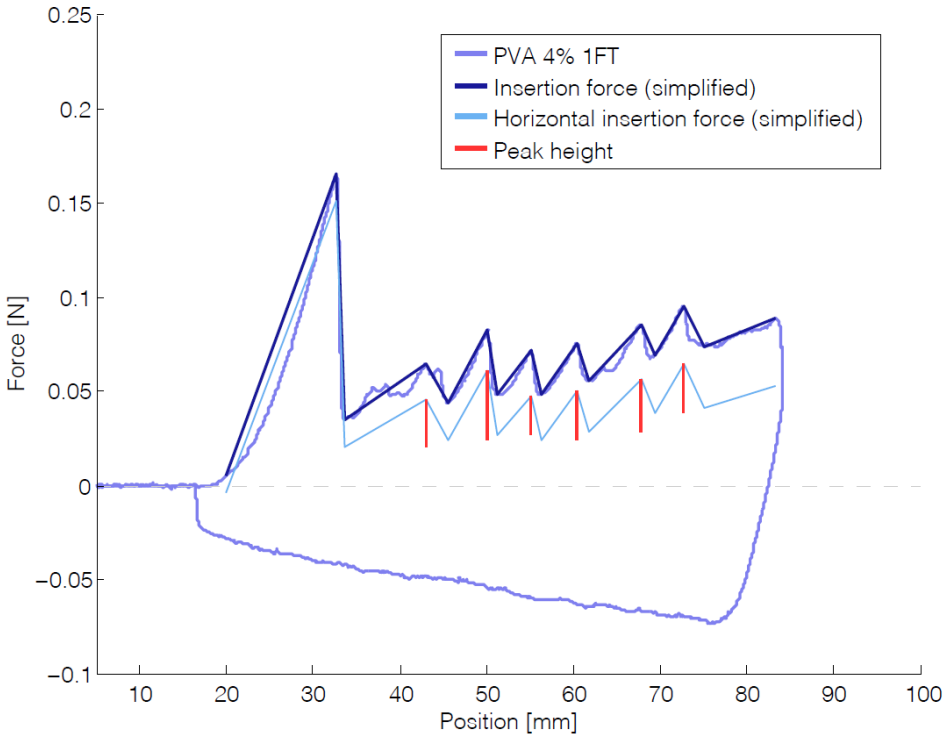

Figure 47 Peaks in PVA

6.2 RESULTS – PEAK FORCES IN PVA

In this section the results of the peak force analysis of PVA are presented.

Peak height and number of peaks differ between PVA samples, as can be seen in the force position diagrams depicted in Figure 48.

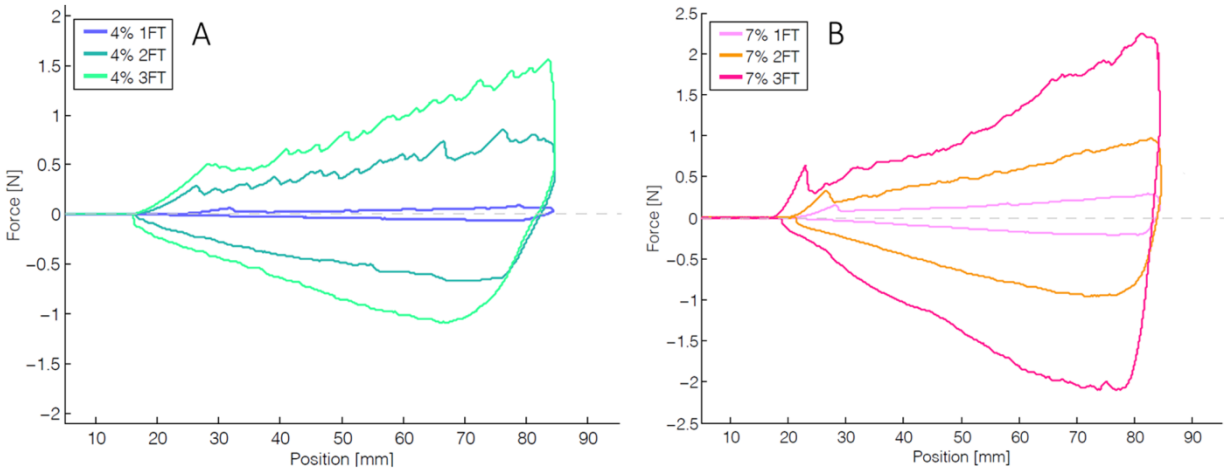

Figure 48 Force position curves A: PVA 4% B: PVA 7%

Median peak height, number of peaks (summed per sample) and number of peaks per dm are presented in Table 9. Peak height in PVA are visualized in Figure 49 and Figure 50 (together with peak height in liver tissue). The median peak height of samples with 3FT lie within the IQR of peak height in liver tissue (0.10N – 0.46N). In Figure 51 the number of peaks per dm are visualized. Samples with 4% 1FT and 4% 2FT have a median number of peaks per dm within the IQR of liver tissue (5.5 -10.0 peaks per dm).

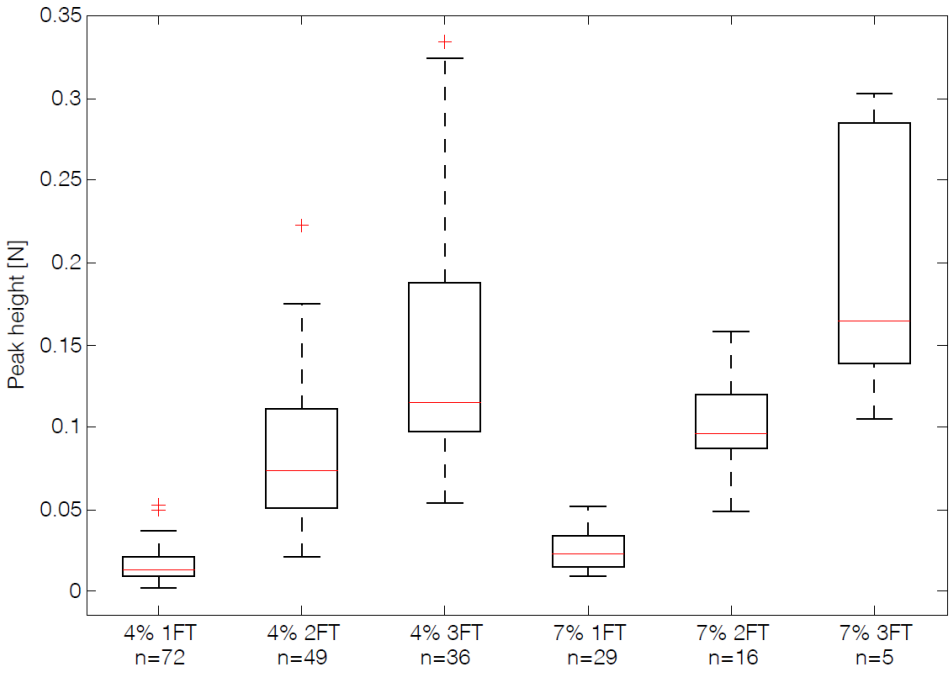

Figure 49 Peak height in PVA

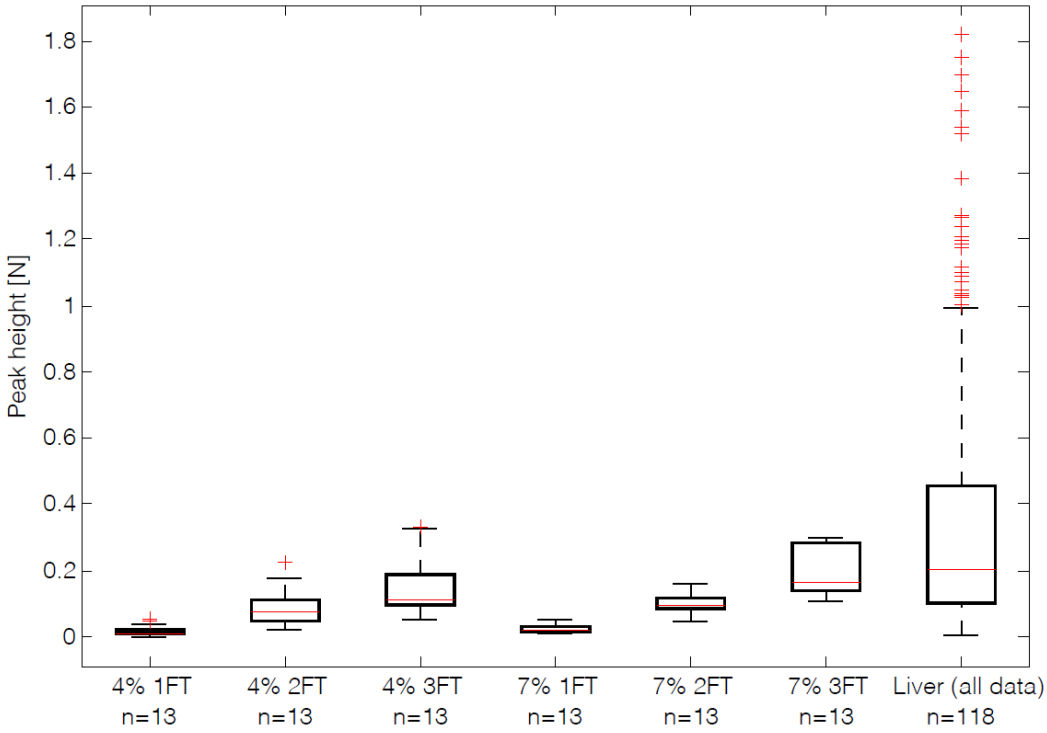

Figure 50 Peak height in PVA compared to liver tissue.

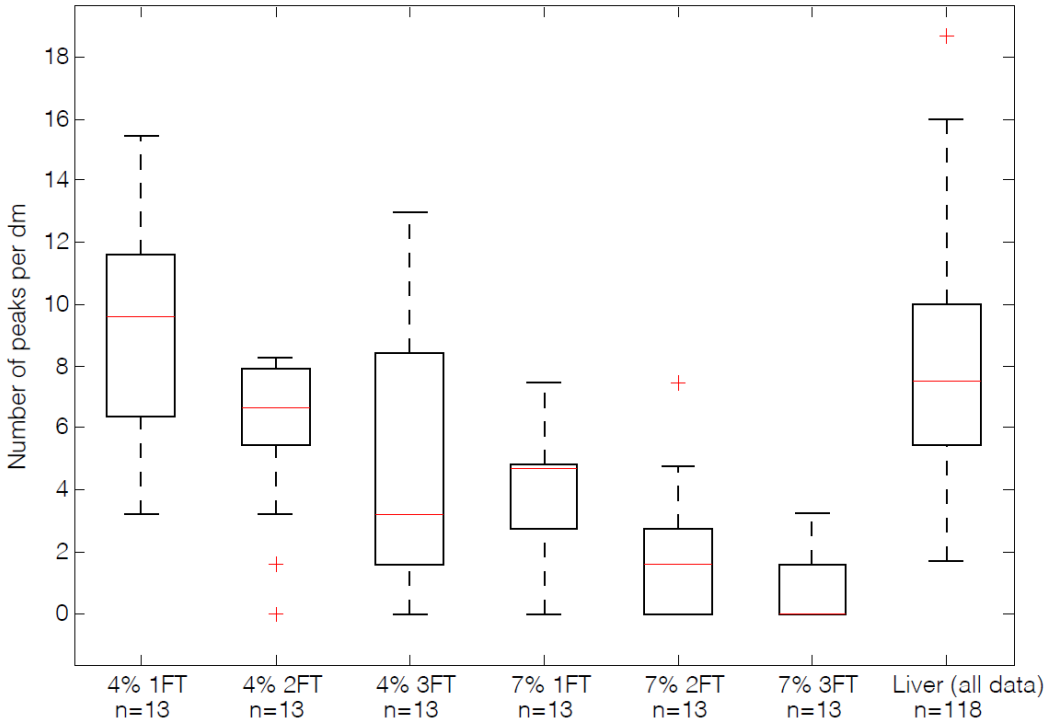

Figure 51 PVA number of peaks compared to liver tissue

Peak forces PVA						
Sample	**4% 1FT**	**4% 2FT**	**4% 3FT**	**7% 1FT**	**7% 2FT**	**7% 3FT**
Median peak height [N]	0.01	0.07	0.11	0.02	0.10	0.16
Number of peaks (per sample)	72	49	36	29	16	5
Number of peaks per dm	9.6	6.6	3.2	4.7	1.6	0

Table 9 Peak forces PVA

6.3 DISCUSSION

In this section the results will be discussed in 6.3.1, followed by the limitations in 6.3.2. The conclusion about the peak forces in PVA will be presented in 6.3.3.

6.3.1. DISCUSSION OF THE RESULTS

We can conclude that the PVA samples that PVA 4%3FT and PVA 7%3FT have suitable peak height. We can conclude as well that PVA 4%1FT and PVA 4%2FT have a similar number of peaks per dm as liver tissue. Samples with 4% PVA that were subjected to 1 and 2 FT cycles have a median number of peaks of 9.6 peaks/dm and 6.7 peaks/dm resp. compared to 8.7 peaks/dm in liver tissue. However the peaks are smaller than those observed in liver tissue (median peak height of 0.01 and 0.07 N resp. compared to 0.20 N in liver tissue). Samples with 4% and 7% PVA subjected to 3 FT cycles show higher peaks (median peak height of 0.11N and 0.16N resp.), but of less occurrence (median number of peaks of 3.2 peaks/ dm and 0 peaks/dm resp.). An increase in concentration of PVA seems to lead to an increase in peak height but also to a lower number of peaks per dm. The same can be concluded for a higher number of FT cycles.

PVA 4%2FT, the sample that met the retraction slope requirement, exhibits a sufficient number of peaks but without adequate peak height.

As explained in 3.3, when a PVA solution freezes, the ice crystals cause the PVA chains to aggregate. Due to hydrogen bonding crystallite formation occurs by which pore walls are formed. During every FT cycle, stronger and more compact bonds are made between the PVA chains leading to an increase in poor size. An explanation for the differences between samples regarding the peak forces is that these forces are influenced by the amount of deformation of the material. We observed that the samples subjected to more FT cycles were stiffer than samples subjected to less cycles. This is also showed by Jiang [72]. The stiffer samples showed less deformation pre puncture. Probably also within the stiffer samples there is less deformation. Therefore inner structures are immediately cut through by the needle instead of being deformed before they are cut, resulting in less peak forces. The occasional peak in PVA 7% 3FT could be caused by an area of substantial PVA accumulation for which more force is required to be cut through. In more elastic samples, the areas of PVA accumulation are substantially thinner and deformation before cutting, resulting in small peaks.

6.3.2. LIMITATIONS

The results are dependent on the amount of simplification that is applied. Using the Douglas Pecker Algorithm, epsilon (the simplification factor) is chosen to define the maximal normal distance from the simplified line to the original line. Concluding from the force-position diagrams of liver tissue and PVA samples, in the liver higher peak forces are present than the peak forces observed in PVA. When a small amount of simplification is applied (e.g. epsilon=0.03), the small peaks during insertion in the liver are included in the analysis, by which the number of peaks increases and the median peak height decreases. The result will be that more PVA samples will have a median peak height and median number of samples within the IQR of liver tissue. This is the reason that in this study an epsilon value of 0.05 N is selected to exclude the small peak forces present during insertion in liver tissue. The influence of the value of epsilon on the results was investigated and is presented in appendix F.

Another limitation mentioned before, is that the experiments of PVA and liver tissue are not conducted with the same needle. Blunting of the needle tip will have an effect on how easily inner structures will be cut through and will therefore influence the measured peak forces. Furthermore, in our experiment the samples were not embedded in gelatin and large deformations were observed in the PVA samples. The influence of these deformations on the measured peak forces is not known.

An aspect to keep in mind is that the properties of PVA are dependent on the freezing and thawing process. As the samples will not be uniformly frozen en thawed, the material properties will vary for different locations within the sample. In the current study, influence of insertion location was not studied.

6.3.3. CONCLUSION – PEAK FORCES IN PVA

None of our samples meets both the requirement defined for the desired number of peaks and peak height. However, possibly by selecting a different combination of concentration and number of FT cycles (or by varying other variables that were kept constant during our experiments such as thawing rate and freezing time) a phantom could be obtained that will fulfil all defined requirements, not only with respect to both peak characteristics during the insertion phase, but as well as to the friction slope during retraction phase. It is recommended that a follow up study, focussed on PVA examines whether true variation of the above mentioned variables can produce a fully suitable phantom for liver tissue.

7. IMAGING TMMS

In addition to comply with the mechanical requirements, the TMM should be usable for training of ultrasound guided procedures, the most commonly used imaging technique as was already outlined in chapter 2. In this chapter a first investigation about the extent to which the materials mimic liver tissue as visualized by ultrasound techniques will be performed.

7.1 METHODS

In this section the materials and the method of analysis will be described.

7.1.1 MATERIALS

In order to obtain images without artefacts, the materials were removed from the beakers. The performance of gellan gum was not assessed, since the gellan gum samples were too soft to retain their shape after removal from the beakers. The candle gel sample could not be removed in its entirety from the beaker, without damaging of the sample. Therefore a new candle gel sample was produced in a paper cup that could be ripped open after gelation was completed. To rule out the possibility on damage to the ultrasound transducer due to possible plasticizer migration out of PVC samples with added softener, only the 100% plastisol sample was evaluated.

Ultrasound images were obtained at different depths, ranging from 2 to 6 cm. 2 PVA samples (PVA 4%2FT and PVA 7% 3FT), 1 PVC (100% plastisol) and 1 candle gel sample were imaged with a Philips HD7 XE ultrasound system (Philips Medical Systems, The Netherlands). A Philips 15-6L high-resolution linear ultrasound transducer was used (Philips Medical Systems, The Netherlands). For PVC and candle gel an ultrasound gel (Aquasonic 100) was applied as coupling agent between sample and transducer to enhance the transmission of ultrasonic waves. Since the PVA samples had a wet surface, no ultrasound gel needed to be used.

7.1.2 ANALYSIS

The obtained images were compared to ultrasound images representing liver tissue presented in section 2.6.2. The comparison was based on echogenicity and homogeneity.

7.2 RESULTS – IMAGING TMMS

PVA

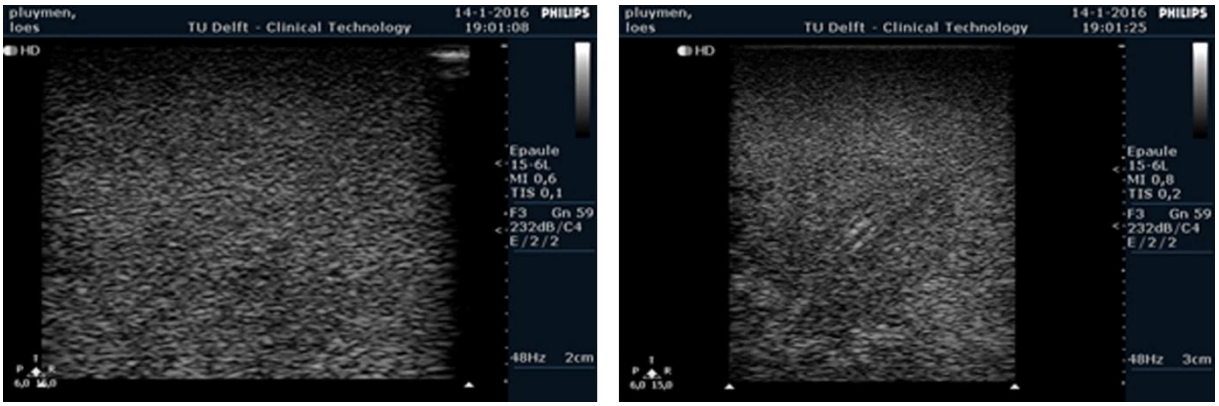

Figure 52 Ultrasound visualization PVA 4% 2FT: 2 images obtained with 2 cm penetration depth

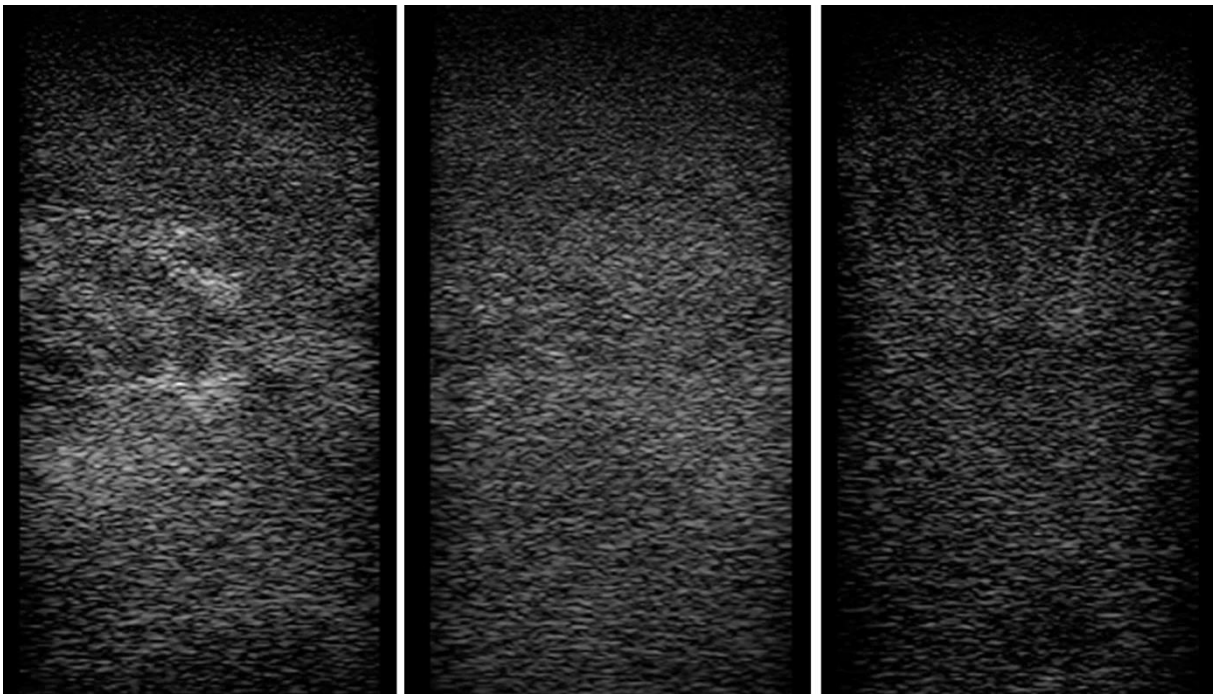

Figure 53 Ultrasound visualization PVA 4% 2FT: 3 images obtained with 5 cm penetration depth

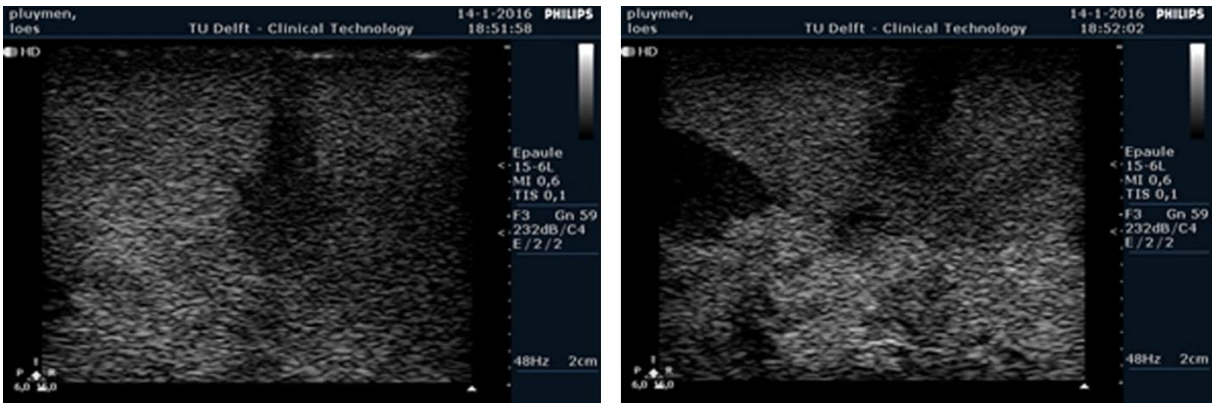

Figure 54 Ultrasound visualization PVA 7% 3FT : Images obtained with 2 cm penetration depth

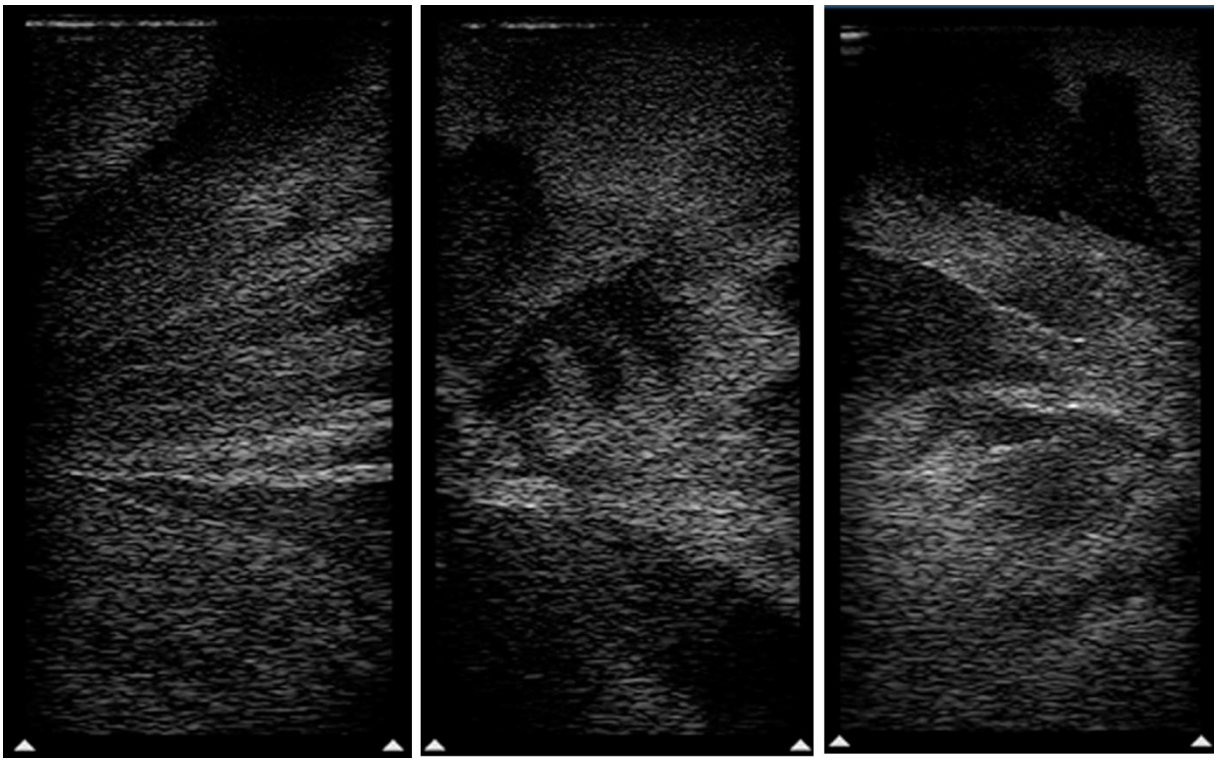

Figure 55 Ultrasound visualization PVA 7% 3FT : Images obtained with 5 cm penetration depth

PVA 4% 2FT, visualized in Figure 52 and Figure 53 has a echogenicity that is comparable to liver tissue. However, the material is not fully homogenous.

Some regions in PVA 7% 3FT, visualized in Figure 54 and Figure 55, have a similar echogenicity as PVA 4% 2FT, while some regions are more hypoechoic. Both whimsical forms and regular patterns are present.

PVC

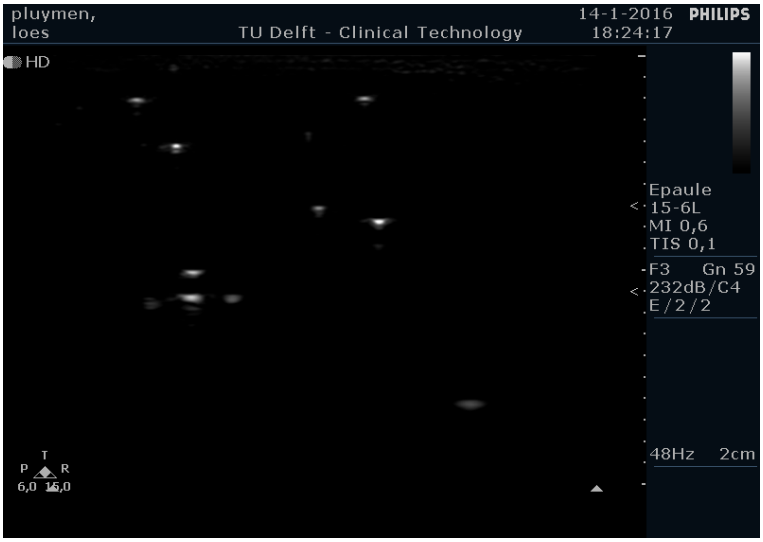

Figure 56 Ultrasound visualization PVC 100% plastisol: Images obtained with 2 cm penetration depth

In accordance with literature [9] , PVC appears anechoic on ultrasound, see Figure 56. The white spots are air bubbles inside the material.

CANDLE GEL

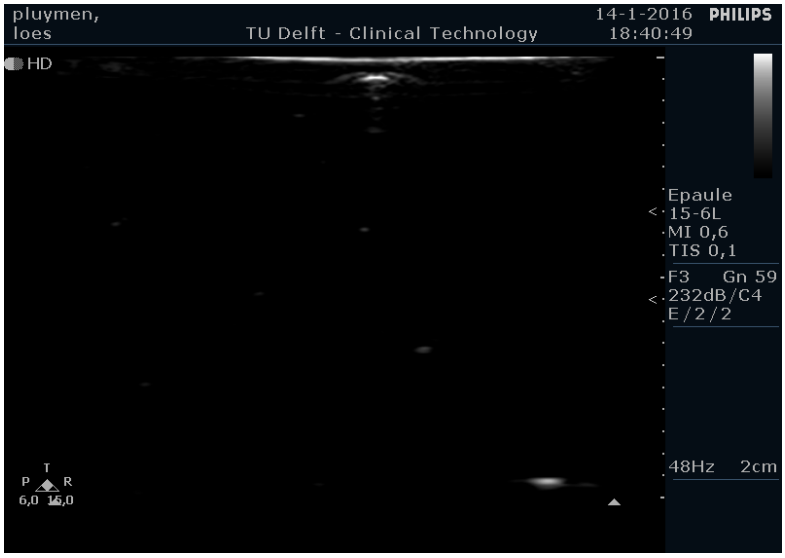

Figure 57 Ultrasound appearance candle gel: Images obtained with 2 cm penetration depth

Also candle gel, visualized in Figure 57 appears anechoic on ultrasound images. The white spots are air bubbles enclosed in the material.

7.3 DISCUSSION

In this section the results are discussed in 7.3.1., followed by a description of the limitations in 7.3.2. Lastly, the conclusion will be presented in 7.3.3.

7.3.1 DISCUSSION OF THE RESULTS

As was expected from literature, PVC and candle gel appear anechoic on US due to the low impedance of the material (the resistance to transmit ultrasound waves). In other words, because all waves are transmitted, none are reflected and therefore no image is produced. When a needle is inserted in an anechoic medium, it will be clearly visible due to its high impedance in relation to the anechoic background.

However, PVC and candle gel can be made more similar to human tissues, by the addition of scattering agents. Cook [73] improved the echogenicity of PVC by addition of graphite powder mixed through the PVC/plasticizer blend. Ceh et al. [9] added cellulose as scattering agent to obtain a speckled texture in PVC. Cellulose can also be added to candle gel to obtain a echogenicity similar to liver tissue, as was shown by Shevchenko [74]. Chmarra [66] added sephadex to a candle gel phantom to obtain a sufficient echogenicity.

Concluding from the images presented in the previous section, PVA has an echogenic appearance similar to liver tissue, even with a liver like speckled pattern. However, the samples are not homogenous. Especially in the PVA 7% 3FT sample, different regions can be distinguished, which are sometimes irregularly shaped and sometimes show a more organized pattern. To be able to conclude whether this inhomogeneity is due to an increase in FT cycles or an increase in concentration, an additional sample (PVA 3% 5FT) was manufactured and imaged. The ultrasound images can be found in appendix G. From these images can be concluded that the inhomogeneity of the PVA 7% 3FT sample is mostly due to its high concentration of PVA, since the 3% 5FT sample almost has the same level of homogeneity as the 4% 2FT sample.

The variation in echogenicity is due to the non-homogenous distribution of PVA inside the samples. The compressed and crystallized zones (described in 3.3) have a higher echogenicity than PVA poor zones. In Figure 55 the freezing direction can be clearly seen.

7.3.2. LIMITATIONS

It should be realised that all observations presented and discussed here are made by a non-trained non-experienced observer. Therefore it is essential that the results will be discussed with clinicians, which will be revisited in chapter 9. However, some conclusions were so evident that there is little doubt that they will be confirmed by more qualified observers.

Another limitation is that the images of liver tissue and TMM are obtained with different devices. In clinical settings in which the liver images are obtained, ultrasound probes are used with a lower frequency spectrum in order to obtain a higher penetration depth. As explained in section 2.5, use of lower frequencies leads to deeper penetration of sound waves but also to decreased resolution. Furthermore, a curved transducer (providing a wide field of view and often used in liver imaging) often generates lower frequency waves than linear transducers. Since our TMM samples have a diameter of only 6 centimetre, a linear probe emitting much higher frequencies was used to image the samples and high resolution images were obtained. Concluding, in addition to a lack of fundamental background, images are hard to compare due to different acquisition parameters.

7.3.3. CONCLUSION – IMAGING TMMS

As described above, PVC and candle gel are not suitable imaging TMM because they are anechoic. As is stated by Chin et al. [75], practising procedures on anechoic phantoms can lead to self-overestimation of inexperienced clinicians regarding their ability to define the position of the needle inside the tissue. In soft tissues the location of the needle is much harder to determine due its speckled echogenic appearance. PVC and candle gel are however, in contrast to PVA, homogeneous. With the addition of echogenic particles (such as graphite powder), possibly a homogenous echogenic phantom could be obtained. As is mentioned before, this is outside the scope of this thesis.

In PVA, the variables that are affecting the amount of friction are influencing the ultrasound properties as well. This can be a disadvantage as production methods to obtain optimal friction properties will not necessarily lead to suitable imaging characteristics. However, with addition of scattering particles in PVC and candle gel, the friction is likely to be influenced as well.

For now our conclusion is that - when evaluating the properties of the samples as how they were fabricated in this study - only PVA shows imaging characteristics that are comparable to liver tissue. Although not mimicking liver tissue fully realistically, PVA could be a suitable material to be used in training settings since contrast between needle and material will probably be comparable to the contrast observed in liver tissue.

8 PRACTICIAL ASPECTS OF TMMS

In addition to fulfilling the requirements defined for the mechanical and imaging aspects, several practical aspects are important regarding the suitability of TMM for image-guided needle interventions. This chapter will focus on the practical aspects of the liver TMMs reviewed in this study.

8.1 CRITERIA

Several features were assessed, including durability, reusability, degradation, ease of production and costs. In this section these aspects are described.

8.1.1. DURABILITY

Durability, defined as the degree to which the material can withstand repeated interventions.

Figure 58 Degradation of candle gel

Durability was analysed by visual inspection of the material after all interventions had been performed. Also the presence and features of needle tracks (which are an aspect of deterioration) was analysed. The presence of needle tracks is seen is as negative.

In the gellan gum samples subjected to needle interventions, the location of insertion was hard to identify afterwards, especially for the HA gellan samples. Since the samples were not transparent, also needle tracks could not be observed.

Also in PVA, locations of insertion could not be derived from inspection of the surface. Due to its opaqueness, needle tracks were not observable either.

On the contrary, in both PVC and candle gel samples, both insertion location and needle tracks were clearly visible. Furthermore, the candle gel sample was considerably damaged due to the needle interventions. During interventions, pieces of candle gel clung to the needle thereby leaving a large hole where the needle was inserted, see Figure 58.

8.1.2. DEGRADATION OVER TIME

Degradation rate was determined based on visual signs of degradation.

Figure 59 Fungal growth in gellan gum

Although the gellan gum samples were stored in the refrigerator, after two weeks all samples were contaminated with fungal growth, as can be seen in Figure 59.

The PVA samples did not show any sign of fungal growth but in some samples a loss of water was observed in which the sample was partially submerged. This effect was more prominent in the samples subjected to 1 and 2 FT cycles than in samples subjected to 3 FT cycles. The loss of water was observed after two weeks, and seemed not to increase over a two-month period. PVA samples were stored in the refrigerator, as was found to be the best option for preservation reported in literature. PVA samples were covered with aluminium foil, since pilot samples were

observed to dry out.

PVC and candle gel did not show any signs of degradation. Plasticizer migration, although observed in samples produced in a pilot study, was not detected in PVC samples used in the experiment.

8.1.3. REUSABILITY

With reusability is meant whether the TMM can be remoulded into a new sample. Gellan gum is a thermo-reversible gel and can be liquefied in order to obtain an intact sample. However, because the material is susceptible to fungal growth, the samples cannot be reused many times.

PVA cryogels are thermo-reversible since the physical crosslinks can be undone when the material is heated. Upon heating the gels liquefy and subsequently they can be subjected to FT cycles again [57]. However, reusing PVA was not tested in this study.

Both PVC and candle gel samples can also be reused by melting the samples. PVC remoulding can be performed a limited number of times due to degradation of the material, while candle gel can be reshaped many times.

8.1.4. EASE OF FABRICATION

Ease of fabrication is determined based on the amount of time that was needed to manufacture the samples and the complexity of the production process.

Gellan gum, PVC and candle gel samples were made relatively fast, while PVA samples required more time and more effort for manufacturing. Gellan gum samples were produced in approximately half an hour per sample. PVC and candle gel required approximately 15 minutes production time per sample. Since the PVA solution needed to be heated to 93 °C and maintained at that temperature for half an hour, this step of the production process required approximately 1 hour per sample. Subsequently the samples were subjected to 1 to 3 FT cycles, which lasted 24 hours per cycle.

Logically, the candle gel sample was obtained most easily, since candle gel was purchased as a ready-made, only to be melted, material. PVA, although this material knows a time intensive production process, was not complicated to handle. PVC demands to be produced in a ventilated room and requires the most cautious approach of all materials. Gellan gum was most difficult to handle. Although several attempts were made it proved to be difficult obtain a homogenous solution.

8.1.5. COSTS

Costs were dependent on amount that was purchased and amount that was needed to produce a phantom. In Table 10 the costs per sample are described.

Costs per sample					
Material	**Components**	**Price per unit**	**Content of unit**	**Amount needed**	**Costs per sample**
Gellan gum	HA gellan gum	€11,77	50 mg	1 mg	€0,24
	LA gellan gum	€11,77	50 mg	1 mg	€0,24
	Total gellan gum				**€0,48**
PVA	PVA	€31,10	100 mg	10 mg	**€3,11**
PVC	Plastisol	€16,67	1000 mg	125 mg	€2,08
	Plasticizer	€16,67	1000 mg	125 mg	€2,08
	Total PVC				**€4,16**
Candle gel	Candle Gel	€12,15	1000 mg	250 mg	**€3,04**

Table 10 Costs per sample

Gellan gum samples were the least expensive samples, followed by candle gel, PVA and PVC. One should note that these prices are dependent on total volume of the materials purchased.

8.2 DISCUSSION

In this section the above described practical aspects are discussed.

8.2.1 DISCUSSION OF THE RESULTS

All practical aspects described in section 8.1 are summarized in Table 11.

Practical aspects TMMs				
Practical aspect	**Gellan gum**	**PVA**	**PVC**	**Candle gel**
Durability	+	+	+	- -
Degradation over time	-*	+	++	++
Reusability	+/-	+	+/-	++
Ease of fabrication	+/-	+/-	+/-	++
Toxicity/Harmfulness	N/A	N/A	- -*	N/A
Costs	++	+	+	+

*Table 11 Practical aspects TMMs. Aspects that were the basis of exclusion as suitable TMM are denoted by *.*

Except from gellan gums low costs per sample, costs of the phantoms are comparable (though PVC is a little more expensive).

As gellan gum is susceptible to fungal growth, it is not suitable to be the basis of a durable phantom. PVC and candle gel show no degeneration over time. But PVC, although durable and reusable, is not a practical phantom material due to its toxicity. Candle gel samples are easy to fabricate but a substantial disadvantage is their rapid deterioration when subjected to needle interventions. On the other hand, the possibility to reuse the material could compensate for the aspect of fast deterioration. Although PVA knows a time intensive manufacturing process, the material deteriorates less rapidly and shows no significant degradation over time.

8.2.2. LIMITATIONS

The practical aspects of the TMMs evaluated in the previous section are heavily dependent on the material and sample composition choices that have been made.

It cannot be ruled out that different sample design choices would lead to other conclusions. In other words, TMMs should not be ruled out prematurely. Especially regarding candle gel, deterioration could be different between different types of candle gel. It could be possible that another type of candle gel would adhere less to the needle and therefore show les deterioration in response to needle interventions. Furthermore, the samples used in this study did not include any additives such as preservatives. In many studies focussing on gellan gum, preservatives (for example potassium sorbate or methyl parabens) are added to prolong shelf life of the phantoms.

8.2.3. CONCLUSION – PRACTICAL ASPECTS OF TMMS

Based on their practical characteristics, gellan gum and PVC are not regarded as suitable phantom materials due to their susceptibility to fungal growth and toxicity respectively. PVA and candle gel would both be suitable phantom materials with respect to their practical characteristics. Both materials have each one significant disadvantage. PVA phantom production involves a lengthy process but results in a more durable phantom than a phantom made from candle gel. Candle gel phantoms on the other hand, will be easy to produce but the production process will have to be repeated many times.

9. CLINICAL EVALUATION

Concluding from the results about mechanical, imaging and practical aspects of the TMMs, PVA exhibits the most suitable properties to be used as liver phantom material. Therefore this material has been presented to clinicians for evaluation of its properties and to get a first validation of our methods. To provide the clinicians with reference materials and to deepen our insight in the relationship between experimental and clinical data, also the PVC and candle gel samples were brought for evaluation. The opinion of the clinicians regarding the properties of these latter two materials can be found in appendix H.

9.1 METHODS

The samples were evaluated by two radiologists in training (AIOS, two year work experience as radiologist) based in the Jeroen Bosch Hospital in Den Bosch. Two samples were used for evaluation: PVA 4% 2FT and PVA 7% 3FT. These specific samples were selected based on their divergent properties.

The radiologists were asked to test the samples with the trocar needle that was used in the mechanical experiment. They used the needle both as it is intended in practice (inner and outer needle are inserted simultaneously) and by using the inner needle only (the method we applied in this research). They were asked to give their opinion about their overall impression of the material, the feeling during insertion and the feeling during retraction. Subsequently, the ultrasound images were presented for evaluation. All feedback was reported.

9.2 RESULTS – CLINICAL EVALUATION

In this section the feedback of the two radiologists M.S. MSc. and B.M. MSc. about the PVA samples are presented.

9.2.1 M. S.

Figure 60 M. S.

MECHANICAL CHARACTERISTICS

M.S. was generally positive about the PVA samples. The first sample that he tested was the 7% 3FT sample and his response to the question to what extent the material mimicked liver tissue was: “Quite good actually!” However, he was of the opinion that the material caused to much friction upon needle insertion. “I have to use too much force that is not realistic. But the overall feeling mimics liver tissue really well.” The retraction phase was perceived as very realistic. The next sample, PVA 4% 2FT, was immediately defined as too elastic. The

material ‘bounced’ according to M.S. and he had never experienced that behaviour in real tissues. The retraction phase was found to be less unrealistic than the insertion phase, but still considerably less representative than the retraction trajectory in PVA 7% 3FT. In all samples (also PVC and candle gel), the stiffness of the sample was experienced as being less stiff when only the inner needle was inserted.

IMAGING CHARACTERISTICS

According to M.S., the ultrasound images visualized a too in-homogenous material to pass for liver tissue. Especially PVA 7% 3FT was described as very unrealistic due to the whimsical forms that were present in this sample. PVA 4% 2FT was considered to mimic liver tissue more realistically. He also denoted some areas in this sample as metastases.

M.S. added that a fully realistic image is not essential in order to be a suitable training material. Since hand-eye coordinating is regarded as the most difficult part of needle interventions, most important characteristic with respect to imaging is that the needle is visualized correctly.

9.2.2 B. M.

Figure 61 B. M.

The first sample tested by B.M. was PVA 4% 2FT. Firstly, he inserted the two parts of the needle simultaneously. A first conclusion was that the material was too stiff to be comparable to liver tissue. Furthermore, he stated that the needle got hitched at some places during insertion which was not realistic. However, when he only inserted the inner needle, he described the needle insertion as ‘very realistic’.

PVA 7% 3FT was subsequently tested. This sample was concluded to be even more stiff than PVA 4%2FT and therefore too stiff to be similar to liver tissue.

IMAGING CHARACTERISTICS

B.M. explained that the ultrasound images had a too coarse structure compared to human tissues. However, like M.S. he also some metastases in PVA 4% 2FT. Also other tissue types were identified, for example one image was typically an ultrasound visualization of the testes. The PVA 7% FT sample was concluded to be very unrealistic due to the stripes that are present in the images. Also M. explained that for ultrasound training, realistic needle visibility is most important and realistic tissue visualization is of secondary importance.

9.3 DISCUSSION

In this section the results of our clinical evaluation are discussed, followed by the limitations of this part of the study. This section will end with a conclusion about the clinical evaluation.

9.3.1. DISCUSSION OF THE OBSERVATIONS

Surprisingly, the two clinicians stated that they perceive the liver as homogenous. Several explanations for this perception can be provided. As is often described in literature, the perfusion of the liver is supposed to influence to a great extent the livers mechanical characteristics, which could be an explanation for the perception of homogeneity. Furthermore, as mentioned before, clinicians avoid to pierce main arteries and veins by which more homogeneous tissue is encountered than during insertion at a random location. Another speculation is that during percutaneous procedures, the friction that is caused by skin, fat and muscle layers, caters for a much larger part of the forces during insertion thereby reducing the relative contributions of peak forces.

Furthermore, both clinicians explained that in practice they do not perceive friction during retraction of the needle. In fact, all materials had comparable friction during insertion as during retraction. The difference between the feeling during insertion and retraction in the liver could be ascribed to the difference in insertion resp. retraction method (for example difference in speed). It could also be possible that in the liver a broader needle track is formed, which causes the decrease in friction during retraction. Another explanation could be that by cutting small arteries and veins during insertion, the leaked blood acts as lubricant during retraction. However, these theories are only speculations.

9.3.2. LIMITATIONS

There are few limitations regarding this part of the study that are worth to be discussed.

Only two clinicians tested our samples. Furthermore they had limited work experience consisting of performing straightforward percutaneous procedures. Neither of them had as yet performed a needle intervention directly in the liver, during open surgery.

Another limitation is that the suitability criterion is based upon the reaction on the inner needle, while in practice this part of the needle is not used without the outer needle (cannula).

For the evaluation an extensively used needle was used, in contrast to a new needle as the clinicians are probably used to. However they were familiar with the type of needle and did not mention anything about different needle characteristics than they expected.

9.3.1 CONCLUSION – CLINICAL EVALUATION

Concluding from the evaluation with clinicians, a phantom made from PVA could realistically mimic liver tissue. However, the PVA should be less stiff than the samples that were used in this study. Furthermore the material should not include inhomogeneities, both with respect to the mechanical performance as for the evaluation by ultrasound. Realistic mechanical properties are most important, the imaging properties should just offer a realistic view on the position of the needle in order to allow for a good training opportunity. With respect to the latter, needle visualization is an important aspect, which should be further examined.

.

10. DISCUSSION

In this chapter an interpretation of the results obtained in the current work is provided. Subsequently, the limitations of this study are discussed. The chapter will end with our final conclusion and recommendations for future research on the topic of liver TMMs for image-guided needle interventions.

10.1 INTERPRETATION OF THE RESULTS

In this study is investigated to what extent TMMs that are suitable for phantom production mimic liver tissue during image-guided needle insertions, with a focus on axial forces during insertion and retraction. Axial forces are selected because they are considered to be the most important force component in needle-tissue interaction [25].

Several aspects of TMMs were investigated: mechanical characteristics, imaging performance and practical aspects. Mechanical and imaging properties of both TMM and liver tissue described in literature served as a basis for selection of potentially suitable phantom materials. The mechanical and imaging selection criteria that were used were Youngs modulus, density, speed of sound and attenuation coefficient. A criterion regarding the practical applicability of the TMMs was the shelf life reported in literature.

The suitability of selected TMMs was assessed by experimental research. Experimental data on liver tissue obtained in a preliminary study performed by T. de Jong served as the basis to define liver behaviour during needle interventions and thereby to formulate a requirement for the behaviour of TMM during needle interventions. Since friction is assumed to play an important role during both the insertion and retraction phase, the first aspect that was examined was the amount of friction during needle interventions. It should be noted that in order to ensure comparability of data, the experimental setup used by T. de Jong was to a large extent copied in these experiment discussed here (e.g. the use of an inner needle without cannula).

A method applied often to study friction is by studying the forces during retraction. Since during retraction no forces are exerted at the tip of the needle, friction is the only force component that is supposed to act [76]. Therefore the slopes of the retraction phase in the force-position diagrams were computed using the data on needle interventions in liver tissue available for this study. The mechanical requirement that followed from this analysis was defined as: A TMM should have a median retraction slope that lies within the IQR of all retraction slopes in liver tissue. An additional mechanical requirement that was made based on the analysis of insertion forces, was that the TMM should have approximately the same number of peak forces during the insertion phase, with a median peak height comparable to that observed in liver tissue. Only PVA showed peaks during the insertion phase and therefore the PVA data were analysed further in order to define the peak force characteristics.

The imaging performance was studied based on two aspects: echogenicity and homogeneity. Ultrasound images of TMMs materials were compared to ultrasound images of liver tissue. Subsequently the practical aspects of the materials were compared and evaluated. To link the results to application in practice, lastly, the samples of the most promising material, PVA, were evaluated by clinicians.

The results of the above mentioned parts of this study are discussed in the sections below.

10.1.1 RETRACTION SLOPES IN TMMS

The experiment that was conducted to examine the retraction slopes in the selected TMMs was described in chapter 5. The retraction slopes of gellan gum, PVA, PVC and candle gel were compared to liver tissue.

None of the gellan gum samples did cause enough friction to be comparable to liver tissue. Two trends were observed:

- An increase in friction with increase of gellan gum mass fraction
- An increase in friction with increase of HA (high acyl) gellan gum mass fraction, with respect to mass fraction LA (low acyl) gellan gum

Concluding from these trends, we had to increase the mass fraction of gellan gum in a 100% HA sample to obtain a gellan gum sample with a steeper friction slope. However, the 2% gellan gum, 100% HA sample was already challenging to manufacture due to difficulties with dissolving the gellan gum powder. After extensive experimenting (including addition of ions and using different dissolving methods), we concluded that our production principles or composition variables could not be chosen so that a suitable gellan gum phantom could be manufactured. Although gellan gum is often used to mimic soft tissues (among others by King [77] and Chen [45]) none of this studies focusses on needle interventions. Therefore our results cannot be compared to results obtained by others.

The PVA samples that were tested for mechanical evaluation showed a wide range of friction slopes. Some samples showed less friction than observed in liver tissue, while others showed more friction compared to liver tissue. Two trends were observed:

- An increase in friction with increase of number of FT cycles
- An increase in friction with increase of mass fraction PVA

From these two trends could be concluded that several combinations of a number of FT cycles and a concentration of PVA in water can lead to phantoms with suitable friction characteristics.

Although the influence on the mechanical properties of PVA of the number of FT-cycles and concentration are described in literature [72] [78], they have not yet been reported with respect to needle-tissue interaction.

It should be noted that the properties of PVA cryogels are influenced by many more variables than those that were studied in the current work. Among these variables are the amount of hydrolysis, the degree of polymerization, the amount of ions present in the solvent, the type of solvent, the freezing rate and duration and the thawing rate [57].

In spite of the many variables of PVA regarding the manufacturing process, that we not systematically varied but instead kept constant in this study, we can conclude that PVA 4% 2FT showed suitable friction properties.

Both PVC and candle gel showed steeper friction slope values than those observed in liver tissue. For PVC a linear trend was observed:

- A decrease in friction with increase of mass fraction plasticizer.

Since plasticizer softens PVC by creating spaces between the polymer chains and furthermore has a lubricating effect, this result was expected. From the observed trend could be concluded that a suitable sample should be possible to obtain with an additional amount of plasticizer. This was confirmed in an additional experiment (presented in appendix E). PVC is used in many studies and is regarded as a suitable phantom material for needle interventions regarding its friction properties by, among others, Hungr et. al [8] and Li et. Al [79]. In these studies less plasticizer was used than in the current work. The suitability of candle gel has not often been reported upon, however the material was found suitable for needle interventions by Vieira et. al [64].

10.1.2. PEAK FORCES IN PVA

In the experiment described in chapter 5, peak forces were observed in the force-position diagrams of PVA. As stated in the first chapter, adjusting the samples characteristics in order to cause peak forces during insertion (e.g. by addition of small particles to increase inhomogeneity) was outside the scope of this thesis. However, because the peak forces in PVA were a natural property of the material, they were worthy of further investigation. This was presented in chapter 6.

The force peaks were analysed using the same method that was applied to analyse the force peaks in liver tissue. Two criteria were defined in chapter 4.4: Peak height and number of peaks per dm. An algorithm was applied to exclude small peaks to allow for better comparison between liver tissue and PVA. Since PVA showed smaller peaks than liver tissue, the forces needed to be simplified to compare significant peak forces only. The influence of the simplifying factor was investigated and a compromise between too much simplification (leading to less informative data) and an insufficient amount of simplification (comparison focusses mainly on small forces and therefore almost all PVA samples fulfil the criteria) was reached.

In this study it was decided to evaluate the number of peaks and the peak height. However, also other aspects can be thought of that are interesting to study. Examples are locations of the peaks, slopes of the rise resp. drop in force in a peak and distance between successive peaks.

However, when analysing results of the two variables studied here, two conclusions can be drawn:

- Both an increase in FT cycles and an increase in PVA mass fraction leads to an increase in peak height
- Both an increase in FT cycles as an increase in PVA mass fraction leads to a decrease in number of peaks

During our experiments, we observed an increase in stiffness with an increase in PVA concentration or increasing number of FT cycles. This is in line with results presented by Jiang [72]. Samples with a higher concentration of PVA or subjected to more FT cycles were stiffer than the other samples and showed less deformation before puncture. Due to the lack of deformation, inner structures are supposed to be cut through more easily. Occasional peaks are probably the result of cutting actions of substantial PVA accumulation.

One should keep in mind that the properties of the PVA samples are influenced by the freezing process. Therefore the properties of the material will be different for different locations within the sample. In this study the influence of insertion location was not taken into account.

10.1.3. IMAGING PERFORMANCE

In chapter 7, the samples are compared to liver tissue regarding their ultrasound properties. Although this part of the study could not be performed in depth due to the inexperience of the observer, it still provided some interesting results. Materials were evaluated based on their echogenicity and homogeneity.

As was expected from literature, PVC and candle gel appeared fully anechoic on the ultrasound images. In other words, the materials had a low impedance and none of the ultrasound waves was reflected. In literature several methods of increasing echogenicity are described, including addition of graphite powder and cellulose [9]. Since both the candle gel and PVC samples were fully homogenous, this might be an interesting option to obtain a homogenous echogenic material. However, this was not investigated in the current study because of the inadequacies of the mechanical characteristics of these materials.

The PVA samples showed a liver like speckled pattern, probably due to the crystalline regions in the material that diffusively reflected sound waves. An obvious difference could be observed between the PVA 4% 2FT and PVA 7% 3FT samples. The latter showed a more inhomogeneous structure with presence of whimsical structures with higher echogenicity. Concluding from comparison between the PVA 3% 5FT sample and the PVA 7% 3FT sample, this inhomogeneity was mostly due to the increase in concentration of PVA.

To allow for better comparison between TMM samples and liver tissue, the materials should be imaged with the same device and analysed by a skilled observer. However, the used setup led to a first indication of the imaging performance of the TMMs. Although the images were not fully comparable to liver tissue, we can conclude that PVA has the most suitable imaging characteristics for an ultrasound compatible phantom.

10.1.4. PRACTICAL ASPECTS

In order to be a suitable phantom material, the TMM should not only have the right mechanical characteristics and imaging performance, but should be practical to handle as well. Several conclusions could be drawn from observations that were made during this study. The samples were evaluated based on the following aspects:

- Durability
- Degradation over time
- Reusability
- Ease of fabrication
- Toxicity/harmfulness
- Costs

Gellan gum and PVC were found to be unsuitable as phantom material based on their practical aspects. Gellan gum appeared to be highly susceptible to fungal growth while PVC (in order to meet the mechanical requirement) needed a substantial addition of plasticizer. Since the toxicity of this plasticizer (used in high concentrations) could not be assessed and furthermore the plastizer could possibly cause damage to the ultrasound transducer, this material was concluded to be an unsuitable phantom material.

Both PVA and candle gel had each one main disadvantage. Manufacturing PVA samples involves a lengthy process, especially when the material has to be subjected to a high number of FT cycles. However, this process leads to a durable phantom. Candle gel on the other hand, has a simple manufacturing process but does not withstand repeated needle insertions. However, the material can be liquefied and recycled into a new phantom.

Both PVA and candle gel can to some extent be seen as suitable phantom materials regarding their practical aspects but cannot be regarded as optimal phantom materials. Their suitability will depend on the indented use.

10.1.5. CLINICAL EVALUATION

An interesting part of the current study was the evaluation with clinicians presented in chapter 9, in which their feedback on the mechanical and imaging performance of the samples was captured. Except from feedback about the properties of PVA also some new insights were gained.

These insights can be summarized as follows:

- The liver is perceived as a homogenous tissue (at least during percutaneous needle interventions)
- Hand-eye coordination is the most challenging aspect of performing needle interventions
- Insertion method and thus tactile feedback differs substantially between clinicians

Most important conclusions about the PVA samples were that the overall feeling was comparable to liver tissue, however the sample subjected to 2 FT cycles (4% PVA) was found to be too elastic while the sample subjected to 3 FT cycles (7%) was found to cause too much friction. Both clinicians concluded that insertion and retraction with the inner needle only was more realistic than with both cannula and inner needle. This is explainable since the friction criterion was based on the amount of friction caused by the inner needle. As the liver is perceived as homogenous, the in homogenous nature of the PVA samples was experienced as non-realistic. The perception of homogeneity could either be explained by the pressure due to vascularization in in-vivo tissues, the avoidance of piercing main arteries and veins during insertion or the high amount of friction during percutaneous interventions.

This part of the study provided a brief insight in the way the PVA samples mimicked liver tissue in vivo. Although the collaborating clinicians had experience with percutaneous interventions only, it did provide some valuable feedback. During percutaneous interventions the friction caused by skin, muscles and fat located

anterior to the liver is added to the forces that are encountered during insertion and retraction in the liver covering up forces caused by encounters with inner structures. Therefore it would be interesting to have the samples tested by a radiologist that is experienced in needle interventions during open surgery.

This master thesis project was performed from a scientific, experimental and literature based viewpoint. When this study would have been initiated from a more clinical starting point, criteria would probably have been defined differently. However, in order to obtain results that could be compared to previously conducted research on TMMs, the applied approach was, in our opinion, the most suitable approach for the current study. Because the relation between research and practice is important to consider, it would be interesting to link the scientific results to a more elaborate practical evaluation.

10.2 LIMITATIONS OF THIS STUDY

The materials that were reviewed in this study were selected based on literature. In studies focussing on phantom design, the presented phantoms often consist of different components. In our study we have investigated the characteristics of the 'pure' materials. Advantage of this approach is that the number of variables is restricted, while a disadvantage is the possible exclusion of a material that would have been a suitable phantom material with addition of other components. Preservatives, mineral oil and echogenic particles are examples of additives that could make the in this study unsuitably declared TMMs potential suitable phantom materials. Logically, a merit of a material that does not need additives is a less complex manufacturing process.

Especially in gellan gum and PVA there a numerous variables that can be varied both with respect to the composition of ingredients as well as to the manufacturing process. Most influential (and best controllable) variables were selected, however other variables could have led to other results.

In addition to the limited studied variables regarding composition and manufacturing process, the results will be substantially influenced by the brand-specific characteristics of materials purchased. Of all materials used in this study different types can be purchased. Our selection was both based on suitability (concluded from literature) and availability.

Another limitation of this work is that the data on livers and TMMs were not obtained in the same experiment. Although the same data collection methods were used, the effects of needle blunting and diminishing of needle coating may have influenced the results. Furthermore, the experiments were not conducted by the same person, thereby possibly causing inter-operator differences.

An aspect to be kept in mind is that the TMM are compared to liver data that did not solely include human livers. Also 4 animal livers have been used as reference, comprising different animals. Furthermore, the data was collected ex vivo. For ethical reasons this is fully understandable, but differences due to among others, lack of perfusion, preservation period and storage conditions cannot be ruled out.

.

10.3. CONCLUSION

Combining the results of all different parts of this study, we can summarize the suitability – the extent to which the TMMs are suitable as liver phantom material – of the TMMs in the following table:

Table 12 Overview of properties TMMs

Requirement	**Gellan gum**	**PVA**	**PVC**	**Candle Gel**
Mechanical requirement 1 (retraction slope)	-	+	+	-
Mechanical requirement 2 (peak forces)	N/A	+/-	N/A	N/A
Imaging performance	N/A	+	-	-
Practical aspects	-	+/-	-	+/-
Overall	-	+	-	-

Table 12 Overview of properties TMMs

As can be concluded from Table 12, PVA is the only material of the TMMs that were studied in this work that fulfils all criteria at least minimally.

PVA fulfils the criterion regarding the required retraction slope. Regarding the criteria for peak forces, some PVA samples show a suitable median peak height while other samples cause a suitable number of peak forces during insertion. It is expected that an optimal PVA phantom can be designed in order to fulfil all mechanical criteria. The same holds for the imaging performance. By tuning the variables, probably a homogeneous sample with the right echogenic properties could be obtained. Ideally, a PVA phantom would be designed with both suitable mechanical as well as imaging properties.

10.3.1. CONTRIBUTIONS

In many studies TMMs are used as a controlled environment to study (axial) forces in needle-tissue interaction. Although providing valuable results, results are hard to compare due to variation in research setups and analysis methods. Some studies compare TMM with liver tissue but focus on one either mechanical or imaging performance. When mechanical and imaging properties are both assessed, in most studies imaging properties of TMMs in combination with elasticity characteristics are compared to liver tissue. This study aimed to provide an overview of TMMs regarding their axial force characteristics and imaging performance under ultrasound. Furthermore, practical aspects are taken into account, which could provide useful information for researchers in need of a realistic liver phantom.

In addition to the information about the suitability of the materials with respect to their mechanical, imaging and practical characteristics, the influence of selected variables on the imaging characteristics of TMMs and the measured axial forces during needle-interventions is showed. To our knowledge, comparable studies have not been performed on the 4 materials selected for this study.

Although the clinical evaluation was performed on a small scale, this part of the study provided some interesting insights. More than the actual results, the importance of combining scientific results with (clinical) practice was emphasized.

10.3.2.RECOMMENDATIONS FOR FUTURE RESEARCH

Depending on specific purpose and deliverables, future research could focus on the following topics.

Mechanical comparison between liver tissue and TMMs:

- Define criteria based on the response of liver tissue upon needle interventions with needles as how they are used in practice (both cannula and inner needle inserted simultaneously, or needles that are used as stand-alone tool).
- Study the behaviour of liver tissue and TMM for different types of needles, different insertion velocities, specific insertion locations in the liver and phantoms.
- Perform a more extensive clinical evaluation of the performance of TMMs

Imaging comparison between liver tissue and TMMs:

- Study needle visibility both inside liver tissue and inside TMMs

Properties of PVA:

- Study the effect of amount of hydrolysis, degree of polymerization, freezing rate and duration, thawing rate, addition of ions, and type of solvent on the mechanical and imaging properties.
- Study the amount of needle deflection and tissue deformation in PVA
- Find the optimal combination of variables to mimic liver tissue

Candle gel:

- Study variable of candle gel that could enhance its mechanical properties
- Optimize echogenicity in candle gel

10.3.3. FINAL CONCLUSION

The aim of this study was to find a liver TMM suitable for image-guided needle interventions. Regarding the defined criteria on friction slope, peak forces during insertion and ultrasound visualization, we can conclude that PVA is a suitable material to mimic liver tissue during image-guided needle interventions.

The properties of PVA are tuneable to mimic a wide range of tissues. From the PVA modalities investigated in this study, the PVA 4% 2 FT sample proved to provide the best match with liver tissue. This sample had a similar friction slope as liver tissue, showed a comparable number of peaks during insertion and showed human tissue-like characteristics when visualized by ultrasound imaging.

APPENDICES

APPENDIX A: CHARACTERISTICS LIVER TISSUE AND TMMS

Healthy liver tissue			
Characteristic	**Value**		**Source**
Young's modulus	6.61 kPa	(human livers, elastography)	[80]
	"Values reported in literature: 4-7.5 kPa"		[80]
	5.7 kPa	(human livers, elastography)	[81]
	4.6 kPa	(69 human livers, elastography)	[82]
	5.9 kPa	(human livers, indentation)	[83]
	0.65 kPa	(human livers, compression tests)	[84]
	11 kPa	(pig livers, indentation)	[85]
Density	1060 kg m^{-3}		[86]
	1070 kg m^{-3}	(pig livers)	[87]
	1060 kg m^{-3}	(pig livers)	[88]
Speed of sound	1540 m s^{-1}		[89]
	1555-1595 m s^{-1}		[90]
	1595 m s^{-1}		[86]
Attenuation coefficient	0.55 dB cm^{-1} MHz^{-1}		[91]
	0.4-0.7 dB cm^{-1} MHz^{-1}		[90]
	0.5 dB cm^{-1} at 1MHz		[86]

Table 13 Healthy liver tissue characteristics

Gellan gum		
Characteristic	**Value**	**Source**
Young's modulus	6 kPa, 15 kPa, 24 kPa for concentration of 0,5%, 0,5% and 1,5% resp. (equal amounts of HA and LA).	[48]
	6 kPa - 250 kPa (dependent of composition and concentration, determined from figure)	[92]
Density	With debubbling 1040 kg m-3, without debubbling 1035 kg m^{-3}	[45]
Speed of sound	With debubbling 1584 m s^{-1}, without debubbling: 1569 m s^{-1}	[45]
	1579 m s^{-1} (with additives)	[77]
Attenuation coefficient	0.64 dB cm^{-1} MHz^{-1} at 20 degrees	[10]
	"close to attenuation in soft tissues"	[77]
Shelf life	Very stable (for at least 60 days) at storage at 4 degrees	[93]

Table 14 Gellan gum characteristics

PVA		
Characteristic	**Value**	**Source**
Young's modulus	3.6 - 11.4 kPa (depending on number of FT cycles)	[94]
	1.6 -16.1 kPa	[95]
	20 kPa	[96]
Density	Around 1270 kg m^{-3}	[97]
Speed of sound	1520- 1540 m s^{-1}	[59]
	1520-1610 m s^{-1}	[98]
	1540-1570 m s^{-1} (with addition of scatterers)	[95]
	1525-1560 m s^{-1}	[99]
Attenuation coefficient	0.07-0.35 $dBcm^{-1}MHz^{-1}$	[98]
Shelf life	Drying out when exposed to air	[100]

Table 15 PVA Characteristics

PVC		
Characteristic	**Value**	**Source**
Young's modulus	50 kPa	[8]
	10-100kPa	[6]
Density	940 kg m^{-3} (for 75% softener)	[8]
Speed of sound	1395 m s^{-1}	[100]
	1420 m s^{-1} (for 75% softener)	[8]
Attenuation coefficient	Very low without additives, with back-scattering agent 0.441 dB cm^{-1} MHz^{-1}	[100]
Shelf life	Little deterioration but approximately stable during at least 26 days.	[8]

Table 16 PVC characteristics

Candle gel		
Characteristic	**Value**	**Source**
Young's modulus	14.7 -34.9 kPa	[64]
Density	810 kg m^{-3}	[64]
	828 kg m^{-3}	[101]
	900 ± 40 kg m^{-3}	[65]
Speed of sound	1424.9 m s^{-1}	[64]
	~1320 m s^{-1}	[101]
	1420 – 1465 m s^{-1}	[65]
Attenuation coefficient	0.63 $dBcm^{-1}MHz^{-1}$	[64]
	~0.54 $dBcm^{-1}MHz^{-1}$	[101]
	0.45 – 4 $dBcm^{-1}MHz^{-1}$	[65]
Shelf life	Very long	[64]

Table 17 Candle gel characteristics

APPENDIX B: FORCE-POSITION DIAGRAMS LIVER TISSUE

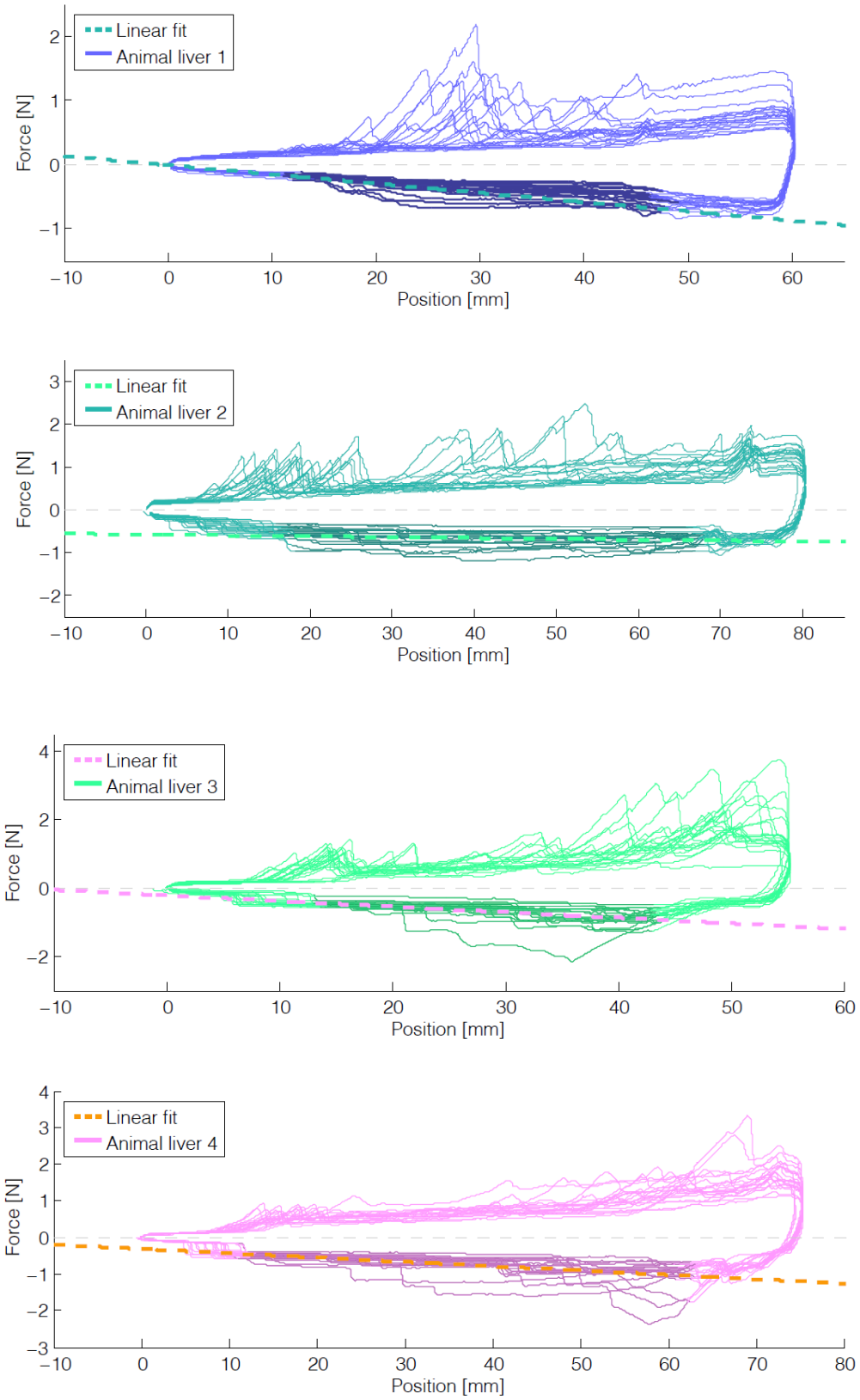

Figure 62 Force-position curves animal livers

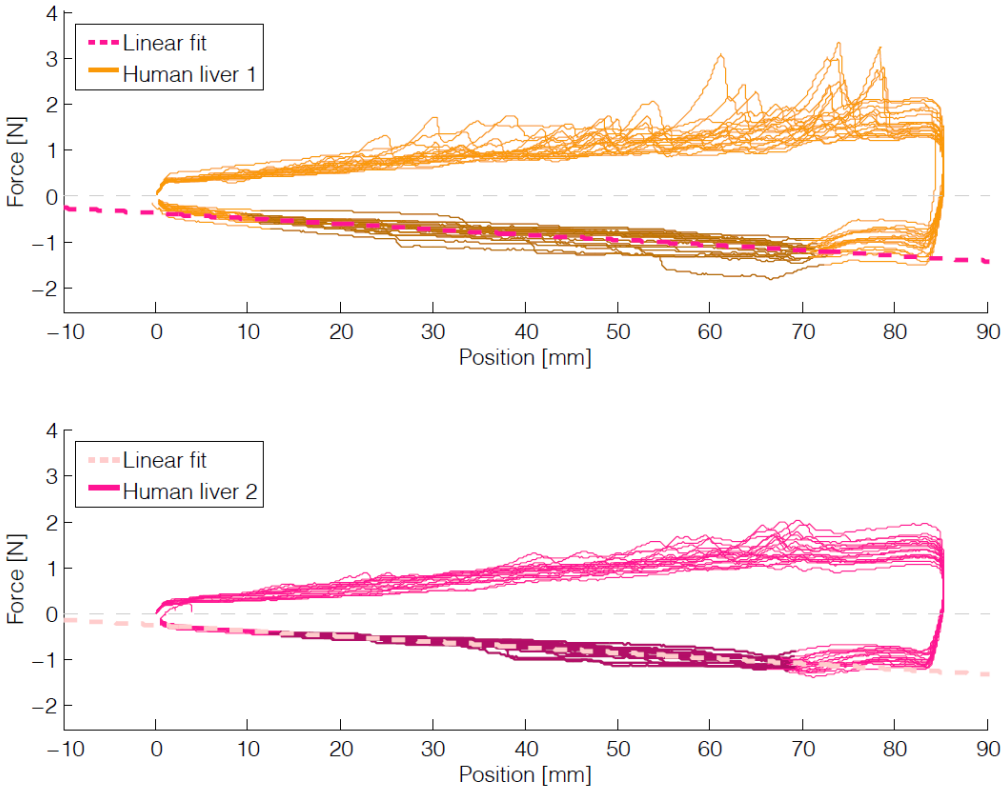

Figure 63 Force-position curves human livers

APPENDIX C: PREPARATION GUIDELINES PVA

The selected type of PVA (Selvol PVOH 165, Sekisui Chemical Group, NJ, USA) contains 5% volatiles. To determine the required amount of PVA granules, the following formula can be used:

$$Polyvinyl\ Alcohol\ (dry\ wt.) = \frac{X * Y}{100\% - 5\%}$$

Where X = Desired solution solids content and Y = Net weight of final solution

For the 4% PVA solution we thus used:

$$\frac{\frac{4}{100} * 250}{100\% - 5\%} = 10.5\ g$$

And for the 7% PVA solution:

$$\frac{\frac{7}{100} * 250}{100\% - 5\%} = 18.4\ g$$

APPENDIX D: FORCE-POSITION DIAGRAMS TMMS

GELLAN GUM

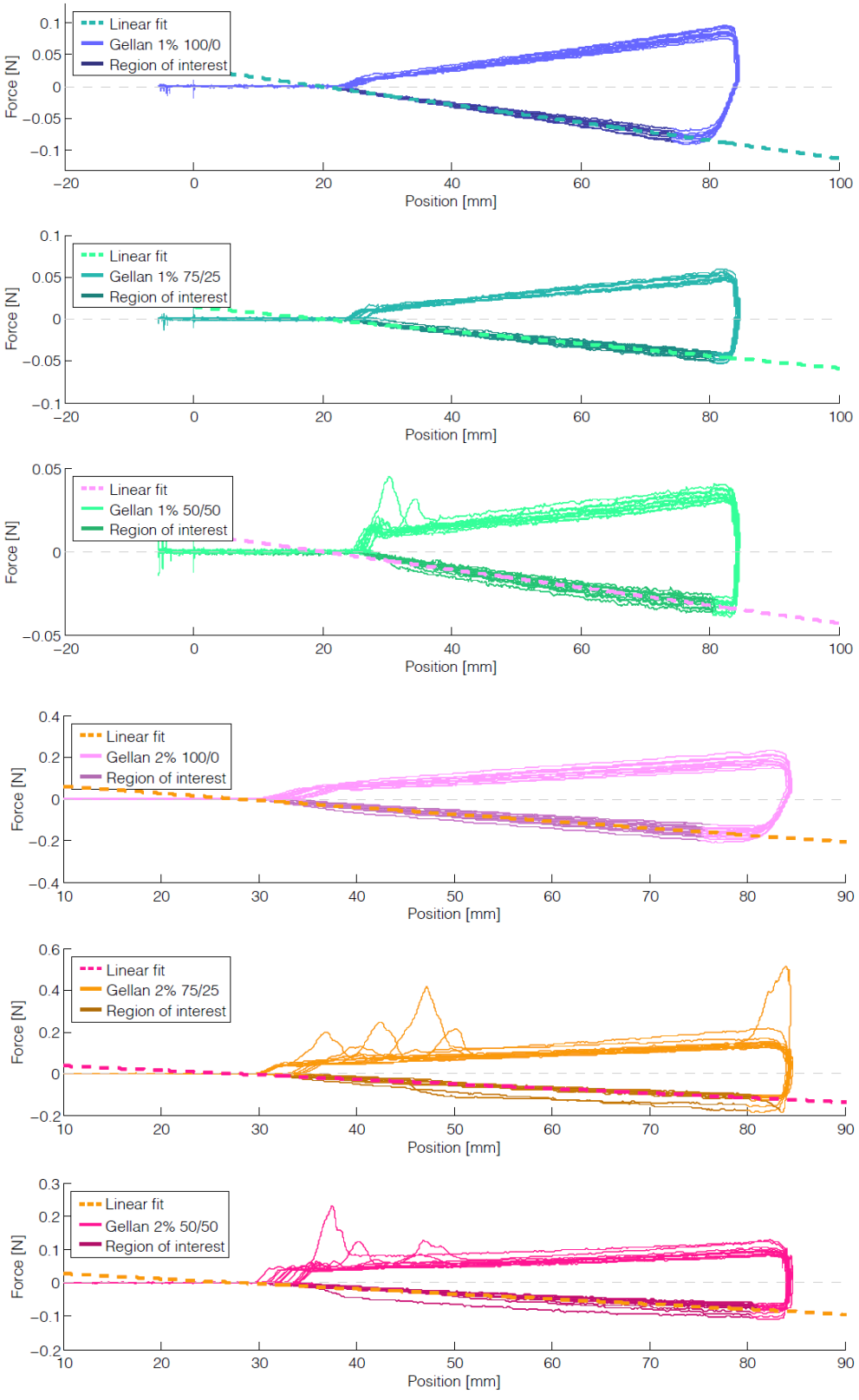

Figure 64 Force-position diagrams gellan gum

PVA

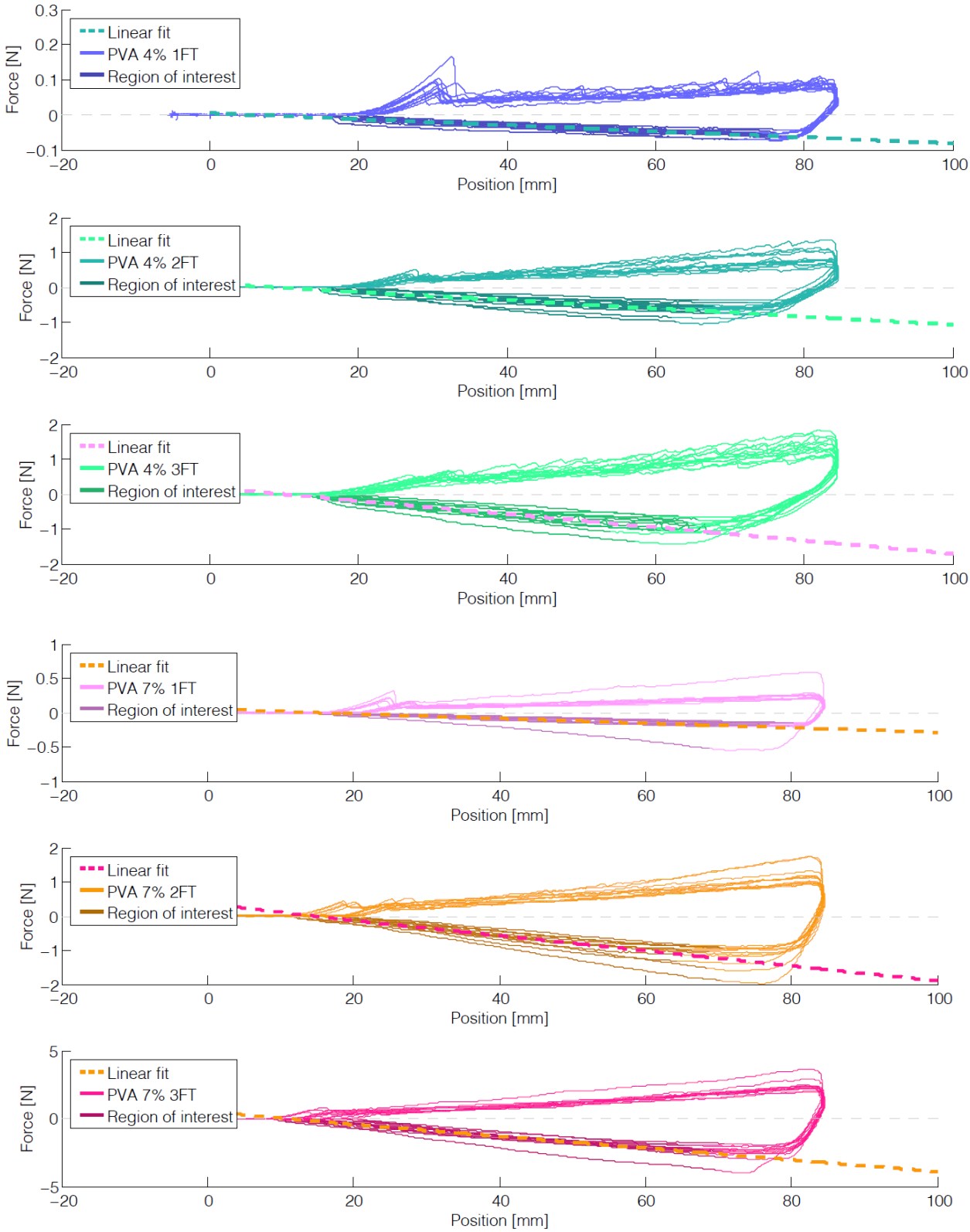

Figure 65 Force-position diagrams PVA

PVC

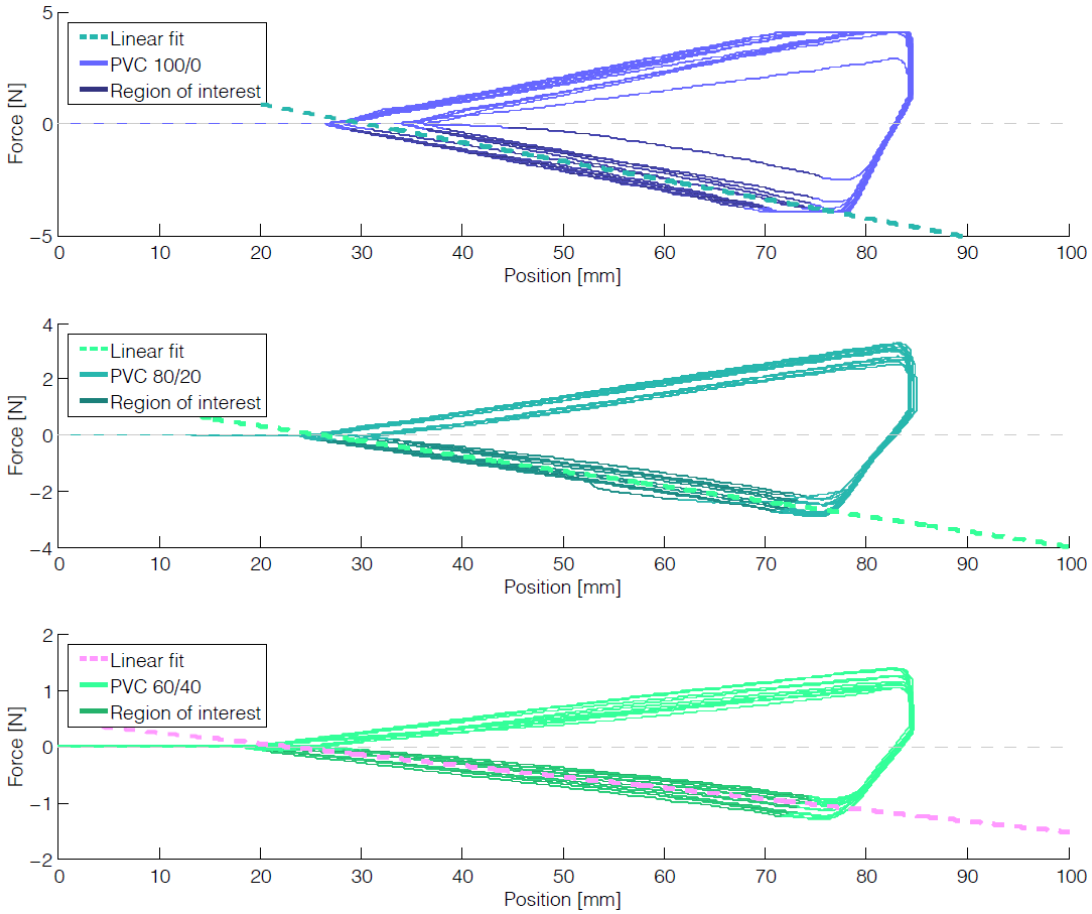

Figure 66 Force-position diagrams PVC

CANDLE GEL

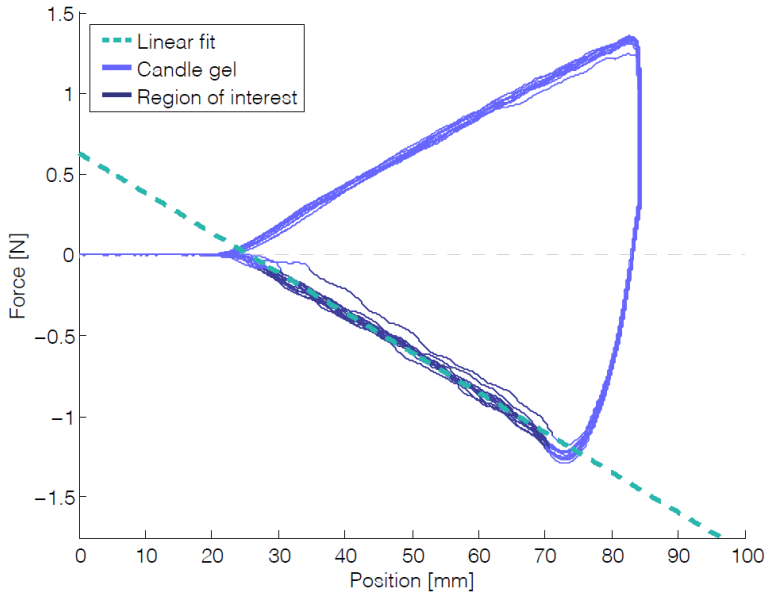

Figure 67 Force-position diagrams PVC

APPENDIX E: RETRACTION SLOPES IN PVC – AN ADDITIONAL EXPERIMENT

From the PVC samples studied the main experiment, the samples with more plasticizer showed results trending in the right direction. Therefore the retraction slopes in PVC samples with a higher concentration of plasticizer were studied in an additional experiment.

METHODS

Additional PVC samples were produced. These samples were obtained by melting a sample consisting of 80% plastisol (true plastisol with 20% plastizer added) and adding an additional amount of plasticizer. With this method samples consisting of plastisol with 50% and 60% additional plasticizer were obtained, referred to as PVC50 and PVC40 respectively (relating to the amount of plastisol the samples consist of).

In order to ensure that the data were not biased by blunting of the needle tip or diminishing of needle coating (the same was needle was used as in the main experiment), the sample with 40% additional plasticizer (referred to as PVC60, of which the properties were already assessed in 5.2) was added to the experimental setup. In addition to quantifying the effect of blunting of the needle tip or diminishing of needle coating, another advantage is that by adding this third sample, trend-lines can be distinguished.

All samples were in randomized order subjected to 5 interventions. Less interventions were performed compared to the previous experiment, as PVC was concluded to be fairly homogeneous in 5.3. The resulting retraction slopes are presented in boxplots, together with the retraction slopes observed in liver tissue.

RESULTS

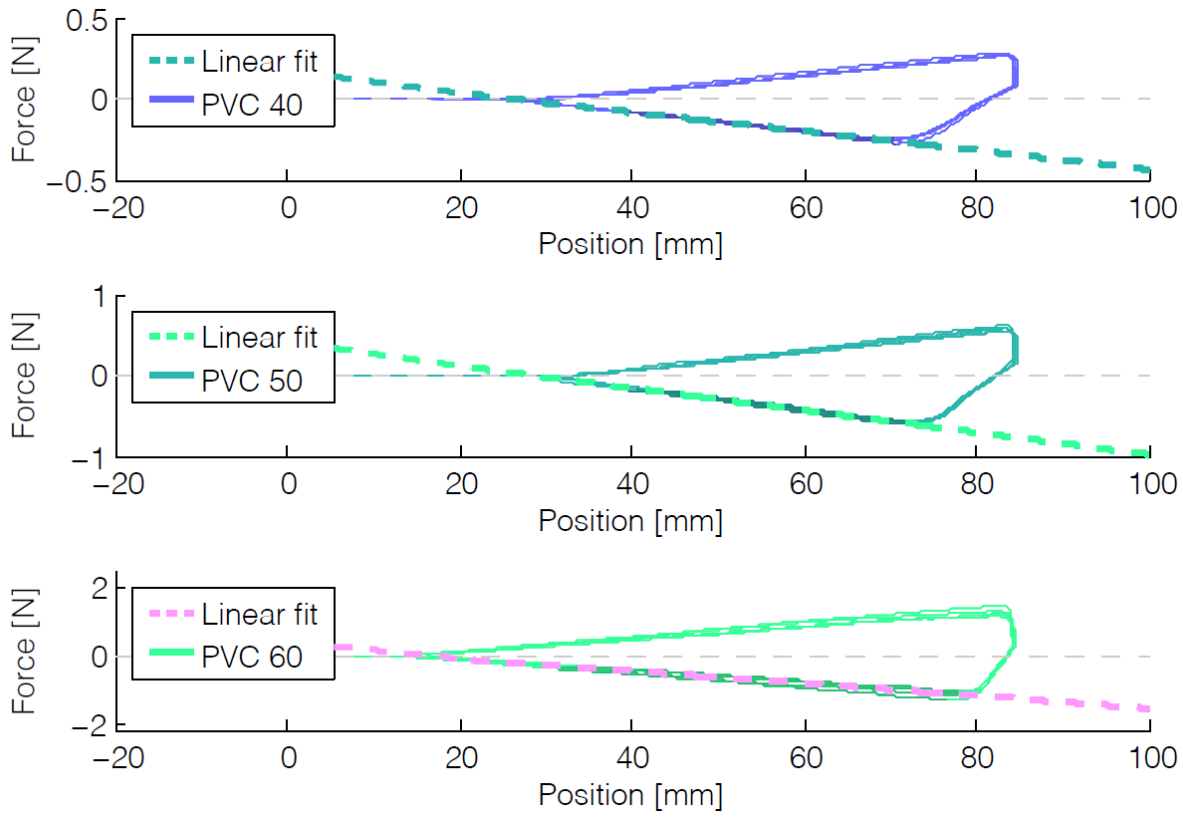

Figure 67 Force-position diagrams in PVC

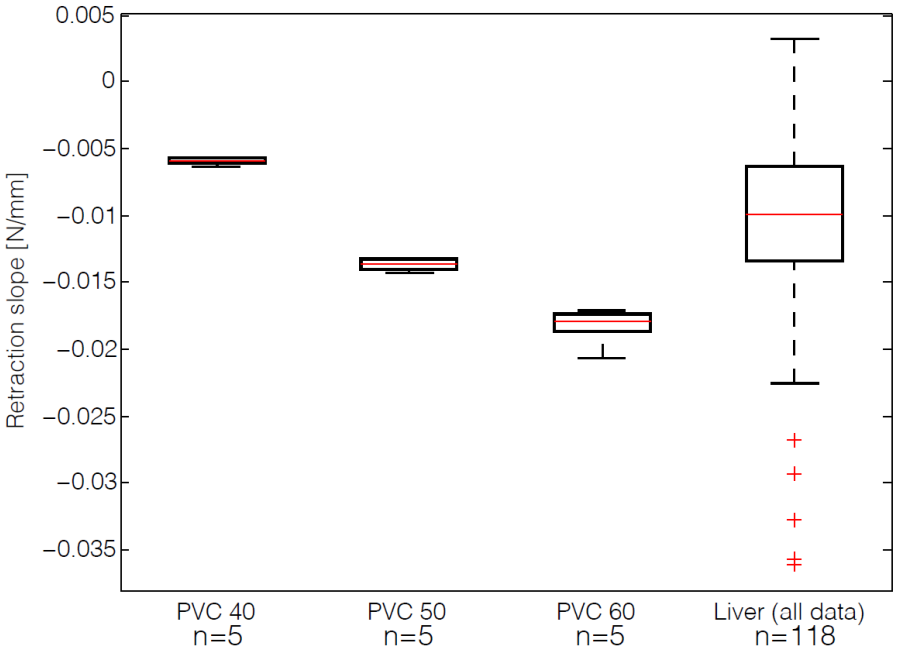

Figure 68 Retraction slopes additional PVC samples together with retraction slopes in liver tissue

The retraction slopes of the three samples are presented in Figure 67 and visualized in boxplots in Figure 68. Median retraction slopes in PVC consisting of 40%, 50% and 60% plastisol are -0.006, -0.014 and -0.018 N/mm respectively. The median retraction slope of PVC40 lies just above the IQR of liver tissue, while the median of PVC 50 lies just below the IQR of liver tissue. As was shown in chapter 5.2, the retraction slopes of PVC 60 are steeper than liver tissue. The results regarding PVC 60 from this experiment (median -0.018 N/mm n=5) and the results obtained in the experiment (-0.020 N/mm n=13) described in chapter 5 are comparable, so needle condition caused disturbances can be neglected.

DISCUSSION & CONCLUSION

From the results can be concluded that a sample consisting of approximately 45% plastisol and 55% additional plasticizer will have a similar median retraction slope as the liver.

As explained above, the PVC samples were produced by melting an existing PVC sample. Although production of the samples was performed precisely, the material properties could be influenced by the different production method with respect to the production method from the first experiment. However, with this additional experiment it has been proven that PVC can have a retraction slope that is similar to those observed in liver tissue. As mentioned before, the high amount of plasticizer remains a critical topic. The samples produced in this experiment remained rather liquid after they cooled down to room temperature. Although the plasticizer involved is presumably (the non-toxic) DEHA, the mixtures should be handled cautiously, not only regarding health issues but also with respect to interaction with the PVC parts of the ultrasound transducer.

APPENDIX F: INFLUENCE OF EPSILON IN DOUGLAS PECKER ALGORITHM

Epsilon = 0.05 N	**Peak Height**	**Number of Peaks per Decimetre**	**Simplification (liver)**
IQR liver tissue	0.10 – 0.46 N	5.5 - 10.0 p/dm	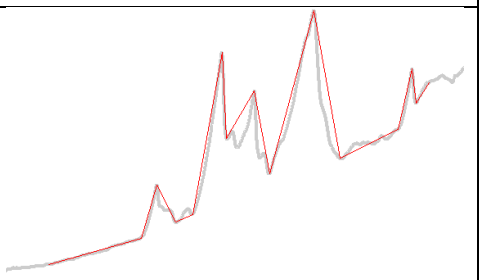
PVA samples with median inside IQR liver	PVA 4%3FT *(median 0.11 N)* PVA 7%3FT *(median 0.16 N)*	PVA 4% 1FT *(median 9.60 p/dm)* PVA 4%2FT *(median 6.66 p/dm)*	

Epsilon = 0.04 N	**Peak Height**	**Number of Peaks per Decimetre**	**Simplification (liver)**
IQR liver tissue	0.09 – 0.42 N	6.40 – 11.19 p/dm	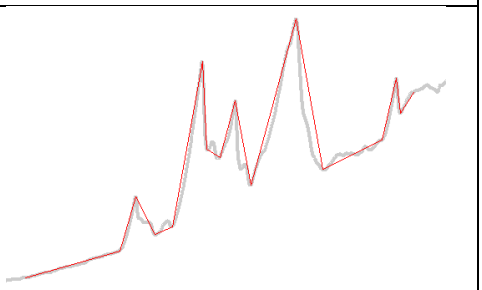
PVA samples with median inside IQR liver	PVA 4% 3FT *(median 0.11 N)* PVA 7% 2FT *(median 0.09 N)* PVA 7% 3FT *(median 0.15 N)*	PVA 4% 2FT *(median 7.92 p/dm)* PVA 4% 3FT *(median 6.49 p/dm)*	

Epsilon = 0.03 N	**Peak Height**	**Number of Peaks per decimetre**	**Simplification (liver)**
IQR liver tissue	0.06 – 0.32 N	8.69 – 13.89 p/dm	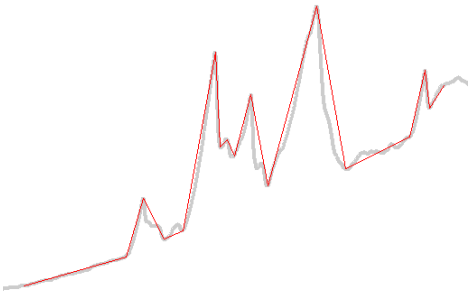
PVA samples with median inside IQR liver	PVA 4% 3FT *(median 0.10 N)* PVA 7% 2FT *(median 0.07 N)* PVA 7% 3FT *(median 0.13 N)*	PVA 4% 2FT *(median 11.01 p/dm)* PVA 4% 3FT *(median 10.97 p/dm)*	

APPENDIX G: ULTRASOUND PERFORMANCE OF PVA 3% 5FT

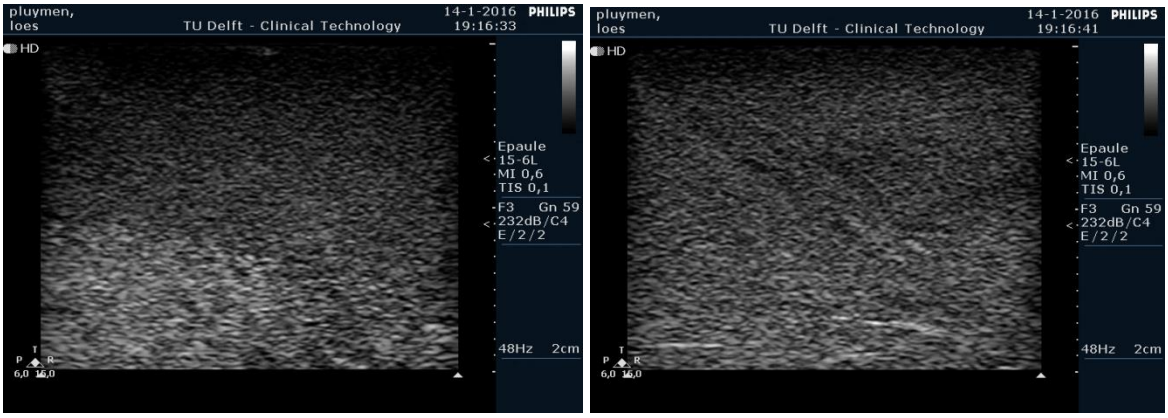

Figure 69 PVA 3% 5FT : Images obtained with 2 cm penetration depth

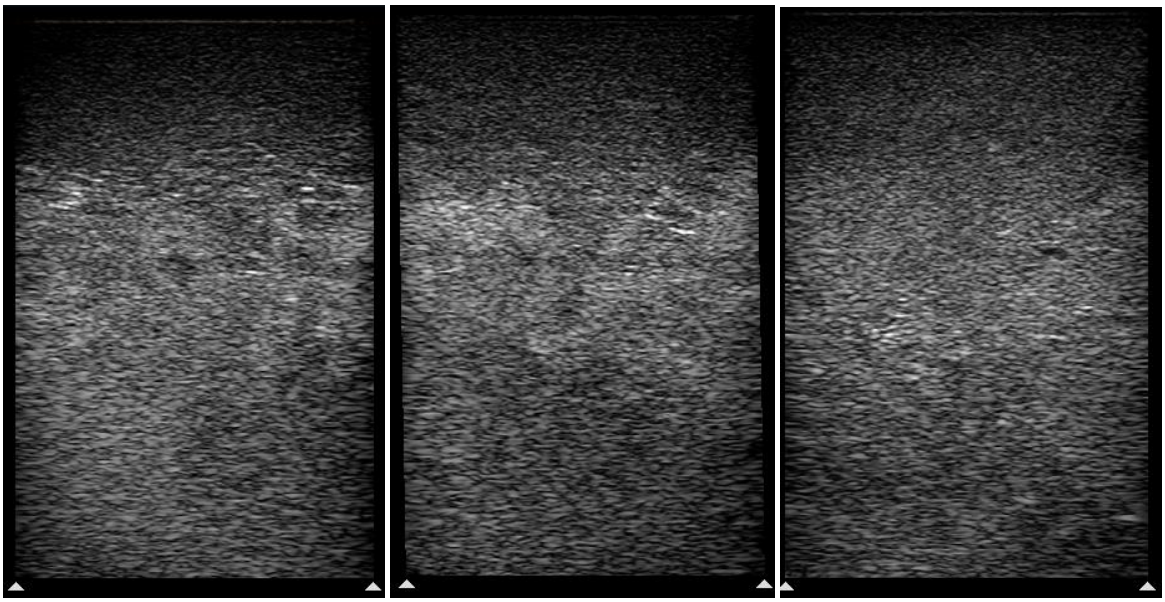

Figure 70 PVA 3% 5FT : Images obtained with 5 cm penetration depth

APPENDIX H: CLINICAL EVALUATION PVC AND CANDLE GEL

In this section the feedback of the two radiologists about the PVC and candle gel samples is captured.

M.S. stated that needle insertions in all PVC samples required too much effort with respect to needle interventions in the liver. During insertion an excessively high amount of friction was experienced, especially in the samples that contained less plasticizer. Furthermore, the material was found to be too elastic to be comparable to human tissues. Also candle gel caused too much friction both during insertion as well as during retraction. M.S. also mentioned the unrealistic aspect of friction in candle gel during retraction. He explained to experience friction only during insertion and not during retraction when performing needle interventions in humans (one should keep in mind that this dissimilarity in perception could be due to the different methods that are applied to insert resp. retract the needle).

B.M. was more positive about the PVC samples. Especially the PVC 60 sample was described as a material suitable to mimic human tissues, due to its properties that allow for smooth needle insertion. The PVC 80 sample was defined as less liver-like and its characteristics were described as more skin mimicking. Also candle gel was assessed rather positively, mainly based on its homogeneous characteristics. B.M. stated that the insertion phase in candle gel was more realistic than the retraction phase, which is in line with M.S.' observations. He also noticed and mentioned the damage that was caused by retraction of the needle. Although to some degree realistically mimicking liver tissue, candle gel was found to be 'too thick' to be a liver mimicking material.

REFERENCES

1. Hunt, A., et al., *Low cost anatomically realistic renal biopsy phantoms for interventional radiology trainees.* European Journal of Radiology, 2013. **82**(4): p. 594-600.
2. Pacioni, A., et al., *Patient-specific ultrasound liver phantom: materials and fabrication method.* Int J Comput Assist Radiol Surg, 2015. **10**(7): p. 1065-75.
3. Hocking, G., S. Hebard, and C.H. Mitchell, *A review of the benefits and pitfalls of phantoms in ultrasound-guided regional anesthesia.* Regional anesthesia and pain medicine, 2011. **36**(2): p. 162-170.
4. Sultan, S.F., G. Shorten, and G. Iohom, *Simulators for training in ultrasound guided procedures.* Medical ultrasonography, 2013. **15**(2): p. 125.
5. Opik, R., et al. *Development of high fidelity liver and kidney phantom organs for use with robotic surgical systems*. in *Biomedical Robotics and Biomechatronics (BioRob), 2012 4th IEEE RAS & EMBS International Conference on*. 2012. IEEE.
6. DiMaio, S.P. and S.E. Salcudean, *Needle insertion modeling and simulation.* Robotics and Automation, IEEE Transactions on, 2003. **19**(5): p. 864-875.
7. Haddadi, A. and K. Hashtrudi-Zaad. *Development of a dynamic model for bevel-tip flexible needle insertion into soft tissues*. in *Engineering in Medicine and Biology Society, EMBC, 2011 Annual International Conference of the IEEE*. 2011. IEEE.
8. Hungr, N., et al., *A realistic deformable prostate phantom for multimodal imaging and needle-insertion procedures.* Medical Physics, 2012. **39**(4): p. 2031-2041.
9. Ceh, D., T.M. Peters, and E.C. Chen. *Acoustic characterization of polyvinyl chloride and self-healing silicone as phantom materials*. in *SPIE Medical Imaging*. 2015. International Society for Optics and Photonics.
10. Culjat, M.O., et al., *A review of tissue substitutes for ultrasound imaging.* Ultrasound in medicine & biology, 2010. **36**(6): p. 861-873.
11. Wedlick, T.R. and A.M. Okamura. *Characterization of robotic needle insertion and rotation in artificial and ex vivo tissues*. in *Biomedical Robotics and Biomechatronics (BioRob), 2012 4th IEEE RAS & EMBS International Conference on*. 2012. IEEE.
12. de Jong, T., *Needle Deflection in Tissue.* 2015.
13. Hall, J.E., *Guyton and Hall textbook of medical physiology*. 2015: Elsevier Health Sciences.
14. Marieb, E.N. and K. Hoehn, *Human anatomy & physiology*. 2007: Pearson Education.
15. Simpson, A.L., et al., *Model-assisted image-guided liver surgery using sparse intraoperative data*, in *Soft Tissue Biomechanical Modeling for Computer Assisted Surgery*. 2012, Springer. p. 7-40.
16. Kumar, V., et al., *Robbins and cotran pathologic basis of disease, Professional Edition: Expert Consult-Online*. 2014: Elsevier Health Sciences.
17. Rockey, D.C., et al., *Liver biopsy.* Hepatology, 2009. **49**(3): p. 1017-1044.
18. Denzer, U., et al., *Prospective randomized comparison of minilaparoscopy and percutaneous liver biopsy: diagnosis of cirrhosis and complications.* Journal of clinical gastroenterology, 2007. **41**(1): p. 103-110.
19. Cakmakci, E., et al., *Percutaneous liver biopsies guided with ultrasonography: a case series.* Iranian Journal of Radiology, 2013. **10**(3): p. 182-184.
20. Vijayaraghavan, G.R., et al., *Imaging-guided Parenchymal Liver Biopsy: How We Do It.* J Clin Imaging Sci, 2011. **1**: p. 30.
21. Abolhassani, N., R. Patel, and M. Moallem, *Needle insertion into soft tissue: A survey.* Medical Engineering & Physics, 2007. **29**(4): p. 413-431.

22. Okamura, A.M., C. Simone, and M.D. O'Leary, *Force modeling for needle insertion into soft tissue.* Biomedical Engineering, IEEE Transactions on, 2004. **51**(10): p. 1707-1716.

23. McGill, C.S., et al., *Effects of insertion speed and trocar stiffness on the accuracy of needle position for brachytherapy.* Med Phys, 2012. **39**(4): p. 1811-7.

24. Podder, T., et al. *Effects of tip geometry of surgical needles: an assessment of force and deflection*. in *IFMBE Proc*. 2005.

25. van Gerwen, D.J., J. Dankelman, and J.J. van den Dobbelsteen, *Needle-tissue interaction forces--a survey of experimental data.* Med Eng Phys, 2012. **34**(6): p. 665-80.

26. Kerdok, A.E., M.P. Ottensmeyer, and R.D. Howe, *Effects of perfusion on the viscoelastic characteristics of liver.* Journal of Biomechanics, 2006. **39**(12): p. 2221-2231.

27. Yarpuzlu, B., et al., *Correlation between the mechanical and histological properties of liver tissue.* journal of the mechanical behavior of biomedical materials, 2014. **29**: p. 403-416.

28. Chatelin, S., et al., *In vivo liver tissue mechanical properties by transient elastography: Comparison with dynamic mechanical analysis.* Biorheology, 2011. **48**(2): p. 75-88.

29. Ling, W., et al., *Effects of vascularity and differentiation of hepatocellular carcinoma on tumor and liver stiffness: in vivo and in vitro studies.* Ultrasound in medicine & biology, 2014. **40**(4): p. 739-746.

30. Podder, T., et al. *Evaluation of robotic needle insertion in conjunction with in vivo manual insertion in the operating room*. in *Robot and Human Interactive Communication, 2005. ROMAN 2005. IEEE International Workshop on*. 2005. IEEE.

31. Webster III, R.J., J. Memisevic, and A.M. Okamura. *Design considerations for robotic needle steering*. in *Robotics and Automation, 2005. ICRA 2005. Proceedings of the 2005 IEEE International Conference on*. 2005. IEEE.

32. Lamouche, G., et al., *Review of tissue simulating phantoms with controllable optical, mechanical and structural properties for use in optical coherence tomography.* Biomedical optics express, 2012. **3**(6): p. 1381-1398.

33. Fu, Y. and C. Chui, *Modelling and simulation of porcine liver tissue indentation using finite element method and uniaxial stress–strain data.* Journal of biomechanics, 2014. **47**(10): p. 2430-2435.

34. Chang, J.M., et al., *Comparison of shear-wave and strain ultrasound elastography in the differentiation of benign and malignant breast lesions.* American Journal of Roentgenology, 2013. **201**(2): p. W347-W356.

35. Özkaya, N., et al., *Fundamentals of biomechanics: equilibrium, motion, and deformation*. 2012: Springer Science & Business Media.

36. Pal, S., *Design of Artificial Human Joints & Organs*. 2014: Springer.

37. Velasco, J.M. and K. Hood, *Percutaneous Ultrasound Guidance Techniques and Procedures*, in *Abdominal Ultrasound for Surgeons*. 2014, Springer. p. 89-107.

38. Silas, A.M., J.B. Kruskal, and R.A. Kane, *Intraoperative ultrasound.* Radiologic Clinics of North America, 2001. **39**(3): p. 429-448.

39. Chan, V. and A. Perlas, *Basics of ultrasound imaging*, in *Atlas of ultrasound-guided procedures in interventional pain management*. 2011, Springer. p. 13-19.

40. Laugier, P. and G. Haïat, *Bone quantitative ultrasound*. Vol. 576. 2011: Springer.

41. DeWerd, L.A. and M. Kissick, *The Phantoms of Medical and Health Physics.* The Phantoms of Medical and Health Physics: Devices for Research and Development, Biological and Medical Physics, Biomedical Engineering. ISBN 978-1-4614-8303-8. Springer Science+ Business Media New York, 2014, 2014. **1**.

42. Callister, W.D. and D.G. Rethwisch, *Materials science and engineering: an introduction*. Vol. 7. 2007: Wiley New York.

43. Maitra, J. and V.K. Shukla, *Cross-linking in hydrogels-a review.* American Journal of Polymer Science, 2014. **4**(2): p. 25-31.

44. Pal, K., A. Banthia, and D. Majumdar, *Polymeric hydrogels: characterization and biomedical applications.* Designed monomers and polymers, 2009. **12**(3): p. 197-220.

45. Chen, R.K. and A. Shih, *Multi-modality gellan gum-based tissue-mimicking phantom with targeted mechanical, electrical, and thermal properties.* Physics in medicine and biology, 2013. **58**(16): p. 5511.

46. Lee, H., et al., *Optimizing gelling parameters of gellan gum for fibrocartilage tissue engineering.* Journal of Biomedical Materials Research Part B: Applied Biomaterials, 2011. **98**(2): p. 238-245.

47. Prajapati, V.D., et al., *An insight into the emerging exopolysaccharide gellan gum as a novel polymer.* Carbohydrate polymers, 2013. **93**(2): p. 670-678.

48. Mao, R., J. Tang, and B. Swanson, *Texture properties of high and low acyl mixed gellan gels.* Carbohydrate polymers, 2000. **41**(4): p. 331-338.

49. Ferris, C.J., K.J. Gilmore, and G.G. Wallace, *Modified gellan gum hydrogels for tissue engineering applications.* Soft Matter, 2013. **9**(14): p. 3705-3711.

50. Gasperini, L., J.F. Mano, and R.L. Reis, *Natural polymers for the microencapsulation of cells.* Journal of The Royal Society Interface, 2014. **11**(100): p. 20140817.

51. Singh, R., et al., *Characterization of the structure and permeability of titanium foams for spinal fusion devices.* Acta Biomaterialia, 2009. **5**(1): p. 477-487.

52. Baker, M.I., et al., *A review of polyvinyl alcohol and its uses in cartilage and orthopedic applications.* Journal of Biomedical Materials Research Part B: Applied Biomaterials, 2012. **100**(5): p. 1451-1457.

53. Surry, K.J., et al., *Poly(vinyl alcohol) cryogel phantoms for use in ultrasound and MR imaging.* Phys Med Biol, 2004. **49**(24): p. 5529-46.

54. Ravve, A., *Principles of polymer chemistry*. 2013: Springer Science & Business Media.

55. Moulay, S., *Molecular iodine/polymer complexes.* Journal of Polymer Engineering, 2013. **33**(5): p. 389-443.

56. Nkhwa, S., et al. *Poly (vinyl alcohol): physical approaches to designing biomaterials for biomedical applications*. in *Conference Papers in Science*. 2014. Hindawi Publishing Corporation.

57. Okay, O., *Polymeric Cryogels: Macroporous Gels with Remarkable Properties*. Vol. 263. 2014: Springer.

58. Brazel, C.S. and S.L. Rosen, *Fundamental principles of polymeric materials*. 2012: John Wiley & Sons.

59. Surry, K., et al., *Poly (vinyl alcohol) cryogel phantoms for use in ultrasound and MR imaging.* Physics in medicine and biology, 2004. **49**(24): p. 5529.

60. Tao, J., *Effects of Molecular weight and Solution Concentration on Electrospinning of PVA*. 2003, Worcester Polytechnic Institute.

61. Zhang, L., et al., *Anisotropic tough poly (vinyl alcohol) hydrogels.* Soft Matter, 2012. **8**(40): p. 10439-10447.

62. Chiellini, F., et al., *Perspectives on alternatives to phthalate plasticized poly (vinyl chloride) in medical devices applications.* Progress in Polymer Science, 2013. **38**(7): p. 1067-1088.

63. Patrick, S., *Practical guide to polyvinyl chloride*. 2005: iSmithers Rapra Publishing.

64. Vieira, S.L., et al., *Paraffin-gel tissue-mimicking material for ultrasound-guided needle biopsy phantom.* Ultrasound in medicine & biology, 2013. **39**(12): p. 2477-2484.

65. Oudry, J., et al., *Copolymer-in-oil phantom materials for elastography.* Ultrasound in medicine & biology, 2009. **35**(7): p. 1185-1197.

66. Chmarra, M.K., et al., *Multimodal phantom of liver tissue.* PloS one, 2013. **8**(5): p. e64180.

67. Van Gerwen, D.J., *Needle-Tissue Interaction by Experiment.* 2013: p. 81-101.

68. Hing, J.T., A.D. Brooks, and J.P. Desai. *Reality-based needle insertion simulation for haptic feedback in prostate brachytherapy*. in *Robotics and Automation, 2006. ICRA 2006. Proceedings 2006 IEEE International Conference on*. 2006. IEEE.

69. Jiang, S., et al., *Experimental study of needle–tissue interaction forces: effect of needle geometries, insertion methods and tissue characteristics.* Journal of biomechanics, 2014. **47**(13): p. 3344-3353.

70. Asadian, A., R.V. Patel, and M.R. Kermani. *A distributed model for needle-tissue friction in percutaneous interventions*. in *Robotics and Automation (ICRA), 2011 IEEE International Conference on*. 2011. IEEE.

71. Dalgaard, M., et al., *Di (2-ethylhexyl) adipate (DEHA) induced developmental toxicity but not antiandrogenic effects in pre-and postnatally exposed Wistar rats.* Reproductive Toxicology, 2003. **17**(2): p. 163-170.

72. Jiang, S., S. Liu, and W. Feng, *PVA hydrogel properties for biomedical application.* Journal of the mechanical behavior of biomedical materials, 2011. **4**(7): p. 1228-1233.

73. Cook, J.R., R.R. Bouchard, and S.Y. Emelianov, *Tissue-mimicking phantoms for photoacoustic and ultrasonic imaging.* Biomedical optics express, 2011. **2**(11): p. 3193-3206.

74. Shevchenko, N., et al. *Evaluation of a resectable ultrasound liver phantom for testing of surgical navigation systems*. in *Engineering in Medicine and Biology Society, EMBC, 2011 Annual International Conference of the IEEE*. 2011. IEEE.

75. Chin, K.J., et al., *Needle visualization in ultrasound-guided regional anesthesia: challenges and solutions.* Regional anesthesia and pain medicine, 2008. **33**(6): p. 532-544.

76. Hing, J.T., A.D. Brooks, and J.P. Desai, *A biplanar fluoroscopic approach for the measurement, modeling, and simulation of needle and soft-tissue interaction.* Medical image analysis, 2007. **11**(1): p. 62-78.

77. King, R.L., et al., *Development and characterization of a tissue-mimicking material for high-intensity focused ultrasound.* Ultrasonics, Ferroelectrics, and Frequency Control, IEEE Transactions on, 2011. **58**(7): p. 1397-1405.

78. Cha, W.I., et al. *Mechanical and wear properties of poly (vinyl alcohol) hydrogels*. in *Macromolecular Symposia*. 1996. Wiley Online Library.

79. Li, W., B. Belmont, and A. Shih, *Design and Manufacture of Polyvinyl Chloride (PVC) Tissue Mimicking Material for Needle Insertion.* Procedia Manufacturing, 2015. **1**: p. 866-878.

80. Muller, M., et al., *Quantitative viscoelasticity mapping of human liver using supersonic shear imaging: preliminary in vivo feasability study.* Ultrasound in medicine & biology, 2009. **35**(2): p. 219-229.

81. Wong, V.W.S., et al., *Diagnosis of fibrosis and cirrhosis using liver stiffness measurement in nonalcoholic fatty liver disease.* Hepatology, 2010. **51**(2): p. 454-462.

82. Kim, S.U., et al., *What are 'true normal'liver stiffness values using FibroScan®?: a prospective study in healthy living liver and kidney donors in South Korea.* Liver International, 2010. **30**(2): p. 268-274.

83. Lim, Y.-J., et al., *In situ measurement and modeling of biomechanical response of human cadaveric soft tissues for physics-based surgical simulation.* Surgical endoscopy, 2009. **23**(6): p. 1298-1307.

84. Yeh, W.-C., et al., *Elastic modulus measurements of human liver and correlation with pathology.* Ultrasound in medicine & biology, 2002. **28**(4): p. 467-474.

85. Wang, Y., et al., *Silicone-based tissue-mimicking phantom for needle insertion simulation.* Journal of Medical Devices, 2014. **8**(2): p. 021001.

86. Mast, T.D., *Empirical relationships between acoustic parameters in human soft tissues.* Acoustics Research Letters Online, 2000. **1**(2): p. 37-42.

87. Niehues, S., et al., *Liver volume measurement: reason of the difference between in vivo CT-volumetry and intraoperative ex vivo determination and how to cope it.* European journal of medical research, 2010. **15**(8): p. 345.

88. Gao, Z., K. Lister, and J.P. Desai, *Constitutive modeling of liver tissue: experiment and theory.* Annals of biomedical engineering, 2010. **38**(2): p. 505-516.

89. Pacioni, A., et al., *Patient-specific ultrasound liver phantom: materials and fabrication method.* Int J Comput Assist Radiol Surg, 2014.

90. Boote, E.J., *Phantoms for Ultrasound Experimentation and Quality Control*, in *The Phantoms of Medical and Health Physics*. 2014, Springer. p. 159-179.

91. Lu, Z.F., J. Zagzebski, and F. Lee, *Ultrasound backscatter and attenuation in human liver with diffuse disease.* Ultrasound in medicine & biology, 1999. **25**(7): p. 1047-1054.

92. Morris, E.R., K. Nishinari, and M. Rinaudo, *Gelation of gellan–a review.* Food Hydrocolloids, 2012. **28**(2): p. 373-411.

93. Mao, R., J. Tang, and B. Swanson, *Water holding capacity and microstructure of gellan gels.* Carbohydrate polymers, 2001. **46**(4): p. 365-371.

94. Jiang, S., S. Liu, and W. Feng, *PVA hydrogel properties for biomedical application.* J Mech Behav Biomed Mater, 2011. **4**(7): p. 1228-33.

95. Cournane, S., et al., *Assessment of the accuracy of an ultrasound elastography liver scanning system using a PVA-cryogel phantom with optimal acoustic and mechanical properties.* Phys Med Biol, 2010. **55**(19): p. 5965-83.

96. Fromageau, J., et al., *Characterization of PVA cryogel for intravascular ultrasound elasticity imaging.* Ultrasonics, Ferroelectrics, and Frequency Control, IEEE Transactions on, 2003. **50**(10): p. 1318-1324.

97. Stasko, J., et al., *Poly (vinyl alcohol) hydrogels.* Proceedings of the Estonian Academy of Sciences, 2009. **58**(1): p. 63-66.

98. Culjat, M.O., et al., *A review of tissue substitutes for ultrasound imaging.* Ultrasound Med Biol, 2010. **36**(6): p. 861-73.

99. Fromageau, J., et al., *Estimation of polyvinyl alcohol cryogel mechanical properties with four ultrasound elastography methods and comparison with gold standard testings.* Ultrasonics, Ferroelectrics, and Frequency Control, IEEE Transactions on, 2007. **54**(3): p. 498-509.

100. Ceh, D., T.M. Peters, and E.C.S. Chen. *Acoustic characterization of polyvinyl chloride and self-healing silicone as phantom materials*. 2015.

101. Jönsson, M., *Utlrasound Artefacts.* 2015.